Bio-oil Generation from Microwave Assisted Pyrolysis of Stockpiled Biosolids

James Schumann (B.Eng)

Submitted on 21st June 2017 in fulfilment of the requirements for Master of Philosophy (Engineering and Related Technologies) at James Cook University.

Primary Supervisor: A/Prof Phil Schneider

Secondary Supervisor: A/Prof Mohan Jacob

Abstract

This project employed microwave assisted pyrolysis (MWAP) to recover resources from stockpiled biosolids from Victoria, Australia. Biosolids are the stabilised sludge that results from sewage wastewater treatment. The presence of contaminants, unpleasant odours and poor public acceptance make biosolids disposal challenging. Over three million tonnes of biosolids are currently stockpiled in Victoria, having no identified end use.

MWAP applies a microwave electromagnetic field to biosolids in a low-oxygen environment, which heats the material, thermally decomposing the organic matter into volatile bio-oils and incondensable gases, leaving behind a biochar. This work focused on assessing the feasibility of generating bio-oil from MWAP of the Victorian biosolids, with a particular focus on analysing the composition of the bio-oil and identifying ways to enhance the process value. A comparative study was also done using local biosolids.

MWAP was carried out using a single-mode microwave pyrolysis unit with a nitrogen-gas purge, enabling condensers to trap the resultant bio-oil. Biosolids mixed with a microwave susceptor that absorbed the microwave energy and re-emitted it as heat (activated carbon) were pyrolyzed in sets of experiments where the oil composition and yield were evaluated. As bio-oil produced from MWAP can contain hundreds of organic compounds, a method was developed to analyse the yield of selected compounds with Gas Chromatography Mass Spectrometry and Gas Spectrometry Flame Ionization Detection. To improve the separation of the bio-oil in the chromatography column, samples were first derivatized using N,O-Bis(trimethylsilyl)trifluoroacetamide (BSTFA).

The bio-oil derived from stockpiled biosolids contained a range of compounds, with the largest groups being phenols and carboxylic acids, and had a calorific value similar to that of bio-diesel. Bio-oil yield was low due to the degradation of the biosolids from the extended periods of stockpiling. The MWAP also consumed a large amount of energy per unit mass of biosolids pyrolysed.

Under some conditions the MWAP was cost competitive against land application, which costs an average $300/dry tonne. MWAP of stockpiled biosolids cost as little as $218/dry tonne, though >90% of the savings were due to mass reduction and not bio-oil in this case. Larger scale tests are needed to determine whether the costs and technical complexity of the

process could be managed. Unidentified components of the bio-oil that were not quantified may improve the economics.

Acknowledgements

Statement of Contribution of Others

Nature of Assistance	Contribution	Contributor
Financial	Scholarship Extension SSA funds Conference Funding	James Cook University Graduate Research School
Financial	Scholarship	Smart Water Fund
Material	Microwave Pyrolysis Unit	Dr. Graham Brodie, Melbourne University
Analytical	Expert advice GC-MS training GC-FID training	Dr. Shane Askew, James Cook University
Analytical	Elemental Analysis	Dr. Michael Nefedov, University of Queensland
Research	Research Assistance	Elsa Antunes
Research	Research Assistance	A/Prof Phil Schneider
Research	Research Assistance	A/Prof Mohan Jacob

Table of Contents

List of Figures

List of Tables

1 Introduction

This section outlines the context for the project and the problem it aims to solve. The goals the project set and methodology used to solve the project problem are stated herein. A brief background on microwave assisted pyrolysis, and why it is being applied to biosolids, is also provided.

1.1 Project Context

This project aims to assess microwave assisted pyrolysis (MWAP) of stockpiled Victorian biosolids with specific consideration given to the generation of bio-oil, its characterisation, and potential for value adding.

Approximately 3.6 million dry tonnes of biosolids are currently stored at the Melbourne Eastern Treatment Plant (ETP) and the Western Treatment Plant (WTP). Biosolids have been stockpiled at these locations for over 25 years, due to the presence of contaminants and lack of viable disposal routes. Melbourne water has a philosophy that biosolids should be minimized, reused or recycled (Melbourne Water, 2014) so is seeking a way to reduce the amount of biosolids kept in stockpile.

There are several types of biosolids stored in Victoria, classified according to their treatment grade and contamination grade. Treatment grade ranges from T1 to T4, with T1 biosolids having been treated to the highest standards. Treatment grade is based upon the treatment process applied, the microbial content of the biosolids remaining under limits, and the steps taken to prevent bacteria regrowth and odour. For contamination grade, C1 is the least contaminated and C3 is the most contaminated. Contaminant grade is based upon the concentration of contaminants, such as heavy metals, in the biosolids, see section 2.3.1.1 for more information on contaminants.

Biosolids that are T1/C1 classification are suitable for "unrestricted use" and can be applied to land (includes agricultural use, forestry, composting, geotechnical fill, etc) with only basic handling and storage safety procedures. Biosolids with T2-T3/C2 grade are suitable for "restricted use" and can be applied to land provided appropriate management procedures are in place, such as limiting public access to the area or not applying the biosolids to crops that are consumed raw. Biosolids that have a C3 grade cannot be applied to land without special approval (EPA Victoria, 2004).

Biosolids that don't meet these treatment and contamination standards, or have no identified route of disposal, are stockpiled in Victoria. 95% of Victorian biosolids are stockpiled at locations at Eastern Treatment Plant (ETP) and Western Treatment Plant (WTP) in Melbourne. These biosolids fall three types;

- T1/C2 biosolids at the ETP stockpiles, totaling approximately 2 million dry tonnes (56% of stockpiles), being produced at a rate of ~40,000 dry tonnes p.a. Approximately 400,000 (11% of stockpiles) dry tonnes of these are unsuitable for agricultural use, due a high clay content, while the rest are suitable for restricted use.

- T1/C2 biosolids at the WTP stockpiles, the total amount of biosolids is less than 200,000 dry tonnes (6% of stockpiles) but the exact mass is not known. These biosolids have been produced only in recent years. These can be applied to land, with restrictions.

- T1/C3 biosolids at the WTP stockpiles, totaling approximately 1.57 million dry tonnes (44% of stockpiles). Biosolids of this contaminant grade are no longer being produced at WTP due to improvements in the treatment process. The biosolids currently produced at WTP are T1/C2 biosolids.

The T1/C1 and T1/C2 biosolids can be applied to land, provided the restrictions on their use are met. There is, however, a limitation imposed by the cost of transporting these biosolids, and the availability of end users, such as farms, construction sites, etc. If there are no appropriate nearby end-users, the cost of disposal is too high. The high clay content T1/C2 cannot be applied to agricultural land, and the T1/C3 biosolids are not suitable for any land application use.

Around the world there are three main fates of biosolids: land application (including use as geotechnical fill), incineration, and landfill (UN-Habitat, 2008). These established methods are not used for the Victorian biosolids. As discussed above, land application is unsuitable for the stockpiled biosolids, due to contaminates. Incineration is not performed in Australia due to the availability of land for biosolids disposal. Incineration comes with significant pollution and capital costs so is unlikely to be a solution for the Victorian stockpiles. Despite the low cost of landfill method, the Victorian EPA has indicated that it is unlikely that landfill will be considered an acceptable end use of biosolids. The aim of this project is to test MWAP as a disposal method for the T1/C3 biosolids and the T1/C2 biosolids that don't have a disposal

plan, representing about 50% of the stockpile or 1.8 million tonnes. MWAP presents an alternative option to these biosolid handling methods and produces valuable byproducts.

1.2 Background Information and Knowledge Gaps

Petroleum consumption is rising around the globe and renewable alternatives need to be found to reduce petroleum consumption and eventually provide a replacement. While primary use of petroleum is for heat and energy generation, an overlooked use of petroleum is also the manufacture of base petrochemicals, which are used in the plastics, chemicals and construction industries to manufacture a wide variety of essential products.

Biosolids contain volatile organic matter that can be thermally decomposed into fuels and chemicals using MWAP, providing a renewable source of fuel and petrochemicals while sterilizing and reducing the volume of the biosolids (Yin, 2012). In MWAP, the entire biomass is heated simultaneously and uniformly by a microwave field. The pyrolysis atmosphere and chamber have poor dielectric properties, meaning that little energy from the microwave field is used to heat them. Due to these advantages in efficiency, a great deal of work has been done exploring the MWAP of biosolids, producing fuels (Beneroso, Bermúdez, Arenillas, & Menéndez, 2014b; Tian, Zuo, Ren, & Chen, 2011) and petrochemicals (Lin, Chen, & Liu, 2012). Alkenes, alkanes, aromatics, fatty acids and ketones are potentially useful groups of compounds that have been detected in MWAP bio-oil (Dominguez, Menendez, Inguanzo, Bernad, & Pis, 2003; Omar & Robinson, 2014; Yin, 2012).

A wide range of biomass sources, including sewage wastes, have been used as MWAP feedstock (Yin, 2012). The biomass in this study was Victorian biosolids that had been stored for an extended period, from several months to greater than 5 years. Due to this age, they are different to fresh sewage wastes that were pyrolysed in previous studies. There is a knowledge gap in what would be the MWAP products from this feedstock, and what would be the value of MWAP. These aspects need to be assessed with the aim being to use MWAP to generate bio-oil from the stockpiled biosolids and safely dispose of the sewage waste.

It is also important to assess MWAP in an Australian context as Australia's geographical and social features, namely low population and large land area, make beneficial use of biosolids expensive with an average cost of $300 per dry tonne (Darvodelsky, 2012). Due to this cost, cheaper methods of beneficially using biosolids are important to Australia, and MWAP may be a candidate process.

A key part of this assessment requires the determination of the composition of the bio-oil to identify any potential products that could be extracted and how processing conditions affect their yield. Some studies report an excess of 100 compounds, as detected by Gas Chromatography-Mass Spectrometry (GC-MS) (Lin et al., 2012). For this reason, many studies have placed the identified compounds into sets based on functional group and structure of the compounds. A semi-quantitative method where the area of peak in a chromatogram is used to assess the proportions of the compounds (I. Fonts, Azuara, Lázaro, Gea, & Murillo, 2009). This approach may not accurate enough to assess the chemical value of the bio-oil.

1.3 Project Goals

There are 4 main goals to this research.

1. To develop the MWAP apparatus and experimental methodologies

To achieve the other goals an experimental methodology needs to be developed. The microwave unit provided by Melbourne University also needs to be modified to allow for instruments to be installed to monitor and record process variables.

2. To determine the bio-oil compounds produced from MWAP of stockpiled biosolids.

This goal aims to identify and quantify components of the bio-oil. As mentioned in section 1.2, most studies do not use standards to identify or quantify compounds in the bio-oil. For this study, a more accurate method is needed to determine the yield of the valuable compounds to properly assess the chemical value (*c.f.* Goal 3) of the bio-oil. In addition, developing a robust and reliable method for improving the analysis of MWAP bio-oil composition is a valuable contribution to the field of MWAP research.

3. To determine the influence of the key process variables on bio-oil yield, composition, and the energy consumption.

Testing the impact of the process variables on the bio-oil yield and composition enables the determination of the benefits of MWAP, through potential value adding. The energy consumption, and how it changes with process variables and the bio-oil production, is an important consideration as energy cost has a significant impact upon the economics of the MWAP.

4. To assess the cost effectiveness of MWAP of Victorian stockpiled biosolids in the broader Australian context.

Small amounts of research have been done on the economics of MWAP of biosolids and none that consider an Australian context. Most of the MWAP research is focused on the calorific content of the products of MWAP. A more complete analysis is needed to determine the costs of MWAP and how much value can be generated from the products, specifically the bio-oil. This project examined the economics of the MWAP of the stockpiled Victorian biosolids, as well as the economics of another biosolids source. The assessment of the other biosolids source was important to evaluate the applicability of MWAP to fresher biosolids. MWAP of fresh Victorian biosolids would prevent the stockpiles growing, or offer an alternative to existing treatment methods in other areas.

1.4 Project Methodology

To achieve project goals, the following methodology was used for each goal. The goals were successive and achieved in order.

Goal 1: To develop the MWAP apparatus and experimental methodologies

The following parts were used as the basis for the MWAP apparatus. An Altair 1200W Single mode magnetron, a Gerling Dual Directional coupler to measure forward and reverse microwave power, a magnetic recirculator to prevent reflected microwaves from damaging the magnetron, as well as the flanges needed to connect the components. A 1.17L stainless steel container was built to serve as the pyrolysis vessel. Figure 12 shows a block flow diagram of the pyrolysis system. The condensable pyrolysis gases were recovered by pumping them through condensers and a water trap, which were configured based on preliminary tests. Temperature was measured with a microwave compatible thermocouple (section 2.5.5.3) and an Arduino datalogging circuit (section 3.1.1) that allowed for a range of values to be viewed and plotted in real time in excel. The MWAP apparatus is shown in Figure 1 with main features labelled.
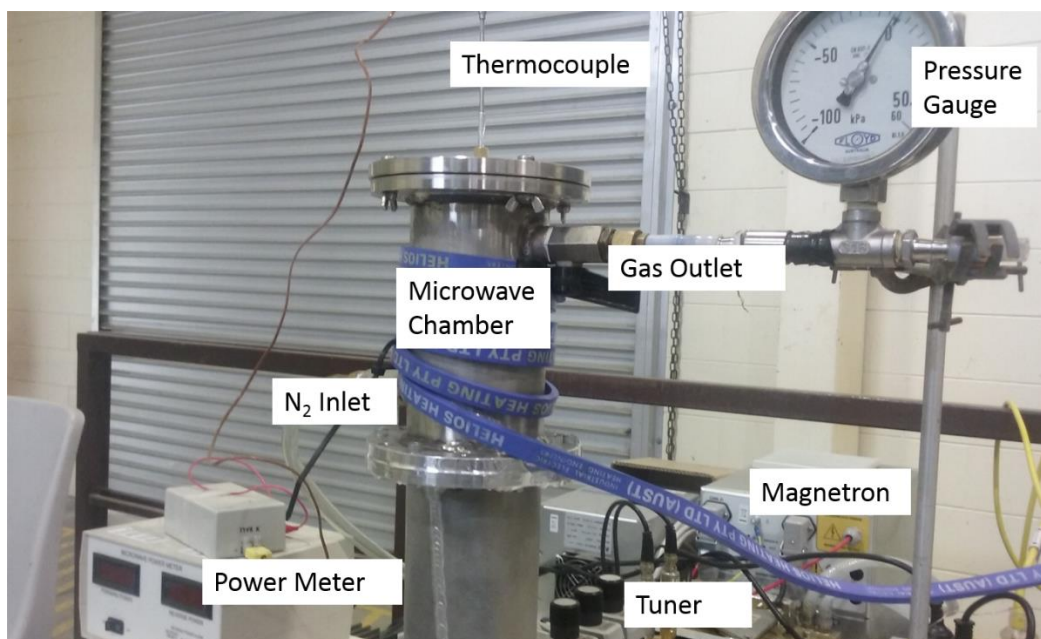
Figure 1. MWAP apparatus

See Table 6 for a full list of the MWAP apparatus and section 3.1 for a complete process description. The received biosolids were analyzed for volatile matter, moisture content, metals, and elemental composition. Methods were developed for preparing sample of biosolids and susceptor and readying the chamber for experiments. A full list of methods and materials is given in section 3.3.

Goal 2: To determine the bio-oil compounds produced from MWAP of stockpiled biosolids.

This project extended the methodology of Dominguez (Dominguez et al., 2003) that used GC-MS with database identification of compounds and peak area fraction to determine the proportion of each identified compound. As mentioned in section 1.2, there are a large number of compounds detected in bio-oils, which makes quantification of the entire range of components in the bio-oil a time-consuming task. However, many of the compounds detected in MWAP bio-oil are present in amounts less than 1% of the total amount of bio-oil (Dominguez, Menéndez, Inguanzo, Bernad, & Pis, 2003) and it is unlikely that their extraction would be feasible. After the composition of the bio-oil was assessed via GC-MS the compounds with the largest peak area fraction were quantified with Gas Chromatography – Flame Ionization Detection (GC-FID). External standards were used for the quantification and definitive identification of those compounds.

Goal 3: To determine the influence of the key process variables on bio-oil yield, composition, and the energy consumption.

Experiments were carried out to identify the impact of the process variables of temperature and pyrolysis time. The effect of aging was also tested on different biosolids. The experimental variables were monitored and recorded using the methods outlined in section 3.1. The produced bio-oils were analysed with the methodology used to fulfil Goal 1 and the mass losses and product distributions were calculated to determine the impact of the process variables.

Goal 4: To assess the cost effectiveness of MWAP of Victorian stockpiled biosolids in the broader Australian context.

With the data gathered from the pursuit of Goals 1 and 2, the monetary value of the quantified chemicals in the bio-oil was determined based upon the wholesale price of these chemicals and the typical profit margins from chemical sales. The monetary value of energy in the bio-oil was also calculated and compared to the chemical value in the bio-oil. There is additional value in the MWAP of biosolids, since it reduces their mass, lowering transport costs and converting the biosolids to biochar. The biochar has value as a phosphorus fertilizer and/or through the reduction of landfill costs. The value generated by different combinations of these options was examined and compared. The value generated was subtracted from the cost of the MWAP to determine the final cost. The cost of the MWAP includes the cost of the energy absorbed by the sample, the cost of the susceptor, and the cost of the nitrogen. When possible, Australian values were used for calculations.

2 Literature Review

The literature review collates the relevant background information on the difficulties in disposal of the Victorian biosolids with conventional methods, the alternative biosolids treatment options and consideration of MWAP as a potential biosolids treatment. Background information on the mechanism of microwave heating is presented, along with a comparison of MWAP to conventional pyrolysis, and what previous studies have learned about bio-oil composition and yield. The information here was used as a basis to design the experimental study on MWAP of the Victorian biosolids.

2.1 Background

Biosolids result from biologically stabilized and dewatered sludge produced by tertiary wastewater treatment processes. Historically, biosolids were recycled by applying them as a fertilizer substitute to agricultural land. Over the last two decades, this method of reuse has come under scrutiny as concerns have emerged over the risks of introducing pathogens, heavy metals and hazardous chemicals into the food chain. There are also social concerns about aspects such as odour and vermin (Pritchard, Penney, McLaughlin, Rigby, & Schwarz, 2010; Sidhu & Toze, 2009). For these reasons, it is important to identify a more suitable disposal route for biosolids.

A process that fulfils both the need of a renewable source of bio-oil and a suitable route for biosolids disposal is microwave assisted pyrolysis (MWAP). MWAP of biosolids and sewage sludge has been shown to produce energy dense liquid and gaseous products. The bio-oil produced by MWAP is also rich in petrochemicals (Yin, 2012). In addition to producing valuable resources, MWAP also sterilizes the biosolids and/or sewage sludge and greatly reduces their mass which allows for safer and more efficient handling (Hong, Park, & Lee, 2004; Menéndez, Inguanzo, & Pis, 2002).

Biosolids are produced from wastewater treatment plants. There are many different methods of wastewater treatment but most large-scale methods of sewage treatment can be broken up into four sections.

Primary Treatment: In the first stage of wastewater treatment large objects, sand, and other materials that could damage equipment further along in the process, are removed from the sewage influent via screening and/or other mechanical separation processes. (ESCWA, 2003).

Secondary Treatment: After primary treatment, the screened wastewater flows into a clarifier. Clarified sludge undergoes a biological digestion process. A wide range of options exist for biological treatment processes, but the aim of all of them is to utilize bacteria to break down the organic matter of the wastewater. After biological treatment the wastewater goes into a secondary clarifier where solids, termed 'activated sludge', are separated and pumped to sludge digestion (ESCWA, 2003).

Tertiary Treatment: Influent to the secondary clarifiers has the solid portion coagulated into flocs, separated and returned to the primary clarifiers. These separated solids are eventually treated in sludge digestion. The supernatant from the secondary clarifier is treated to meet the required standards for sewage effluent. A wide variety of processes including disinfection by chlorine, ozone or UV light, reverse osmosis and nutrient capture are used in this step. (ESCWA, 2003; Okuda et al., 2014).

Sludge Handling: The separated solids are stabilized in biological digesters. The purpose of this step is to reduce the amount of pathogens, prevent the waste fermenting, and minimize odour. The stabilized sludge is usually dewatered to some extent. The organic solid portion of this stabilized sludge is termed 'biosolids'(NRMMC, 2004; Turovskiy, 2000).
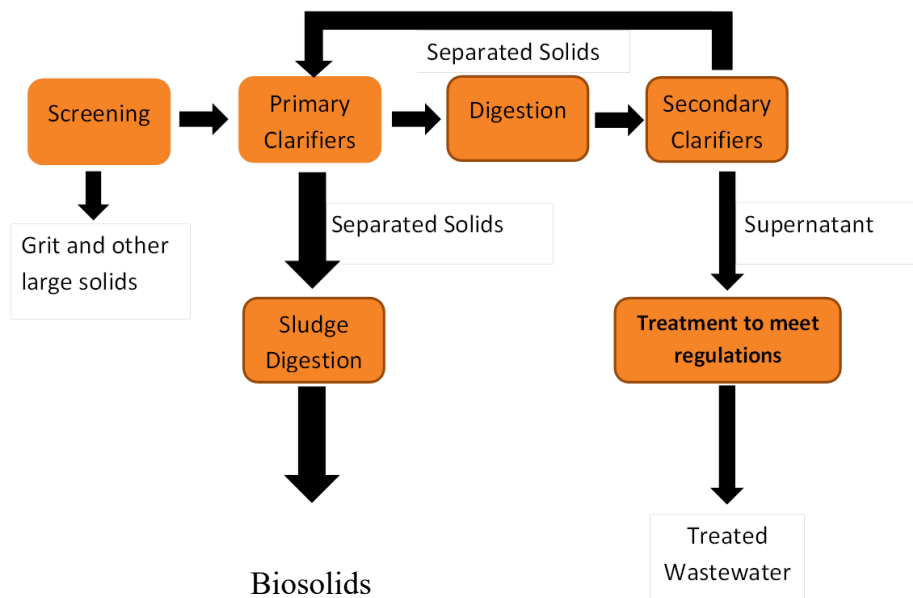
Figure 2. Block flow diagram of a wastewater treatment plant.

2.2 Biosolids Disposal in Australia

Australia produced 329,500 dry tonnes of biosolids in 2012-13, with a typical moisture content of 60-90%, corresponding to 1.32 million wet tonnes of biosolids (Darvodelsky, 2012; Department of the Environment AUS, 2013). The distribution of biosolids end use in Australia is shown in Table 1.

Table 1. End use of biosolids in Australia (dry tonnes/yr), adapted from (Department of the Environment AUS, 2013)

Region	Land Application	Landfill	Ocean Discharge	Stockpile	Unspecified/ Other	Total
NSW & ACT	73434 (75%)	1500 (1.5%)	3942 (4%)	239 (0.2%)	19017 (19.3%)	98131
QLD	64819 (92%)	2961.5 (4%)	-	-	2391.5 (4%)	70172
SA	30477.5 (100%)	-	-	-	-	30477.5
TAS	3466 (51%)	3359.5 (49%)	-	-	-	6826
VIC	33269 (35%)	-	-	62051 (65%)	317 (0.3%)	95637
WA & NT	22447.5 (79%)	2875 (10%)	-	2935 (11%)	-	28257
National	227913 (69%)	10695 (3%)	3942 (1%)	65225 (20%)	21725 (7%)	329500

As can be seen from the above Table 1, 69% of Australian biosolids are disposed of via land application, 20% are in storage and the remaining 11% is either dumped to landfill or the ocean or unknown. Globally, the most common biosolids disposal methods are land application, incineration and landfill, shown in Figure 3 for some regions.
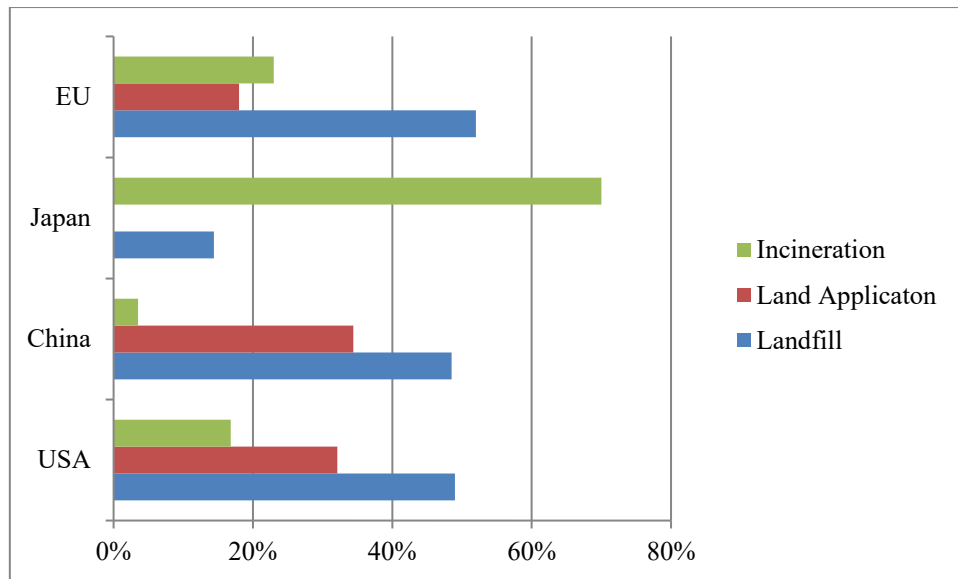
Figure 3. Global biosolids disposal methods, compiled from (UN-Habitat, 2008)

2.3   Current Biosolids Disposal Methods

This section will examine the three globally dominant methods of biosolids. Land application, landfill and incineration, what are the pros and cons of each method, and how they can be applied in the Victorian context (Isabel Fonts, Gea, Azuara, Ábrego, & Arauzo, 2012).

2.3.1   Land Application

Land application of biosolids is by far the most common method of biosolids disposal in Australia as it utilizes the nutrient content of biosolids and is simple to implement. Land application incorporates applying biosolids directly to farmland (agricultural), applying biosolids as a composted mixture with other green waste (Key, 2005) and applying biosolids to improve soil properties, such as porosity (Navas, Machín, & Navas, 1999). Typical Australian biosolids contain 2% and 0.9% dry weight of nitrogen and phosphorus, respectively. The value of the total nutrients in biosolids is 40-140 $/tonne on a phosphorus content basis (Darvodelsky, 2012), however, not all of the nutrients can be utilized by plants (are *bioavailable*). A 2008 paper by The National Biosolids Research Program (NBRP) conservatively estimates the value of Australia's biosolids to be about $11/dry tonne (McLaughlin et al., 2008). This estimate accounts for the fact that not all the nutrients in biosolids are plant available, nor are all of the available nutrients taken by the plant due to leaching, and possibly gas-phase emissions. It should be noted that both the Darvodelsky and NBRP estimates only consider the phosphorus and nitrogen content of the biosolids.

Biosolids contain other macronutrients such as potassium and micronutrients such as copper and magnesium (Department of the Environment AUS, 2013). The carbon content of biosolids also has been shown to improve soil quality properties (García-Orenes et al., 2005). These additional benefits are shown in the NBRP paper where three farms are reported to have benefited from biosolids application of $7.68, $12.54 and $5.38 per wet tonne. With an assumption of 75% moisture content, this is equivalent to a value per dry tonne of $30.72, $50.16 and $21.52 (McLaughlin et al., 2008). These findings demonstrate applying biosolids to agricultural land can be an effective method of beneficial reuse.

2.3.1.1 Issues with Land Application

Cost: The cost is generally between $150-$500 with the average cost being $300 with transportation accounting for 70-90% of this cost (Darvodelsky, 2012). The benefits of the land application of biosolids is far less than the cost of this method. However, the cost of transportation is reduced the more the biosolids are dewatered onsite.

Contaminants: Biosolids can contain contaminants that pose a risk to the health of the environment and community when the biosolids are applied to land. Some common classes of contaminants present in biosolids that have been examined in literature are;

Pathogens; e.g. *Salmonella, Giardia*, noroviruses.

As biosolids are derived from sewage sludge, pathogens are still potential hazards even after the sludge has been stabilized. Tests by the NBRP found that numbers of indicator microorganisms decreased over time and the chance of transmission to humans through grain crops was unlikely. The pathogenic risk of biosolids can be further reduced if the biosolids are composted before being applied (Pritchard et al., 2010).However, diversity in pathogens present in biosolids as well as the of lack data on many of these pathogens a definitive assessment of the pathogenic risk cannot be made (Sidhu & Toze, 2009)

Heavy metals; e.g. copper, zinc

Research has shown that even when biosolids are applied at rates far higher than recommended (based on nitrogen requirements of the soil) heavy metal concentrations in the soil were still below the allowable limit. This research suggests that the heavy metal limits in biosolids are over-regulated, even in acidic soils that have a higher uptake rate of metals. Biosolids could safely be applied at 450% of the recommended rate for the biosolids examined in one study (Pritchard et al., 2010).

Chemical; e.g. persistent organic pollutants (POPs) and pharmaceutical and personal care pollutants (PPCPs)

POPs are organic compounds that resist degradation by photolytic, chemical and biological means. They also display low water solubility, but high lipid solubility. These characteristics cause POPs to have a year's long half-life in soil (exact half-life varies between POPs) and have a high rate of bio-accumulation. PPCPs are a broad category of chemicals that encompasses any chemicals used for personal hygiene or cosmetic purposes. A recently identified health risk, PPCPs have a shorter half-life than POPs, but this shorter half-life is compensated by their higher rates of introduction to the environment through domestic wastewater where pharmaceutical and personal care products are frequently used (Clarke & Cummins, 2014). As domestic wastewater is the source of many of Australia's biosolids (Pritchard et al., 2010), PPCP contamination may be a risk of biosolids land application.

2.3.2 Incineration

Incineration is one method of biosolids/sludge disposal that is unused in Australia, but is common in countries where available land is limited. Sewage sludge and biosolids can be mono-incinerated when the water content is low enough, while wetter sludge or biosolids can be co-incinerated, often with municipal solid waste (Lin & Ma, 2012). Incineration has several key advantages as a wastewater treatment technology;

- Reduces the volume by occupied in landfill by roughly 70% compared to disposal of biosolids directly into landfill (Isabel Fonts et al., 2012)
- A life cycle assessment, or LCA, conducted on sewage sludge in 2005 found that incineration technologies have a smaller cradle-to-grave global warming potential than land application, due to the oxidation of high global warming potential gases such as methane, which are emitted during land application. For the sludge considered in the LCA, land application produced approximately 480 kg CO_2eq./dry tonne while incineration in a fluidized bed produced 180 kgCO_2equiv/dry tonne. Incinerating the sludge in a cement kiln to produce klinker further reduced the emissions by approximately 50 kg CO_2eq./dry tonne (Houillon & Jolliet, 2005).
- The combustion can be used to produce heat and power to offset the cost of incineration. The energy content of biosolids/solid portion of sewage sludge is around 16-21 MJ/dry kg, which is comparable to that of brown coal at 10-20 MJ/ dry kg. In the European Union, dried sewage sludge has been used as fuel for coal fired power

stations (Mills, Pearce, Farrow, Thorpe, & Kirkby, 2014). However, the heating duty of the combustion is increased by the often >50wt% water content of the material (Murakami et al., 2009).

- Nutrients such as phosphorus can be recovered from the ash produced in biosolids incineration through chemical processes. For example, in the Bio-con process the ash and slag are dissolved in sulfuric acid and pass through a series of ion exchangers before the phosphorus collected as phosphoric acid via hydrochloric acid regeneration (Lundin, Olofsson, Pettersson, & Zetterlund, 2004). These technologies have yet to see full scale testing (Egan, 2013).

2.3.2.1 **Issues with incineration**

While incineration is a common method of biosolids disposal around the world (Figure 3) it has several disadvantages.

Moisture content: The efficiency of thermal treatment processes of biosolids or sewage sludge, including incineration, depends upon the efficiency of the drying method. High moisture content feedstocks have a low net calorific value, which lowers the net energy recovery from the process (Houillon & Jolliet, 2005).

Ash: The volume reduction during incineration concentrates the heavy metals present in biosolids. Shown in Table 2 below, adapted from Cyr *et al.* (Cyr, Coutand, & Clastres, 2007) is the heavy metal content of incineration ash from sewage sludge ash.

Greenhouse Gases: The combustion gases of sewage incineration contribute to global warming and air pollution.

Table 2. Heavy metal content of incineration ash (Cyr et al., 2007)

Element mg/kg	As	Ba	Co	Cr	Cu	Pb	Sn	Zn
Min. from literature	0.4	90	19	16	200	93	539	1084
Mean from literature	87	4142	39	452	1962	600	539	3512
Max from literature	726	14600	78	2100	5420	2055	539	10000
From Cyr et. Al.	23	1430	669	2636	2483	720	623	7103

The cleaning and disposal of this ash can be costly and require special landfill sites (Lin & Ma, 2012). Work has been done to find a recovery method for the incineration ashes, though few full-scale processes exist. Identified methods include;

- Sintering the ash into pavers, bricks and ceramics (Donatello & Cheeseman, 2013)
- Acid leaching phosphorus from the ash (Donatello & Cheeseman, 2013)
- Using biosolids ash in lieu of fly ash as an adsorbent to remove copper from wastewater, removal rates of 98% have been achieved with this process (Pan, Lin, & Tseng, 2003)
- Using the ash as an additive in cement (Cyr et al., 2007)

2.3.3 Landfill

One of the key advantages of landfill is that it is inexpensive and simple (Kim & Owens, 2010). In many jurisdictions biosolids can be disposed in existing municipal solid waste (MSW) facilities. There is also the potential to recover energy from the landfill disposal via landfill gas (LFG) recovery technology. During the anaerobic decomposition of biosolids or other organic wastes by microbes, LFG is produced. LFG is a varying mix of gases, usually consisting of between 35-55% methane, 30-44% CO_2, 5-25% N_2O and a small amount of other gases (Clarke Energy, 2014). Methane has a gross calorific value of 39.82 MJ/m and

methane recovered from landfill is used for energy production around the world, including Australia (SITA Australia, 2010). This technique of landfill resource recovery is more effective in landfill where both biosolids and municipal solid waste are landfilled together. A study of biosolids stockpiles in Victoria found that biosolids on their own produce small amounts of methane when compared to CO_2 and N_2O, due to the predominately aerobic reaction conditions (Majumder, Livesley, Gregory, & Arndt, 2014).

2.3.3.1 Issues with landfill

Landfill is a waste disposal practice that has significant disadvantages. This section however will focus on the issues resulting directly from landfill of biosolids.

Greenhouse gas emissions: The Victorian study that tracked emissions from stockpiled biosolids of different ages, found that biosolids emit 10,000-60,200 CO_2 equiv kg .yr^{-1}, although the amount of greenhouse gases emitted per tonne of biosolids decreased with the age of the biosolids, reaching a minimum after around three years (Majumder et al., 2014). Most of the gaseous emissions were unusable gases, such as CO_2 or N_2O.

Landfill space usage: Biosolids have a low bulk density which causes them to occupy a large amount of landfill space per unit mass. Disposal of biosolids to landfill is becoming increasingly costly as available landfill space decreases (AWA, 2012).

2.4 Pyrolysis

2.4.1 Pyrolysis Fundamentals

Pyrolysis is the thermal decomposition of organic matter at high temperatures in an oxygen-free environment, producing three product types; biochar, bio-oil and gas (Houillon & Jolliet, 2005). The ratio and composition of the product types depends upon the mode of pyrolysis used (Bridgwater, 2012). Pyrolysis processes can be categorized based on the values of the process parameters, a description of several major modes of pyrolysis and the obtained product distribution is shown in Table 3.

Table 3. Comparison of pyrolysis modes, data from (Bridgwater, 2012; Yin, 2012)

Mode	Temperature	Heating Rate*	Vapour Residence Time	Product Yield Distribution
Carbonization	300-500ºC	Very Low	Hours - Days	Biochar=Gas>Bio-oil
Slow Pyrolysis	400-900ºC	Low	Minutes - Hours	Biochar=Gas>Bio-oil
Intermediate Pyrolysis	400-600ºC	Moderate	10-30 seconds	Bio-oil>Gas>Biochar
Fast Pyrolysis	500-3000ºC	High	<2 seconds	Gas>Bio-Oil>Biochar

*There is a lack of definition about what constitutes a high or low heating rate, (Yin, 2012) recommends that heating rates >10ºC/s be considered a high heating rate. 1°C/s to 10°C/s considered medium, others slow.

The general trends that can be deduced from Table 3 are; as the temperature increases the product distribution shifts from biochar →bio-oil→gas and as vapour residence time increases the product distribution shifts from gas→bio-oil→biochar.

2.4.2 Pyrolysis for wastewater treatment processing

Pyrolysis is an emerging technology for WWTP and the most researched application for pyrolysis in this area is bio-fuel production from the biosolids/sludge. Due to the oxygen-free environment, functional groups that would otherwise be oxidized in an incinerator, will be preserved in the bio-oil product. Pyrolysis produces bio-fuel at a very high fuel-to-feed ratio, making it one of the most efficient thermal processes for bio-fuel production. Certain fractions of the produced bio-oil display high gross calorific values of between 30-40 MJ/kg and, as a whole, the bio-oil has a gross calorific value of around 17 MJ/kg. The bio-oil is also able to be stored and transported for use offsite (Isabel Fonts et al., 2012; L. Zhang, Xu, Champagne, & Mabee, 2014). In addition to bio-fuel production some other benefits of the pyrolysis process are;

- Heavy metals and other inorganics found in biosolids and sewage sludge are better incorporated into the biochar than they are in incineration ash, making the biochar more environmentally benign than incineration ash (Mills et al., 2014). The only

heavy metals that are detected in the bio-oil or gas portion of the products are volatile metals such as cadmium and mercury (Isabel Fonts et al., 2012).

- An LCA carried out by Mills *et al.* (Mills et al., 2014) found that pyrolysis, when integrated into a wastewater treatment process, could be used to produce syngas for combined heat and power generation (CHP) from biosolids, which improved the energy efficiency of the process and produced only biochar as a by-product. Wetter sludge is somewhat advantageous in this process, since the syngas produced from this process has a higher hydrogen content than that produced from dry sludge, but the higher water content in the feedstock increases the required heating duty (Domínguez, Menéndez, & Pis, 2006).

2.4.2.1 **Issues with pyrolysis**

Pyrolysis technology has had some commercial success with plants in Europe and Asia and research is continuing in this field. However, pyrolysis does not have the same level of implementation as the previously mentioned disposal methods. The general issue with pyrolysis of sewage sludge is that it lacks full scale implementation, as well as markets for the products (Jahirul, Rasul, Chowdhury, & Ashwath, 2012). In addition, there is a need to upgrade the pyrolysis products before they can be used as a complete replacement for non-renewable products (Isabel Fonts et al., 2012).

Bio-fuels often contain water, small particulates and have a different composition to conventional fuels, causing them to have different combustion characteristics to conventional fuels. The quality and composition of bio-fuels also depends upon the composition of the feedstock which varies between WWTPs. These factors present a barrier to using bio-fuels in engines that are designed to operate using conventional fuels. Before bio-fuels can be used in to power these engines an upgrading process needs to be designed to produce a fuel of consistent composition and quality. The gases also need to be scrubbed and dried before use (Beneroso et al., 2014b). One method that has been examined is upgrading the products via pyrolysis or gasification at a central facility from decentralized bio-oil producing facilities (Jahirul et al., 2012).

2.5 **Microwave Assisted Pyrolysis**

MWAP is similar to conventional pyrolysis in that organic matter is heated to high temperatures in an oxygen-free environment; the key difference is that MWAP uses dielectric heating, generated via applying a microwave field, instead of conventional heating.

2.5.1 Generating a microwave field

A microwave field is generated using a magnetron, shown in Figure 4.
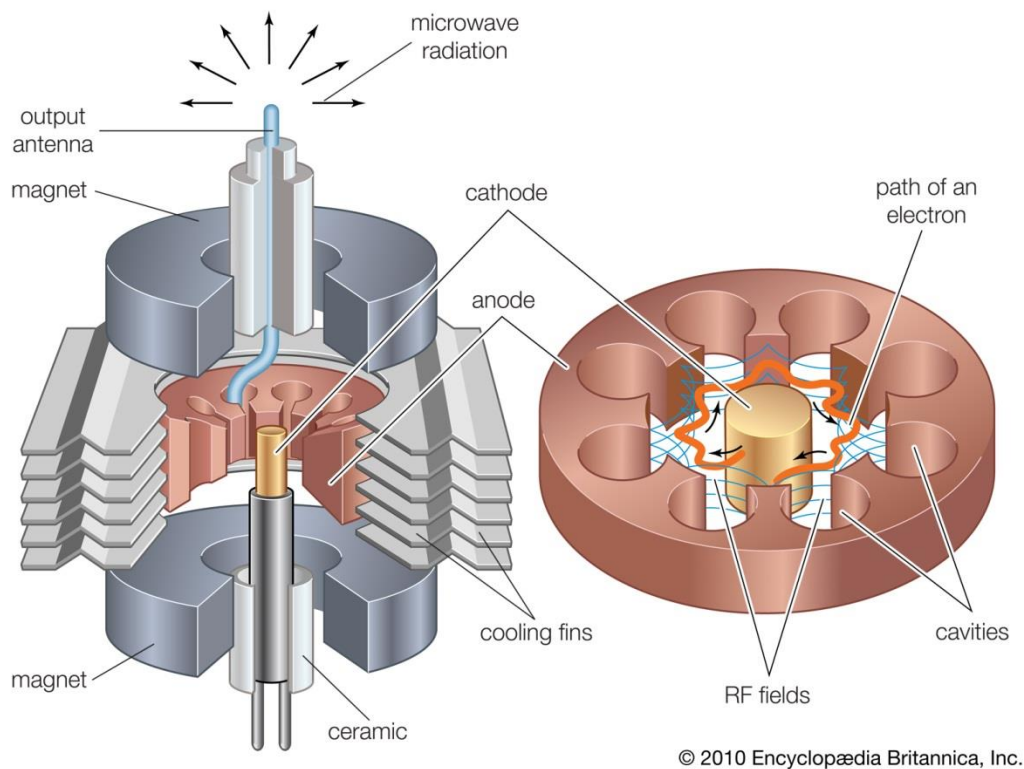
Figure 4. Schematic of a magnetron (Britannica, 2014)

A heated cathode emits electrons that are attracted to the anode. Simultaneously, the magnet is producing a magnetic field perpendicular to the electrical field, attracting the electrons to the anode. The two forces cause the electrons to curve towards the anode at varying angles, depending upon their emission velocity. As they pass the resonant cavities in the anode they induce a radio frequency (r.f.) field on the edges of the resonant cavity. This r.f. field then slows or accelerates the electrons. This causes areas of positive and negative charge to build up on the anode, when excessive negative charge builds up in an area of the anode, the charge shifts around the cavity at a frequency that depends upon the cavity design. As the charge shifts, electromagnetic radiation in the form of microwaves is emitted. A waveguide (not shown) is used to direct the microwave field and a filter box (not shown) prevents reflected microwaves from damaging the magnetron (Beverly Microwave Division; Nave. R, 2014).

2.5.2 Fundamentals of MWAP

To understand how microwaves heat materials a background of the mechanisms of dielectric heating is necessary. As great deal of work has been conducted on this topic only a brief background will be presented here.

Microwaves are electromagnetic radiation with frequencies between 300 MHz and 300 GHz. For domestic and industrial microwaves the most commonly used frequencies are the ISM bands centred on 0.915GHz and 2.45GHz (Datta, 2001).

Materials can be classed into three categories, based on their behaviour when placed in a microwave field.

1. Insulator; the material does not interact with the microwave field and microwaves pass through unimpeded
2. Conductor; the material reflects microwave radiation
3. Susceptor; the material absorbs energy from the microwave field

Microwave susceptors absorb microwave energy and convert it to thermal energy through two mechanisms; dipole polarization and Maxwell-Wagner polarization (Fernandez, Arenillas, & Angel Menendez, 2011). In dipole polarization, the dipoles of the susceptors, which can be pre-existing or induced by the microwave field, continuously realign with the oscillating microwave field. As this realignment matches the frequency of the microwaves the dipoles are realigning 2.45 billion times/second (2.45GHz). This motion causes the dipoles to rotate and generate heat from intramolecular resistance to this rotation. This is shown in Figure 5.
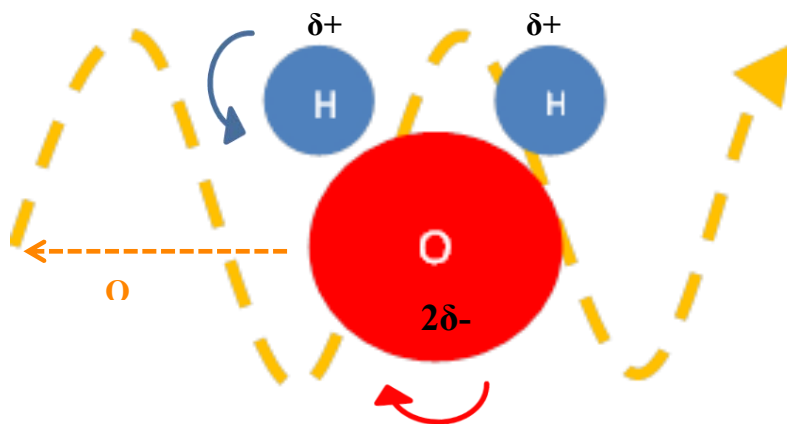
Figure 5. Dipole Polarization of a water molecule; heat (Q) is released due to molecular friction caused by the rotating water molecule.

Maxwell-Wagner polarization occurs at the boundary between materials with different dielectric properties or within susceptors where electrons are free to move within the electron cloud of the susceptor. This is shown in Figure 6. Carbon is a good example of this effect. When charged particles in the material are unable to follow the oscillation of the electric field of the microwave, this causes a charge to build up at the boundary of the particle and heat is released due to the effect (Fernández, Arenillas, & Menéndez, 2011).
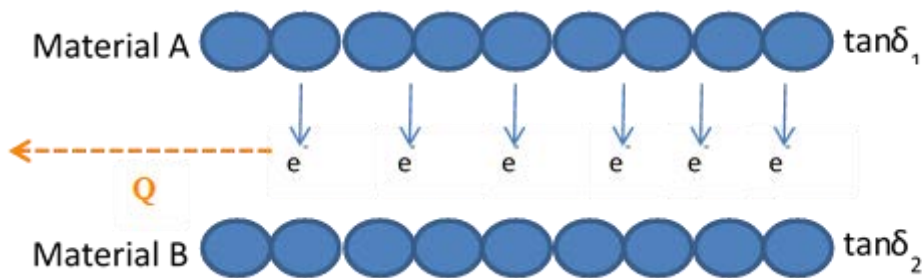
Figure 6. Maxwell-Wagner polarization; heat (Q) is released due to a build-up of charge between two materials with different tangent loss factors.

The effectiveness of a susceptor is given by the dissipation factor, tanδ;

$$\tan \delta = \frac{\epsilon''}{\epsilon'}$$

(1)

where; ϵ' is the dielectric constant, which indicates how well the material can be polarized by the microwave field; ϵ'' is the dielectric loss factor measures the efficiency of the conversion of electromagnetic to thermal energy by that material, the higher the tan δ of a material the better its dielectric properties (Sturm, Verweij, Stankiewicz, & Stefanidis, 2014).

The inherent tan δ of the organic component of biosolids is very low; dry biosolids tested had a tangent loss factor of essentially zero at a frequency of 2.45GHz. Wet biosolids can be heated via microwave pyrolysis, but this is due to the dielectric properties of water rather than the biosolids. Once the water is removed the biosolids cannot be heated well. To overcome the poor dielectric properties of biosolids, a microwave susceptor needs to be mixed into the biosolids to act as a heat source (Y Yu, J Yu, B Sun, & Z Yan, 2014). When susceptor material is uniformly distributed throughout the biosolids and in sufficient quantity, the heating of the mixture is similar to that of a material with inherent dielectric properties. Thus,

bulk of the material is heated by the microwave field. In this case though, the heat is generated by dielectric heating of the susceptor, which transfers heat via conduction to the surrounding biosolids. Some microwave susceptors that have been used in past works are: the biochar remaining after biosolids pyrolysis (Dominquez, Fernandez, Fidalgo, Pis, & Menendez, 2009), various metallic oxides (Y Yu et al., 2014) and many carbonaceous materials (Menedez et al., 2010).

2.5.3 Comparison of Conventional Pyrolysis and MWAP

Many similarities exist between MWAP and conventional pyrolysis. Both are carried out in an oxygen-free environment and have solid, liquid and gaseous products. The effects of the mode of pyrolysis used are also comparable between the two processes, such as a high pyrolysis temperature producing a high yield of gas (Domínguez, Menéndez, Inguanzo, & Pis, 2005). However, the heating behaviour and composition of the product portions differ.

2.5.3.1 Heating comparison

The dielectric heating in MWAP produces different heating effects to conventional pyrolysis, presented in Table 4 below.

Table 4. Comparison of MWAP and conventional pyrolysis, adapted from (Fernandez et al., 2011; Tyagi & Lo, 2013; Yin, 2012)

	Microwave Pyrolysis	Conventional Pyrolysis
Heating mechanism	Energy conversion of electromagnetic to thermal via dielectric heating. Heat from the susceptor is then transferred to the biosolids via conventional heating mechanisms Figure 7.	Transfer of thermal energy via convention, conduction and radiation from heating element through the pyrolysis oven cavity to the feedstock. See Figure 7 below for a visual representation.
Heating rate	The entire material is exposed to the microwave field at the same time; the heating rate at any given point in the material is determined both by the dielectric properties of that point and the heat transfer to adjacent points. In a homogenous material, the heating rate is the same throughout the material.	Heating occurs from the surface of the material, inwards and is limited by the thermal properties of the material and the pyrolysis atmosphere. This causes the process to require time before the heating rate is the same throughout the material.

Heating dependence on material	The effectiveness of MWAP heating depends heavily on the dielectric properties of the material. Insulators and conductor materials cannot be effectively heated in a microwave field.	Limited by material properties, but all materials can be heated by conventional pyrolysis to some extent.
Control	Heating stops/starts immediately when the magnetron is turned off or on. The heating rate can rapidly increase as biochar is produced. The biochar acts a susceptor itself, increasing the heating rate.	As the surroundings and the heating element are still hot the samples cooling is slowed down by thermal inertia.
Efficiency	As dielectric heating effects heat the sample directly, the heat loss due to convection and conduction are minimized.	Energy losses during the transfer of heat from the element, through the pyrolysis cavity and to the centre of the sample, due to convection and conduction.
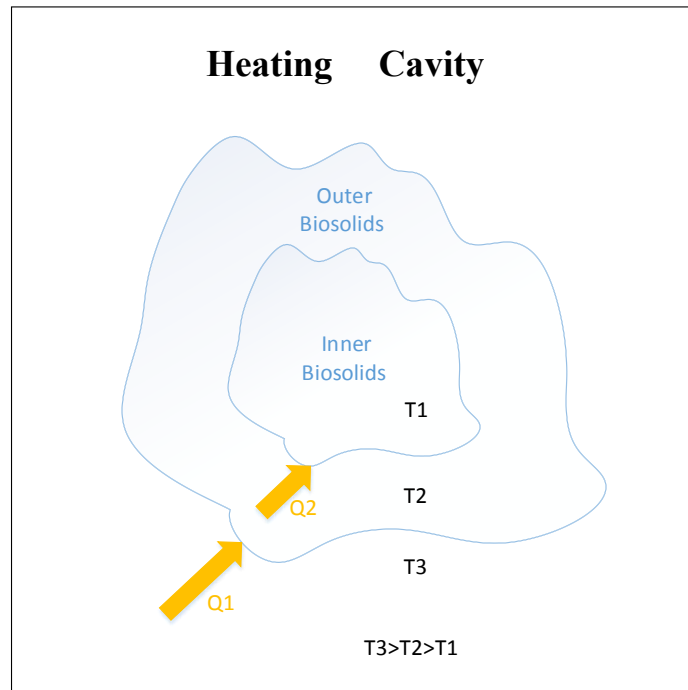
Figure 7. Conventional heating; the heat (Q1), is transferred from the heating cavity to the surface of the biosolids, the heat is transferred from the surface of the biosolids to the sample core (Q2).
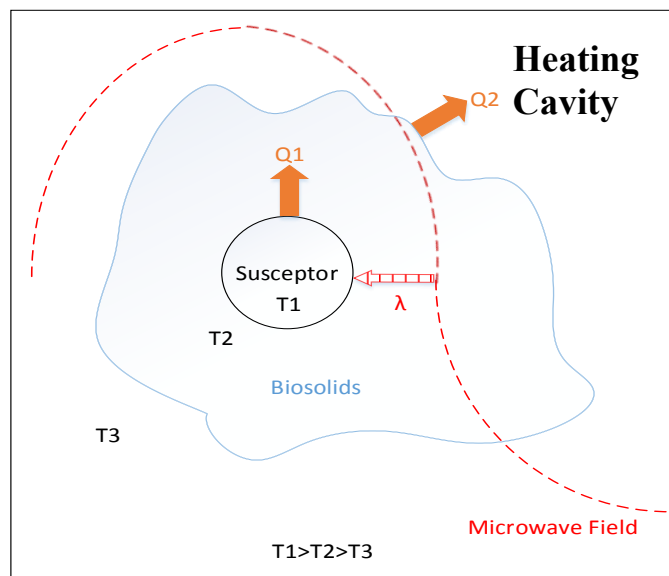
Figure 8. MWAP heating; the microwave energy (λ) is absorbed by the susceptor which re-emits it as heat (Q1) to the biosolids sample, the heat is transferred from the surface of the biosolids to the heating cavity (Q2).

2.5.3.2 **Comparison of products**

Numerous works have studied the products of MWAP compared to conventional pyrolysis, which is summarized in Table 5. The work in the third row used coffee hulls instead of sewage sludge but was included as it compared conventional and microwave pyrolysis.

Table 5. Studies comparing MWAP products to conventional pyrolysis products

MWAP products	Conventional pyrolysis products	Reference
• Produced bio-oils were highly aliphatic • H_2+CO concentration in the gas portion was 59.4-66.4% • Low amounts of hydrocarbons in gas portion • Gross calorific value of gas portion ranged from 7.43-9.52MJ/m^3 • No hazardous polycyclic aromatic hydrocarbons (PAHs) detected in products	• Produced bio-oils contained a large amount of aromatic hydrocarbons including PAHs • H_2+CO concentration in gas portion was 45.1% • Roughly double the amount of hydrocarbons in gas portion when compared to MWAP. • Gross calorific value of gas portion was 13.85MJ/m^3 due to the additional hydrocarbons	(Domínguez, Menéndez, Inguanzo, & Pís, 2006)
• Many of the functional groups of the sludge feedstock remained in the bio-oil after the pyrolysis • Some produced bio-oils had a large amount of mono-aromatic hydrocarbons but no heavy PAHs • The bio-oils where more highly oxygenated than those in conventional pyrolysis	• Secondary cracking reactions destroyed many of the functional groups present in the sludge • Other secondary reactions lead to the formation of heavy PAHs	(Domínguez et al., 2005)
• The H_2 concentration in the produced gas was between 35.6-40% and the combined (H_2+CO) was 61.4-72.8% of the gas fraction • Similar to sewage sludge syn-gas the coffee hull, MWAP produced syn-gas had lower concentrations of other hydrocarbons and CO_2 but a lower gross calorific value	• The H_2 concentration in the produced gas was 9.3-27% and the combined (H_2+CO) was 29.9-53.9% of the gas fraction • The yield of gas product was lower but the yield of bio-oil was higher at 11.2-13.6% compared to 7.9-9.2%	(Domínguez et al., 2007)

• The gas product yield was higher for MWAP at 61.9-68.2% compared to 57.2-66.6%		
• Produced bio-oils were less dense and less viscous than conventional pyrolysis bio-oil for power levels <600W • Bio-oils produced at <800W had a HHV of 28- 37MJ/kg • Bio-oils produced had a monoaromatic HC concentration of 15.5-29.5% • Bio-oil PAH content was between 6-7% • Oxygen content was between 0.015-0.024% • N-alkane content was between 14-21%	• Bio-oils were denser and more viscous than MWAP bio-oils produced at >600W power • Bio-oils had a HHV of 30MJ/kg which is greater than the 28MJ/kg of MWAP bio-oils produced at >800W • Bio-oil contained 12% monoaromatic HCs • Bio-oil PAH content was 9% • Bio-oil Oxygen content was 0.027% • N-alkane content was 16% and was higher than MWAP bio-oils produced at >800W	(Tian et al., 2011)

As can be seen from Table 5 the general differences between the products of MWAP and conventional pyrolysis are:

- H_2+CO concentrations are higher in MWAP gas

- PAH concentrations are lower in MWAP

- MWAP preserves the functional groups found in the feedstock

- Monoaromatics yields are higher in MWAP

- MWAP bio-oils are more highly oxygenated and aliphatic

- At higher temperatures, conventional pyrolysis produces bio-oils with a higher calorific value and greater alkane content

Bio-oils produced via MWAP contained a greater range of compounds than those produced by conventional pyrolysis and preserved the functional groups. So MWAP bio-oil may be better for chemical recovery. Conventional pyrolysis produced greater amounts of bio-oil, with higher energy content, but the bio-oil contained a greater proportion of toxic PAHs.

2.5.4 Microwave Assisted Pyrolysis Process Variables and their Effects

This section provides the key findings of previous projects on the impact of MWAP process variables. The process variables covered in this section are the most common process variables studied.

2.5.4.1 Temperature

Temperature is an important process variable for MWAP, it has both a great impact on the products formed, and is easily controlled via the magnetron power output. Thermogravimetric (TG) analysis of sewage sludge/biosolids pyrolysis shows three main stages of mass loss during the pyrolysis process (see Figure 9) shows typical TG and differential thermogravimetric (DTG) curves obtained from pyrolysis (Dai, Jiang, Wang, Chi, & Yan, 2013).

Drying: In the temperature range 41-167°C the free and bound moisture is removed from the sample (Dai et al., 2013).

Organic decomposition: In the temperature range of around 200-600°C, for different sludge or biosolids (Beneroso et al., 2014b), the organic compounds such as dead bacteria and cellulose decompose to form volatiles. This organic decomposition can be broken into two distinct steps (Jindarom, Meeyoo, Rirksomboon, & Rangsunvigit, 2007). The first step is the decomposition of long chainlike molecules such as aliphatic hydrocarbons and cellulose, while the second step is the decomposition of complex structures and aromatics (Neves, Thunman, Matos, Tarelho, & Gómez-Barea, 2011).

Inorganic decomposition: A slight weight loss is observed at temperatures greater than 800°C, which is attributed to the decomposition of inorganic compounds, such as phosphates (J. Zhang, Tian, Zhu, Zuo, & Yin, 2014).
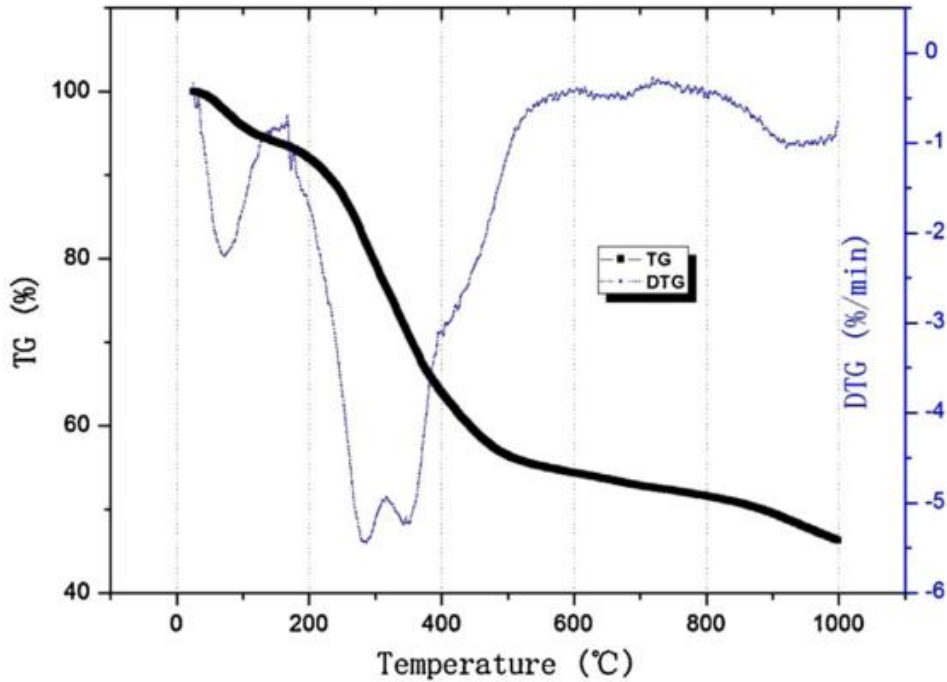
Figure 9. TG and DTG of sewage sludge pyrolysis- taken from (Dai et al., 2013)

As mentioned in Table 3, the distribution of pyrolysis products tends to shift to gas > bio-oil > biochar as the temperature increases. Three recent studies report the maximum bio-oil yield to occur at 490°C (Tian et al., 2011), 500°C (J. Zhang et al., 2014) and 550°C (Xie et al., 2014). It should be noted that this temperature range for maximum bio-oil yield is similar to that for conventional pyrolysis which is reported as 450-550°C (Isabel Fonts et al., 2012). It was also reported that above the temperature of maximum bio-oil yield the bio-oil yields decreased while the gas yields increased, likely due to secondary cracking reactions down to a minimum bio-oil yield at 800°C. At temperatures higher than 800°C, the biochar undergoes cracking reactions, increasing the gas yield further while decreasing the biochar yield (Tian et al., 2011).

2.5.4.2 **Moisture Content**

The moisture content of the MWAP feedstock is important as higher moisture content impacts the process by increasing the heat duty as well as lowering the organic content per unit mass of feedstock. It has also been shown to have an impact on the products of the process by causing certain reactions to be favoured.

In syn-gas production, moisture content has been shown to affect gas yields and composition. The reactions that have been found to be significant have been provided below (Beneroso, Bermúdez, Arenillas, & Menéndez, 2014a):

$$C + H_2O \leftrightarrow H_2 + CO \qquad \Delta H^0 = 131 kJ.mol^{-1} \tag{2}$$

$$C + 2H_2O \leftrightarrow 2H_2 + CO_2 \quad \Delta H^0 = 90 kJ.mol^{-1} \tag{3}$$

$$CH_4 + 2H_2O \leftrightarrow 3H_2 + CO \quad \Delta H^0 = 205 kJ.mol^{-1} \tag{4}$$

$$C_nH_m + nH_2O \leftrightarrow \left(\frac{n+m}{2}\right)H_2 + nCO \tag{5}$$
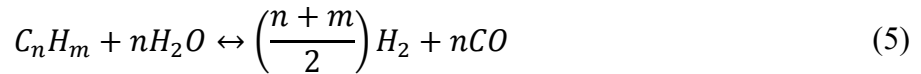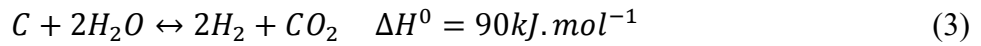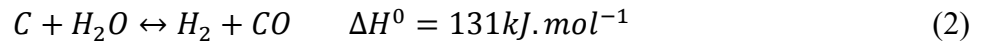
The rapid heating of the entire sample in MWAP (J. Zhang et al., 2014) allows the moisture to come into contact with the produced volatiles, allowing the above reactions to occur. Equation (4) and (5) are the likely reason for syn-gas produced via MWAP to have lower hydrocarbon content, but a higher H_2 content than syn-gas produced in conventional pyrolysis as reported in other studies (Domínguez, Fernández, Fidalgo, Pis, & Menéndez, 2008). Equations (2) and (3) are the steam gasification of the carbon in the sample and contribute to the consumption of the carbon in the biosolids/susceptor mix (Beneroso et al., 2014b).

Insofar as this literature review has been able to determine, no comparable work has been done on the impact of moisture on the bio-oil product portion with MWAP.

2.5.4.3 Susceptor Type

Susceptors are added to the MWAP feedstock to heat the biomass via the mechanisms discussed in section 2.5.2. Susceptors with different material structure, chemical composition and tangent loss factor affect the process conditions and reactions that occur, due to the different heating effects they produce. A variety of susceptors have been used in literature, the most common susceptors used are carbon based susceptors (Yin, 2012) but some studies have used metallic susceptors (Ying Yu, Junqing Yu, Bing Sun, & Zhiyu Yan, 2014). Some susceptors that have been used are:

Activated Carbon: A very commonly used susceptor. Activated carbon is cheap and has a very high tangent loss factor of between 0.5-2.95, depending on the type. It also does not introduce any new elements into the sewage waste that it is mixed with. Activated carbon has been found to have positive effects on the products of MWAP, reducing SO_x and NO_x emissions, catalysing methane decomposition and enhancing the yield of aliphatic HCs (J.A. Menéndez et al., 2009) (Beneroso et al., 2014b).

Biochar: Similar to activated carbon in that it is a carbon susceptor. For this reason, it has effects on MWAP products (J.A. Menéndez et al., 2009). The main differences between biochar and activated carbon are that biochar has a generally lower tangent loss factor, which varies depending on the source material of the biochar, but is generally lower than activated carbon. The advantage of biochar over activated carbon is that biochar is a by-product of the pyrolysis process so is essentially free, and can be fed back into a continuous MWAP process as a susceptor in a recycle stream (X. Wang et al., 2012). Biochar forming during the pyrolysis process and acts as a microwave susceptor, increasing the heating rate, which further increases the formation of biochar, further increasing the heating rate. This leads to a thermal runaway effect and the controllability issue noted in Table 5.

Graphite: A carbon susceptor that is not used as extensively as activated carbon or biochar. Graphite is interesting in that it is both a carbon material, which have good tangent loss factors, and an electrical conductor, which tend to reflect microwaves (J.A. Menéndez et al., 2009). The combination of these properties means that graphite can act as a susceptor but absorbs a lower amount of energy than activated carbon, decreasing the chance that the susceptor will generate very small, short lived microplasmas. This allows for a more even heating of the sample and a more easily controlled process. Graphite has also been found to favour the cracking of heavier aliphatic (long chain) hydrocarbons (HCs) into lighter HCs (Tian et al., 2011; Zuo, Tian, & Ren, 2011).

Silicon Carbide: Has not been studied to the extent of carbon based susceptors. One study that did consider SiC as a susceptor found that the samples mixed with silicon carbide reached a higher maximum temperature than those mixed with the other susceptors studied. Silicon carbide mixed samples reached a peak of 1130°C compared to those mixed with activated carbon, biochar and graphite, which reached a peak of 1000°C, 970°C and 800°C respectively (Zuo et al., 2011). The heating rate when silicon carbide was used was also rapid and linear when compared to the other susceptors.

2.5.4.4 Heating Rate

The impacts of heating rate are difficult to distinguish from the impacts of temperature. Studies on the effects of heating rate found that it does appear to impact product composition and yield. One of the most comprehensive studies of heating rate effects on MWAP used wood biomass as the feedstock and made the following findings:

Heating rate increased the temperature at which CO and CO_2 peaked during the pyrolysis (Wu et al., 2014). The study considered microwave power settings to be analogous to heating rate and used three power settings; 600W, 900W and 1200W to pyrolyse 154g of 10% moisture sewage sludge. Of these settings 1200W produced the maximum amount of CO and CO_2 at 175ºC. 600W and 900W produced the maximum amount of CO and CO_2 at temperature ranges of 60-125ºC and 150-175ºC respectively.

The CH_4 yield appeared to increase with heating rate; in that study, negligible amounts were detected at all power settings except 1200W.

- The organic volatiles measured were mostly limited to phenols (typical of woody biomass). The yield of these was found to increase with an increase in heating rate.
- Higher heating rates decreased biochar yields and the amount of carbon in the biochar, while increasing the yield of the gas and bio-oil fractions.

Some findings of other studies are shown in brief below:

- A high heating rate and short pyrolysis times were found to maximize bio-oil yield (Tian et al., 2011).
- Somewhat contrary to the above finding, some researchers found that a high heating rate (200°C/min) increased gaseous yields, but decreased bio-oil yields (Menéndez, Domínguez, Inguanzo, & Pis, 2004).
- Low heating rates favour biochar production (Domínguez et al., 2007)
- A high heating rate was found to increase the yield of hydrocarbons (HCs) with –OH groups, which is considered to be due to a high heating rate (>200°C/min) increasing the rate of addition reactions between C-O and water bonds (Zuo et al., 2011)

2.5.5 Products of MWAP

The main products this project seeks to generate with MWAP are volatile compounds from the bio-oil portion. While the gas portion also contains valuable products, it is not a focus of this project.

2.5.5.1 Aromatics

Aromatics - the broad group of chemical compounds containing one or more unsaturated cyclic carbon rings. The most desired aromatic HCs are monoaromatic (single ring) HCs (Domínguez et al., 2005), while compounds with multiple aromatic rings, such as PAHs are

generally undesirable but are present in only small amounts in MWAP bio-oil (N. Wang et al., 2014).

The most widely used aromatics are monoaromatic base petrochemicals, such as benzene, phenol and xylene which can be processed into precursor chemicals to be used in the plastics, cosmetics and pharmaceutical industries or used as solvents. Some examples are shown in **Error! Reference source not found.**. Global production of the most common aromatics, benzene and xylene, is around 75 Mt/yr. The majority of this amount is produced via distillation and conversion of crude oil (Centre for Industrial Education, 2014).

The amount of low molecular mass aromatics produced in MWAP is very high relative to the amount produced in conventional pyrolysis, which is advantageous as higher weight aromatic compounds include harmful PAHs (Tyagi & Lo, 2013) (Omar & Robinson, 2014). Monoaromatic HC contents of 25 wt% or greater have been produced from sewage sludge MWAP (Tian et al., 2011; Zuo et al., 2011).

2.5.5.2 Alkenes

HCs containing at least one carbon-carbon double bond are also called olefins. Important alkenes include ethene and propene. Alkenes are used extensively in plastics production; many plastics are named after the alkene that forms the basis of the monomers that form the plastic polymer e.g. polyethylene and polypropylene. Examples are shown in **Error! Reference source not found.**. Polyethylene is the most important of these as it and its derivatives are the most commonly used plastics in the world and the majority of ethene produced is used to manufacture polyethylene. Other uses of alkenes include: fuel and illumination, base petrochemical manufacture, and agriculture. Larger alkenes are often used as additives in lubricants and surfactants (Lappin & Sauer, 1989; Petroleum UK, 2013). Alkenes are produced via steam cracking of light HCs from crude oil to produce lighter alkenes which can then be combined to produced larger alkenes.

Aliphatic alkenes in the size range of 10-22 carbons are present in the bio-oil produced from the MWAP of sewage sludge (Dominguez et al., 2003) with other authors reporting a wider size range of alkenes using different biomass feeds (Omar & Robinson, 2014). The amount of alkenes present in bio-oil is usually presented as a percentage of the GC-MS chromatogram area or incorporated into the measurement of the amount of aliphatic HCs present but MWAP has been reported to favour the production of alkenes over other aliphatic HCs (Dominguez et al., 2003).

2.5.5.3 Alkanes

Organic compounds consisting only of single bonded carbon and hydrogen. Examples of this group of hydrocarbons include methane, octane and decane. Lighter alkanes, 3-16 carbons chain length, such as octane, are used for fuel, while heavier alkanes are used as lubricants and anti-corrosion coatings, alkanes with a chain length of 35 carbons or greater are used in bitumen or cracked into smaller alkanes (Lohninger. H, 2011). The generalized structure of alkanes is shown in Figure 10. Alkanes are produced via fractional distillation of crude oil and lighter alkanes such as methane are produced from natural gas.

Lighter alkanes are not present in the bio-oil product portion, but in the gas portion, which is due to lighter alkanes being non-reactive and having boiling points lower than ambient temperature, where, in general, alkanes with a chain length less than 5 carbons are gases (Roberts, 1977). It has been reported that the majority of alkanes in MWAP bio-oil are between 10-18 carbons long (Domínguez, Menéndez, Inguanzo, et al., 2006), which includes chain lengths useful as fuels. In most of the literature surveyed in this work alkanes were reported as aliphatic HCs, which includes alkenes and alkynes. Those that measured alkanes separate from other aliphatic HCs reported the amount as around 17wt% (N. Wang et al., 2014).
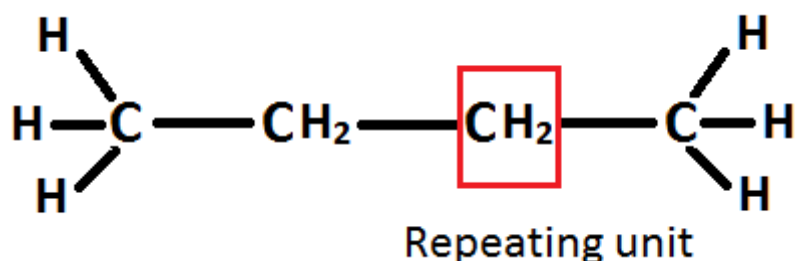
Figure 10. Butane, shown in the red box is the repeating unit of alkanes

Aromatics, alkanes and alkenes are the most desirable organic volatile products of MWAP as they are the most widely used petrochemicals and most other petrochemicals are derived from them. Other organic volatile groups are present in MWAP bio-oil however and a non-exhaustive list is provided below.

- Ketones (Dominguez et al., 2003)
- Aldehydes (Yin, 2012)
- Carboxylic acids (Yin, 2012)

- Alkynes(Domínguez, Menéndez, Inguanzo, et al., 2006)
- Alcohols (N. Wang et al., 2014)

2.5.6 Temperature measurement

A common issue encountered in MWAP research is temperature measurement. Temperature measurement in a microwave field is difficult due to the electromagnetic field, which induces arcing between the thermocouple and the sample, as well as the electric field producing currents that interfere with the measurement circuit (Dominguez et al., 2003; Yin, 2012). Metal thermocouple sheaths can also intensify the microwave field via conduction effects, causing the temperature around the thermocouple to be higher than that in the rest of sample (Evan Pert et al., 2001). This is a major problem in studying MWAP as temperature is one of the most important process variables in pyrolysis. Several solutions exist that allow temperature measurement in the microwave field.

- Using an infrared optical pyrometer in lieu of a thermocouple. This is a commonly used solution in literature (Domínguez et al., 2005) but has the disadvantage of only measuring the surface temperature of the sample. As shown in Figure 8, the temperature is the highest at the centre of the sample, whereas the temperature is lowest at the surface, which may cause pyrometers to under-report the temperature. An unobstructed view of the sample is also required, so biochar and gases can block the reading.

- Controlling the microwave field to limit interference to the thermocouple. In systems where a waveguide is used to direct the microwave energy a thermocouple that has dimensions that are small compared to the wavelength of the field (~12.5cm for 2.45 GHz) can be placed parallel to either the electric or magnetic component of the electromagnetic field. In this configuration the interference caused by the thermocouple is negligible (van de Voort, Laureano, Smith, & Raghavan, 1987). Controlling the microwave field is not possible in conventional domestic microwave ovens as multiple modes form and their location and intensity depend upon the type and volume of the material being heated.

- Shielding and grounding the thermocouple. Covering the sheath of the thermocouple with a reflective material and electrically grounding the thermocouple prevents induction of the interfering current. Grounding when combined with a 2-3mm diameter thermocouple sheath minimizes arcing and the intensification of the

microwave field around the thermocouple (van de Voort et al., 1987) (Evan Pert et al., 2001).

2.6   Key findings and knowledge gap

The key findings from the literature review on the current state of technology for biosolids treatment, the advantages of MWAP for treating the Victorian biosolids, and the knowledge gaps in MWAP, are presented below.

- The dominant methods of biosolids end use are not suitable for treating the entire 3.6 million dry tonnes of stockpiled biosolids in Victoria due to cost, environmental regulations and/or ease of implementation. In particular, the stockpiled T1/C3 biosolids can't be used for land application. MWAP is a technology that offers a potentially beneficial end use for Victorian biosolids, including the T1/C3 biosolids.

- The bio-oil produced as a product of the MWAP has value for fuel, chemicals, and has the potential to be a saleable product; in the way that biogas from wastewater treatment generates income and cuts costs for WWTPs. The bio-oil contains a wide range of compounds, the most valuable of which are aromatics, alkanes and alkenes.

- The most important process variables that impact on the bio-oil production are temperature, which maximizes bio-oil yield around ~550°C according to literature, choice of susceptor, and moisture content. It is important that this study identify the process values that perform best for this specific biosolids feedstock.

- As the stockpiled biosolids are different to fresh biosolids there may be little applicability of the findings of previous studies to the situation in Victoria. This study will fill this knowledge gap about the behaviour and products of MWAP of stockpiled biosolids.

- Most of the work classifying the compounds of MWAP bio-oil has focused on groups of compounds, rather than specific compounds. This knowledge gap in bio-oil component identification and quantification means that the chemical value of the bio-oil cannot be properly assessed. Bio-oil contains a large number of chemical components so this avenue of value generation from MWAP warrants investigation.

2.7 Focus Areas for this Study

Based on the findings and knowledge gaps in the literature review, and the goals in section 1.3, several areas were identified for this study to focus on.

- Maximizing the production of bio-oil components that have potential to value add to the process, such as the examples given in section 2.5.5. This will be accomplished by determining how process variables impact product composition and how they favour the production of desired bio-oil components.

- Identifying components should have their yield maximized, a method will be developed to definitively identify and quantify components in the bio-oil. This will extend the bio-oil characterization of previous studies and allow for the bio-oils value, under the tested conditions, to be calculated.

- Assessing the overall feasibility of MWAP for the treatment of the Victorian biosolids using the calculated value of the bio-oil. By considering the value of the bio-oil, the benefits of treating the biosolids, and the process costs, MWAP will be evaluated as a beneficial use and be compared against other beneficial use methods.

- Provide greater insight on the impacts of process variables on product composition and provide a basic methodology for assessing whether MWAP is a feasible method for treating certain biosolids.

3   Methodology

The methodology section discusses the methods and materials used in the experiments, and in the analysis of the produced bio-oils. As part of this section, chromatographic results from the bio-oils analysis are provided to better discuss the method development for the chromatographic analysis of the bio-oils.

3.1   Experimental Apparatus

The experiments were carried out in a single mode microwave cavity. A single mode cavity is microwave cavity where the microwave field strength is concentrated into one area. This differs from a multimode cavity, which is the configuration used a kitchen microwave. In a multimode cavity the microwave field forms multiple standing waves, distributing the energy across a greater volume than a single mode (see Figure 11) (Hayes. B, 2002).
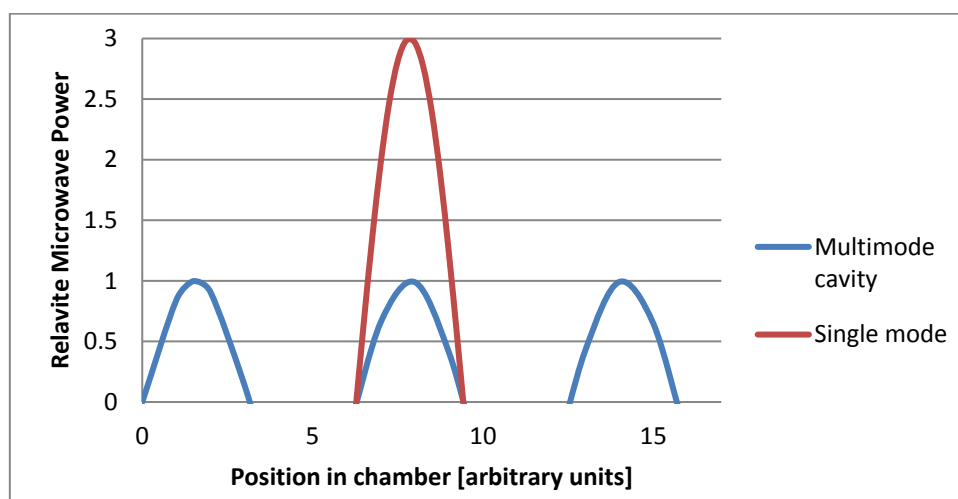
Figure 11. Comparison of relative power distributions in single and multimode microwave cavities.

Single mode microwaves produce higher power densities at the same microwave power and allow for more efficient heat transfer. The position of the sample in the cavity is important in a single mode, as the microwave energy is concentrated into one area. If the sample is placed outside of this area it will not be heated well. The microwave energy is supplied to the microwave cavity by the magnetron; the experimental apparatus also has several components to prevent damage to the magnetron, measurement and data logging instruments, and a condensing system to recover the bio-oil. A block diagram of the apparatus, and a description of each block and flow, can be found in below in Table 6.
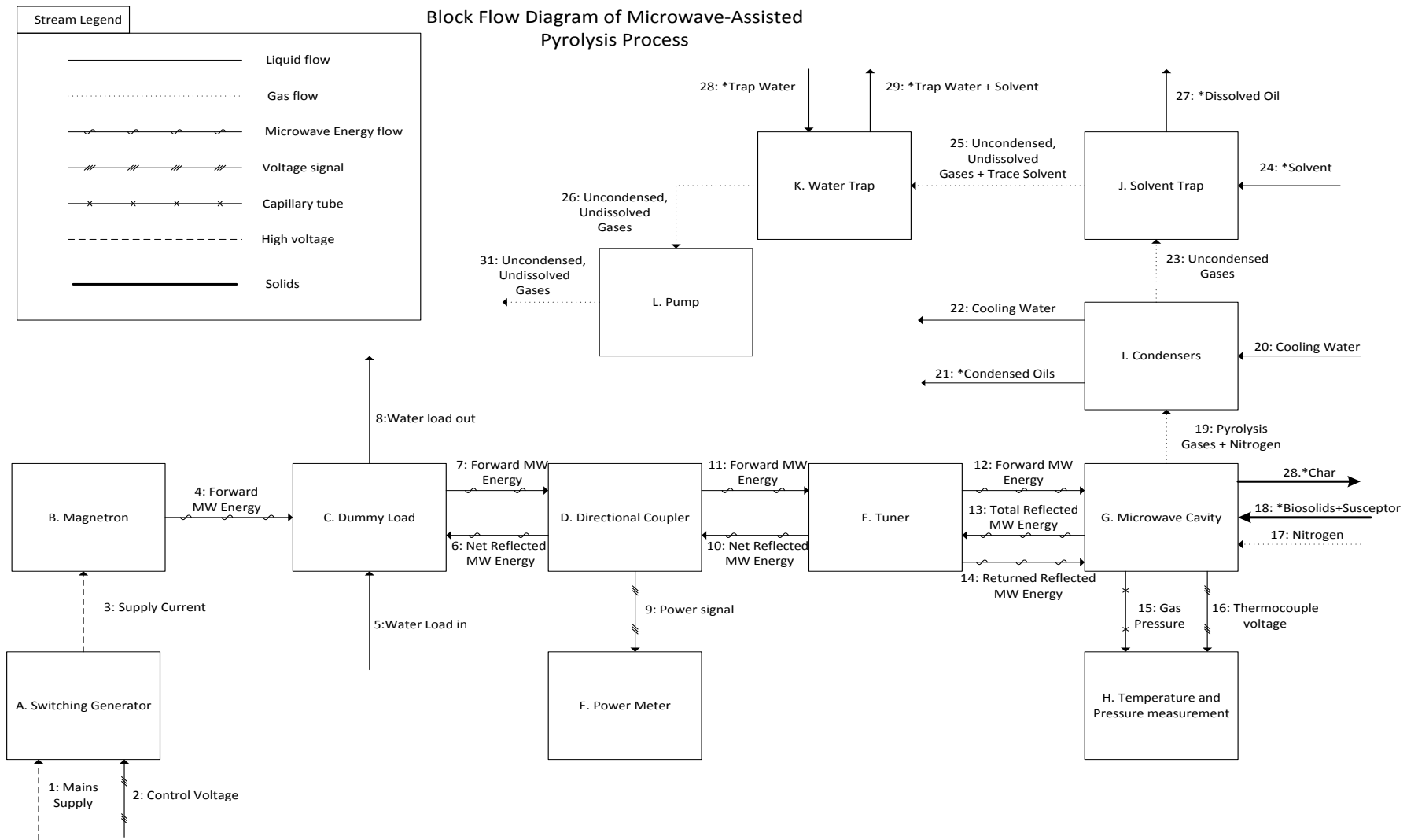
Figure 12. Block flow diagram of microwave pyrolysis apparatus

Table 6. Inflows and outflows of each block of the MWAP process

Block	Component Name	Function	Inflow Stream/s	Inflow Stream/s Type	Outflow Stream/s	Outflow/s Type
A. Switching Generator	Alter CM-440 Switching Power Generator (Alter power Systems, 2006)	Remotely supply current to power the magnetron and control the power output of the magnetron through the control voltage.	1: Mains 230 VAC 50Hz power supply	1: Energy	3: Supply current	3: Energy
			2: Control voltage	2: Signal		
B. Magnetron	TM0120 (Alter power Systems, 2003)	Supply an adjustable amount of microwave energy to the pyrolysis chamber.	3: Current Supply	3: Energy	4: Forward MW energy	4: Energy

Component	Product	Function	Input		Output	
C. Magnetic Isolator	National Electronics-Industrial Isolator (National Electronics, 2007)	Redirect reflected microwave energy from the pyrolysis chamber to a water load using a magnetic circulator.	4: Forward MW energy	4: Energy	7: Forward MW energy	7: Energy
			5: Water Load in	5: Liquid Flow	8: Water Load out	8: Liquid Flow
			6: Net Reflected MW Energy	6: Energy		
D. Dual Directional Coupler	GA3106 Dual Directional Waveguide Coupler (Gerling Applied Engineering, 2005)	Measures the forward and reflected microwave power.	7: Forward MW energy	7: Energy	6: Net Reflected MW Energy	6: Energy
			10: Net Reflected MW Energy	10: Energy	9: Power Signal	9: Signal
					11: Forward MW Energy	11: Energy
E. Power Meter	GA3213	Displays the forward and reflected power, as measured by the dual directional	9: Power Signal	9: Signal	N/A	N/A

			coupler.				
F. Tuner	Alter Manual AG340 3 Stubs Tuner	Matches the impedance in the forward and reflected directions to minimize the amount of reflected power.	11: Forward MW Energy	11: Energy	10: Net Reflected MW Energy	10: Energy
			13: Total Reflected MW Energy	13: Energy	12: Forward MW Energy	12: Energy
					14: Returned Reflected MW Energy	14: Energy
G. Microwave Cavity	N/A	The sealed 1.35L 316 steel vessel which serves as the pyrolysis chamber	12: Forward MW Energy	12: Energy	15: Gas Pressure	15: Signal
			14: Returned Reflected MW Energy	14: Energy	16: Thermocouple Voltage	16: Signal
			17: Nitrogen Flow	17: Gas Flow	19: Pyrolysis Gases + Nitrogen	19: Gas Flow
			18: *Biosolids + Susceptor mix	18: Feed stock	28: *Biochar	28:*Biochar

H. Temperature and Pressure Measurement	Thermocouple: Microwave compatible thermocouple from microwave research applications lab, inc. Pressure Gauge: Bourdon style pressure gauge, -100/0/50 kpa range from Floyd instruments	This process block consists of two parts; 1) a K-type thermocouple connected to a data acquisition system that allows for real time monitoring and recording of the temperature and, 2) a pressure gauge	15: Pressure signal	15: Signal	N/A	N/A	
			16: Thermocouple voltage reading	16: Signal			
I. Condensers	N/A	2x250mL volume Dimroth coil condensers operating in series that condense the	19: Pyrolysis Gases + Nitrogen	19: Gas Flow	21: *Condensed Bio-oil	21: Liquid Flow	
			20: Cooling Water	20: Liquid Flow	22: Cooling Water	22: Liquid Flow	

			pyrolysis vapours.			
J. Solvent Trap	N/A	100mL Cold finger containing solvent to recover the uncondensed portion of the gases.	23: Uncondensed Gases	23: Gas Flow	25: Uncondensed, Undissolved Gases + Trace Solvent	25: Gas Flow
			24: *Solvent	24: Liquid Flow	27: Dissolved bio-oil	27: Liquid Flow
K. Water Trap	N/A	To scrub the entrained solvent from gas flow to prevent damage to the pump.	25: Uncondensed, Undissolved Gases + Trace Solvent	25: Gas Flow	26: Uncondensed, Undissolved Gases	26: Gas Flow
			28: Trap Water	28: Liquid Flow	29: Trap Water + Solvent	29: Liquid Flow
L. Pump	Vacuum pump	Provide suction	26: Remaining gases	26: Gas Flow	30: Uncondensed, Undissolved Gases	30: Liquid Flow

3.1.1 Process Description

The switching power generator (A) supplies the necessary current to run the magnetron and controls the magnetron (B) power output, in response to a 0-10V analogue control voltage, by adjusting the pulse width of the current supplied to the magnetron. The switching power generator also preforms other monitoring and control functions for the magnetron, such as: powering the cooling fan and other peripheries, monitoring the voltage and temperature across the magnetron, and shutting down the apparatus to prevent damage to the magnetron if necessary.

The magnetron produces microwave (MW) energy via the mechanism discussed in section 2.5.1. This energy from the magnetron is directed forward by the magnetic isolator (C). A magnetic isolator is a two-port passive ferromagnetic component that uses a generated magnetic field to transfer MW energy to the next clockwise port (Meca Electronics, 2010). The theory behind these devices is out of the scope of this thesis but the effect of the device is that the energy from the magnetron enters port 1 and is passed to port 2, towards the pyrolysis chamber. Reflected MW energy entering port 2, from the pyrolysis chamber, is passed to port 3 where it is directed towards a dummy load water flow (Figure 13), away from the magnetron. Redirecting the reflected power in this manner prevents damage to the magnetron. Both the forward and reflected powers are measured by the dual directional coupler (D), and the measured values are displayed on the digital power meter (E).
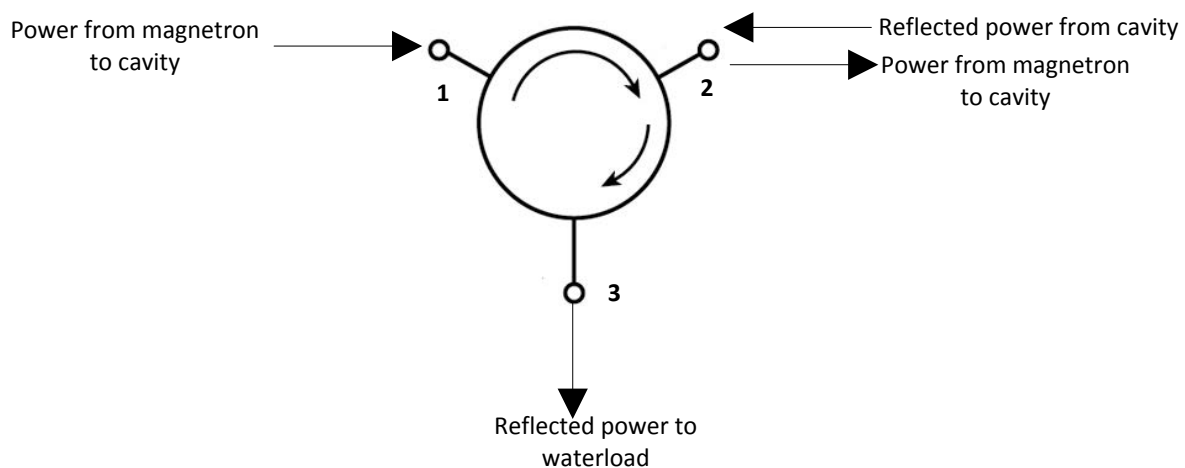
Figure 13. Magnetic circulator schematic

The tuner (F) is used to minimize the reflected power by adjusting the depth of penetration of three steel rods into the microwave field. This allows for the impedance of the waveguide

where the tuner is attached to be matched to the impedance of the microwave cavity (G). When impedance is matched the reflected power is minimized. During experiments, the impedance inside the microwave cavity changed too rapidly to allow the impedance to be accurately matched, so the tuner was not utilized for the experiments.

For clarity, the microwave cavities used and their connections are shown Figure 15. The original microwave cavity Figure 15 is a sealed 1.35L flanged steel cylinder with a height of 190 mm and a 95 mm internal diameter. A quartz plate sits between the bottom flanges to allow microwaves to enter the cavity and a silicone O-ring keeps the join airtight. A plate is bolted to the top flange to act as a lid, and the join is sealed with an O-ring. The lid plate has two hosetail fittings to act as a gas inlet and outlet, a pressure relief valve, and a compression fitting for a thermocouple to be inserted through the centre of the sample. The chamber is wrapped in heating tape to preheat the walls before experiments, to prevent the moisture in the sample from re-condensing on the chamber walls and refluxing.

During the project, the chamber had to be rebuilt. The impetus for the chamber rebuild was the significant corrosion caused by the heat, moisture and fatty acids in the bio-oils (shown in Figure 14). The chamber was rebuilt after the temperature effects experiments (3.2.1) and the first pyrolysis time (3.2.2). The new chamber was constructed out of 316 Stainless Steel, which has better corrosion resistance. As there was still moisture remaining in the chamber after the experiments, it was also suspected that the gases were not being properly entrained by the nitrogen flow. During the rebuild, the gas inlet and outlets were modified; the inlet was positioned at the base of the chamber and the outlet was positioned on the opposite side at the top of chamber. This new position would allow the nitrogen gas to better flow over the sample and entrain the pyrolysis gases. The chamber dimensions and the inlet, outlet, and thermocouple connections remained the same.

Figure 14. Corrosion of the 304 carbon steel chamber
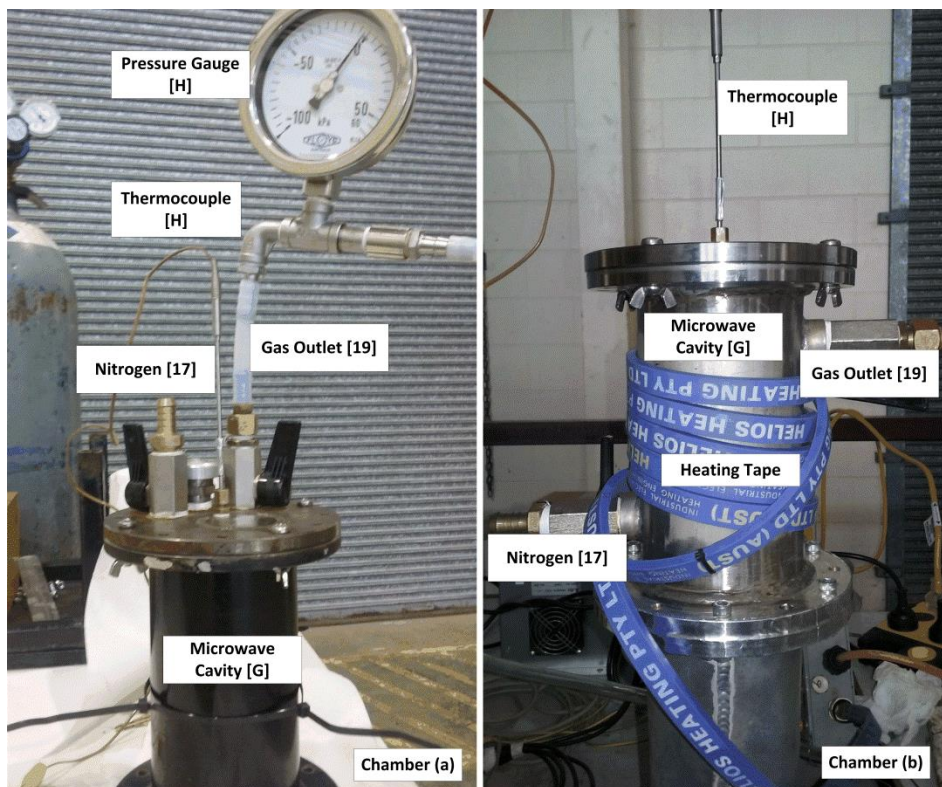
Figure 15. Image of Microwave Cavity - original chamber (left) and the rebuilt chamber (right).

Before the pyrolysis begins the sample is placed into the microwave cavity. The sample is contained in a fused quartz beaker and rests on the fused quartz plate at the bottom flange (see Figure 15). Fused quartz is used for the plate and the beaker as fused quartz has a low loss factor ($<4x10^{-4}$), so does not block the microwave radiation from the sample. Fused quartz also has both a high melting point (1683°C), and a low coefficient of thermal expansion ($5.5x10^{-7}$ cm/cm.°C) (Technical Glass Products, 2010). The high melting point means the fused quartz is resistant to the high temperatures in the pyrolysis while the low coefficient of thermal expansion means that it won't crack when exposed to high heating rates. A nitrogen gas flow is used to purge the oxygen and provide the inert atmosphere needed for pyrolysis; the nitrogen flow is maintained throughout the experiment to elute the pyrolysis gases. The nitrogen stream [17] enters through the hosetail fitting at the base and is removed, along with the pyrolysis gases through the outlet hosetail [19]. The thermocouple (H) inserted through compression fitting is connected to a datalogger and the temperature measured by the thermocouple is recorded and displayed real time. The gas outlet has a connected pressure gauge (H) that measures the pressure at a point just after the gas outlet [19], the pressure at this point is assumed to be the pressure of the microwave cavity. At the end of the experiment the chamber is unsealed and the biochar produced from the sample is removed, and the chamber prepared for the next experiment.

The gases leaving through the outlet are pumped through two ambient temperature condensers (I), condensing the majority of the gases. The gases which are not recovered in the condensers flow into the solvent trap (J) where they are dissolved in dichloromethane (RCI Labscan Ltd- LC1040A-G4L). To remove the condensed gases from the condenser at the end of the experiment, the pump action is maintained, the pressure gauge is removed, and DCM is poured through the connection and is pumped through the condensers and into the solvent trap, collecting the condensed bio-oils in the process.

Downstream of the solvent trap is a water trap (K) that serves to prevent any remaining condensable and dissolvable volatiles, as well as any solvent overflow, from damaging the vacuum pump (L). The pump provides the suction necessary to draw the gases through the gas system, between the pump and the water trap is a needle valve that is opened or closed during the experiment to maintain the correct pressure.

3.2 Experimental Design

The experiments conducted aim to identify the impact of process variables on the bio-oil yields and composition. The process variables selected were those reported to have largest impact on products and efficiency, such as, temperature and pyrolysis time. Goal 4 of project was to assess the feasibility of generating the bio-oil from the Victorian biosolids. For this reason, the experiments carried out were adapted as necessary to identify ways to improve low bio-oil yields, or better assess the bio-oils value, to maximize the cost-effectiveness of the process, whether by increasing overall bio-oil yield or the yield of valuable products. Figure 17 shows the progression of the experiments over the course of the project, as the experimental sets were adapted to tackle challenges that arose, such as bio-oil yields and energy efficiency being too low to make the process feasible.

The sets of experiments are outlined in this section, the general experimental procedure is given in section 3.3 and activities specific to each set of experiments are noted in the relevant experiment set section.

3.2.1 Temperature Effects Experiments

The goal of this set of experiments was to develop a GC-MS analysis methodology (explained further in section 3.4), determine the impact of the temperature on the distribution of the compounds in the bio-oil, and to identify what compounds are the major products of the pyrolysis. In the experiments, samples were pyrolysed at 300, 400, 500, 600, 700 or 800°C, held for 10 minutes at that temperature, and each experiment was executed three times. The bio-oils produced during the experiments were collected in the manner described in section 3.1.1. At the end of the experiment the condensed bio-oils were flushed through the condenser, with DCM, into the solvent trap for collection. The bio-oils were then prepared and analysed via GC-MS. At 300°C there was no recoverable amount of bio-oil, so these experiments were not reported on.

3.2.2 Pyrolysis Time Effects Experiments

The goal of this set of experiments was to determine the effect of pyrolysis time on the bio-oil yield and the bio-oil composition. In the experiments, samples were held at pyrolysis temperatures of 500°C, which was the temperature that bio-oil yields are maximized, according to literature (Tian et al., 2011) (J. Zhang et al., 2014) and at 700°C. At 700°C in the Temperature Effects Experiments the bio-oil yield was 11% less than the maximum (at 800°C) while consuming 22% less energy (see Table 11), so this temperature was chosen.

The samples were held at these temperatures for; 5 min, 10 min, 15 min, 30 min and 45 min. Experiments were done in duplicate with 5 min, 20 min and 30 min being done in triplicate. These times were tested in succession to determine when the bio-oil yield begins to plateau. 45 minutes was determined to be the point where bio-oil yield begins to plateau and the process is just consuming energy. Figure 16 shows an example temperature curve with how pyrolysis was time was defined.
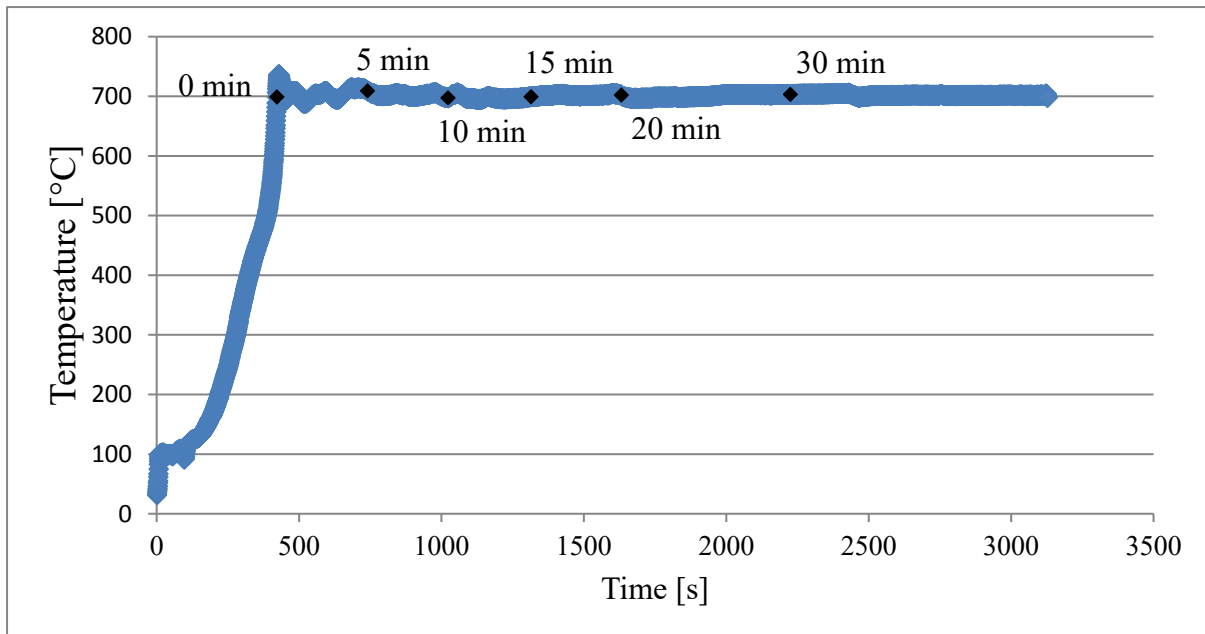
Figure 16. Example temperature curve with pyrolysis time indicated

From the previous Temperature Effects Experiments it was known that bio-oil was not produced until 400°C, even then only a small of bio-oil was produced over a 10 minutes pyrolysis time. The heating rate rapidly increases after 400°C due to the thermal runaway effect (see 2.5.4.3), causing the sample to spend only a small amount of time being heated above 400°C, relative to the total pyrolysis time. Some pyrolysis and bio-oil production will be occurring, but would be relatively constant across the samples and is considered negligible compared to the bio-oil production over the total pyrolysis.

The bio-oils were collected and prepared in the same way as in section 3.2.1 and then analysed using the GC-MS methodology developed in the Temperature Effects experiments (see 3.2.1). The calorific value bio-oil of the bio-oils was determined via combustion elemental analysis to determine the energy efficiency of the MWAP, to assess whether there was any potential to use the bio-oil as fuel. The original intent was to do a set of experiments at 600°C or 800°C, after 700°C, depending upon the results of the 700°C tests, but the 700°C

needed to repeated after the chamber rebuild described in section 3.1.1 this decision to continue with the rebuilt chamber is explained and justified in section 4.1.3.

3.2.3 Effect of Biosolids Storage Time

The goal of this experiment set was to determine how storing biosolids impacts upon the bio-oil yields and volatile matter content. This set of experiments was done in response to the low bio-oil yields observed during the Temperature Effects Experiments and Pyrolysis Time Effects Experiments. The effect of biosolids storage is also an important variable to consider for the wider application of MWAP as a WWTP technology. MWAP can be operated in batch mode, and stop and start more efficiently than conventional pyrolysis (see 2.5.3); biosolids could be stored and processed in large batches. If this did not adversely impact the bio-oil yields, it may be advantageous for smaller WWTP's with lower biosolids production to store biosolids until they have a sufficient amount to process. Due to difficulties in obtaining fresh biosolids from the Victorian WWTP, biosolids from a local wastewater treatment plant were used for this set of experiments. It was necessary to know the age of the biosolids precisely and to refrigerate the biosolids as soon as possible after collection to prevent degradation. Biosolids that were stored outdoors for 4 days to a month were pyrolysed. Experiments were done in duplicate, except for 14 and 21 days storage time at 500°C, which were done in duplicate. The bio-oil yield was compared to biosolids collected off the belt press and immediately refrigerated. The change in the volatile solids content over the storage time was also measured.
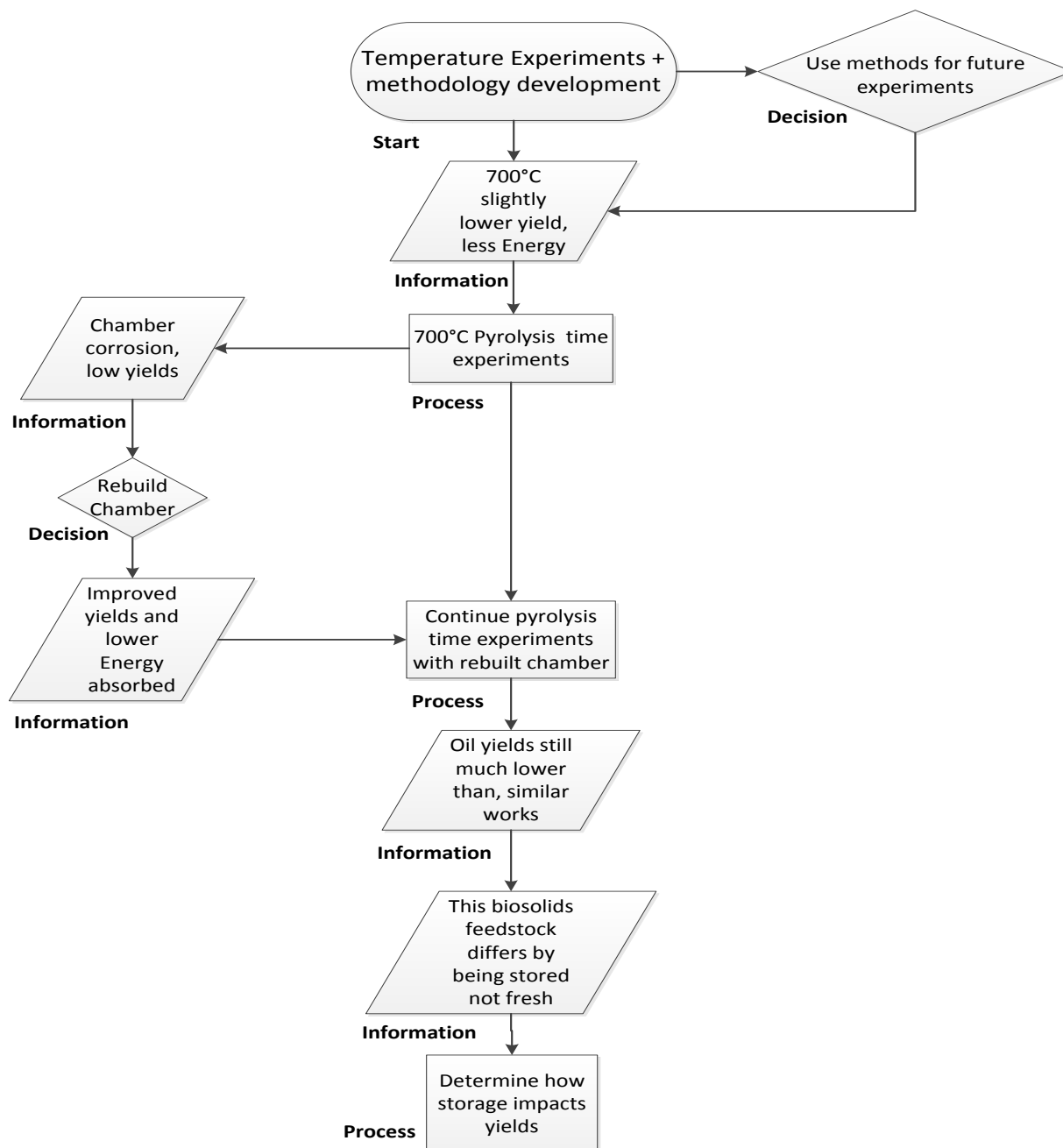
Figure 17. Experimental design flowchart

3.3 Experimental Procedure

The purpose of this section is to outline the analytical and experimental methods used and to present the starting composition of the biosolids used.

3.3.1 Biosolids Composition

The biosolids used were treated with anaerobically digestion and collected from stockpile at Euroa Wastewater Treatment Plant, Victoria, Australia, the biosolids were stored for approximately one month before being transported to Queensland. Two lots of biosolids were delivered that were from Euroa WWTP but had a slightly different composition. The Lot 1 was used in the temperature effects experiments and the Lot 2 was used for the pyrolysis time. The local biosolids from Mt St John WWTP were treated with an aerobic/anoxic cyclic digestion process. The moisture content was determined by analyzing three samples of the biosolids, prepared using the cone and quarter method, in a moisture analyzer (Sartorius MA 45) and taking the average of the three measurements. Volatile solids content was determined by firing the biosolids at 550°C for 3 hours in an oven, based on EPA method 1684, with a longer firing time based on recommendations from WWTP operators. Table 7 shows the composition of the biosolids used.

Table 7. Biosolids composition assay

	N %[a]	C %[a]	H %[a]	S %[a]	O %[b]	Volatile Solids %[a]	Moisture %
Lot 1 Delivery	2.20	19.9	3.5	1.0	17.8	43.5	50
Lot 2	3.05	26.30	4.31	1.03	15.81	50.1	40.4
Local Biosolids	6.04	34.12	5.61	0.68	37.50	83.96	60[c]

[a] Dry Basis; [b] Calculated by difference; [c] Adjusted to 60% for experiments

A Fourier transform infrared (FTIR) spectrum (shown in Figure 18) of the Lot 1 biosolids was obtained in a Perkin Elmer Spectrum 2000 FTIR spectrometer between 650 and 4000cm^{-1}. Prior to analysis, biosolids were dried at 100°C, ground and sieved. A sample of biosolids less than 75 microns in diameter was used to perform the analysis. The FTIR analysis of biosolids showed the presence of several functional groups in biosolids. The broad peak around 3320cm^{-1} corresponds to hydroxyl groups, which is common in organic matter. Aliphatic bonds can be identified by the peaks at 2920cm^{-1} and 2853cm^{-1}, and the stretching of C-H bonds in aromatic structures can be also visible in this region. The peaks around

1644cm^{-1} correspond to amide bonds typically present in biosolids. The presence of PO$_4$ groups can be visible in the range between 1000cm^{-1} and 1200cm^{-1}. The presence of phosphorus groups was expected because these biosolids are from a domestic wastewater treatment plant.
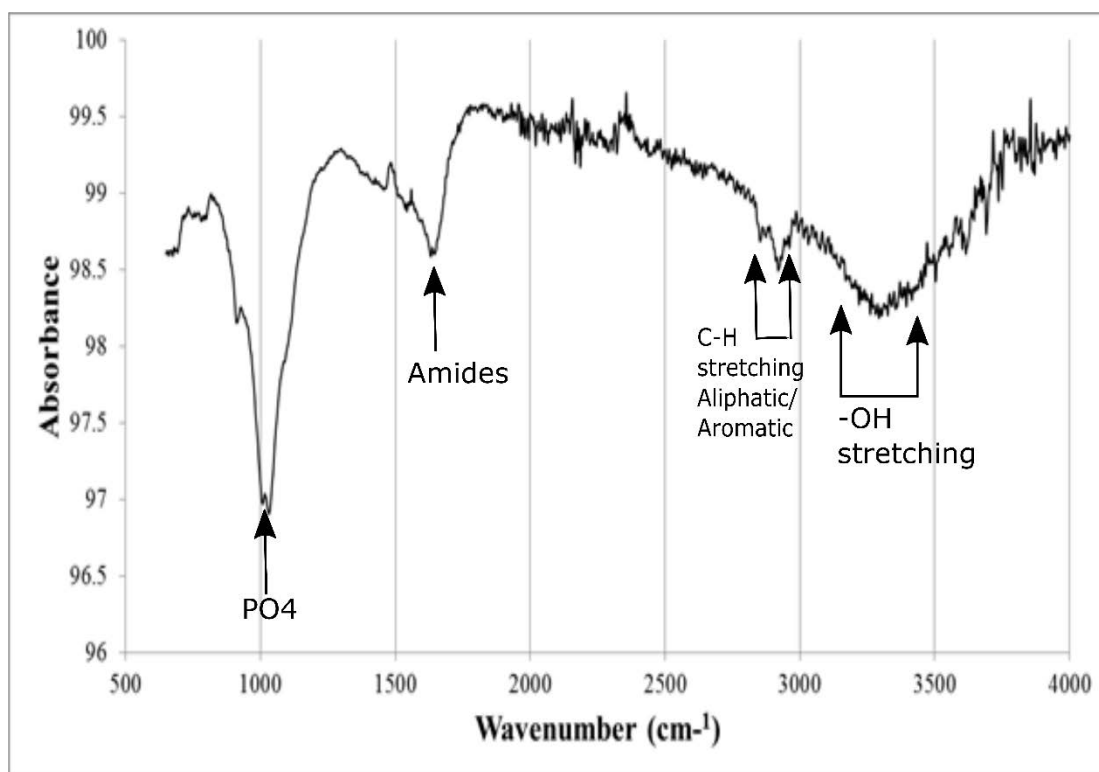
Figure 18. FTIR of Lot 1 biosolids

3.3.2 Biosolids Sample Preparation

The samples used during the Temperature effects experiments consisted of 80g of 50wt% water biosolids mixed with 1:10 ratio activated carbon (AC) (Sigma Aldrich- 242276) dry biosolids mass, producing a sample of 84g total mass. This was chosen based on preliminary tests, which showed that a 1:10 ratio of susceptor to biosolids sufficient to ensure a homogenous heating of the sample (see 2.5.2). For the experiments in section 3.2.2 the supplied biosolids had lower moisture content of 40%, and 4.768g of activated carbon was added to 80g of wet biosolids. For the Storage effects experiments, stored biosolids had their water content adjusted to 60%, as required and a 75g sample containing AC and dry biosolids in the same 1:10 ratio was prepared. For all experiments, the biosolids and AC were mixed in a grinder for 5 seconds to ensure that the AC was homogenously distributed throughout the biosolids. The mixture was then placed into a quartz beaker, to allow the biochar to be easily removed after the experiment, and then the beaker was placed into the pyrolysis chamber.

3.3.3 Pyrolysis Conditions

The microwave chamber was prepared for the experiment by purging it for one minute with 11L/min of nitrogen, corresponding to 8.2 residence times, which is sufficient to inert the atmosphere for pyrolysis. The nitrogen flow was maintained throughout the experiment to entrain the gases and provide a stable atmosphere. The initial power level of the magnetron was set to 750W to rapidly remove the moisture content of the biosolids and limit the time taken to reach the pyrolysis temperature. When the desired pyrolysis temperature was reached, the power level was continuously adjusted by changing the control voltage to maintain the temperature for the desired pyrolysis time. This power was monitored via the dual directional coupler and the forward and reverse power was recorded every minute, or when the magnetron output power was adjusted. The temperature was monitored and recorded with the data logging circuit. The pressure within the pyrolysis chamber was monitored with the pressure gauge and maintained at 12-15kPa vacuum for chamber (a) and 8-10kPa for chamber (b) by adjusting the needle valve (see Table 6) between the pump and water trap. By maintaining a constant pressure the residence time of the pyrolysis gases and moisture was kept consistent.

The bio-oils were collected using the method in described in section 3.1.1 and mixed with the bio-oils recovered in the DCM column. DCM was selected as the solvent for collecting the pyrolysis gases as its relative polarity of 0.309 (compared to 1 of water) allows it to dissolve a wide range of both polar and non-polar compounds. Due to the wide range of compounds produced by the pyrolysis (see 2.5.5) it is necessary to use a solvent such as DCM. Any produced bio-oils that entered the water trap were not considered for analysis. An inspection of the small amount of DCM that entered the water trap found that both the DCM and the water remained clear so the amount of bio-oils lost in this manner was considered to be negligible, as none could be extracted from the water with a solvent wash.

3.3.4 Moisture and Mass Loss Determination

At the completion of the experiment, the biochar was removed from the pyrolysis chamber and placed into a desiccator to cool. Once the biochar had cooled sufficiently it was weighed to determine the total mass loss from the initial sample. The moisture of the biochar was determined using the moisture analyzer with the same method as in section 3.3.1. The difference between the moisture content of the sample and the biochar was taken as the moisture loss. The char resulting from the pyrolysis was almost completely dry, see **Table 11** for example moisture contents.

3.3.5 Bio-oil Yield Determination

The bio-oil/DCM solution from the experiments was placed into a separatory flask to separate the organic and the aqueous layer. The organic layer was drained and the aqueous layer was then washed with a volume of DCM approximately equal to the volume of the aqueous layer three times and the resulting organic layers separated and added to the initial organic layer. The combined organic layer was dried with Sodium Sulfate, filtered with a Buchner flask and Microscience Qualitative MS2 filter paper. Roughly 1-2mL of this dried and filtered solution was placed into a weighed vial, the vial reweighed with the solution and the solvent was removed by vacuum boiling. After the solvent had visibly boiled off the container was reweighed at regular intervals until the change in the mass was less than 1 mg. The mass of bio-oil per mL and mass of bio-oil per gram of solution was then determined by weighing the container once the solvent had completely boiled off. The mass of bio-oil per gram of solution was used to calculate the total bio-oil produced during the pyrolysis and the bio-oil yield, in terms of the biosolids dry, ash-free (DAF) mass.

3.3.6 Elemental Analysis and Calorific Value

The elemental composition of the bio-oils and biosolids was also determined to calculate the calorific value. The samples were analysed for carbon, hydrogen, nitrogen and sulphur content, oxygen was calculated as the balance. The calorific value of the bio-oils was determined from the Boie equation, which relates the Higher Heating Value of a fuel to the mass fractions of carbon, hydrogen, nitrogen, sulphur and oxygen. This equation was selected as it is suitable for liquid fuels (K.Annamalai, J.M. Sweeten et al. 1987).

$$
\begin{aligned}
HHV, \frac{kJ}{g} = {} & 0.3516\,[C\%] + 1.16225\,[H\%] - 0.11090\,[O\%] \\
& + 0.06280\,[N\%] + 0.10465\,[S\%]
\end{aligned}
\tag{6}
$$

The following equation was used to calculate the higher heating value (HHV) of the sludge, this equation was selected as it has previously been used on solid biomass fuels (T.J. Buckley & E.S. Domanski, 1988);

$$
\begin{aligned}
\frac{kJ}{gDrySludge} = {} & 0.3515[C\%] + 1.617[H\%] + 0.1232[S\%] - 0.1198[O\% + N\%] \\
& - 0.0153[A\%]
\end{aligned}
\tag{7}
$$

The LHV was then calculated from the value of HHV using the following equation from (US EPA, 2007)

$$LHV\left[\frac{kJ}{g}\right] = HHV - 0.0236([M\%] + 9[H\%])$$

(8)

[M%] is the moisture content of the material and is zero for the bio-oils as they were dried prior to analysis.

Using the calculated LHV's the energy density increase of the material was calculated by subtracting the initial LHV of the biosolids from that of the produced bio-oil.

$$Energy\ Density\ Increase = LHV\ Oils - LHV\ Biosolids\ feedstock$$

(9)

The energy efficiency of the bio-oil production was calculated by dividing the energy density increase by the total energy absorbed by the biosolids over the course of the pyrolysis. The total energy absorbed is the difference between the forward and reflected powers measured by the dual directional coupler over the course of the experiment (see 3.1.1).

$$Energy\ Efficiency$$
$$= \frac{LHV\ Oils\ [kJ] - LHV\ Biosolids\ feedstock[kJ]}{Total\ Forward\ Power\ [kJ] - Total\ Reflected\ Power[kJ]}$$
$$* 100\%$$

(10)

The $Total\ Forward\ Power - Total\ Reflected\ Power$ value is used instead of the total forward power applied by the magnetron as the reflected power isn't absorbed by the biosolids and couldn't be reduced in our apparatus as the manual tuner was insufficient to control the reduced power (see 3.1.1). An automatic tuner would be able to eliminate reflected power without requiring a human to adjust the penetration depth of the rods.

3.4 Chromatographic Methods

The bio-oils were analyzed using Gas Chromatography (GC) using both mass spectrometry (MS) and flame ionization detection (FID). A sample preparation method and GC program was developed to allow for the major components in the bio-oil to be identified and quantified. Quantification of the largest components is an important step in assessing the

value of the bio-oil and was an extension of the semi-quantitative methods used in previous studies (see 2.6).

3.4.1 Sample Derivatization

Derivatization is a procedure to improve the chromatographic properties of a sample. Certain functional groups possess the ability form hydrogen bonds which can cause them to have low volatility, low thermal stability and interact with the GC column (Schummer, Delhomme, Appenzeller, Wennig, & Millet, 2009); these effects cause them to show up as 'smears' rather than peaks when analyzed with GC-MS. In the produced MWAP bio-oils the main functional groups present that contain hydrogen bonds are –COOH (carboxylic/fatty acids) and -OH (phenols). In order to improve the response of the compounds with these functional groups the samples are derivatized via silylation where the hydrogen in the functional groups is replaced with a silicon based functional group. The silylation was carried out with a commonly used silylating reagent N,O-Bis(trimethylsilyl)trifluoroacetamide (BSTFA) , BSTFA replaces the hydrogen in the functional groups with the more volatile trimethylsilyl $(Si(CH_3)_3)$ group (Le Barc'H, Grossel, Looten, & Mathlouthi, 2001).
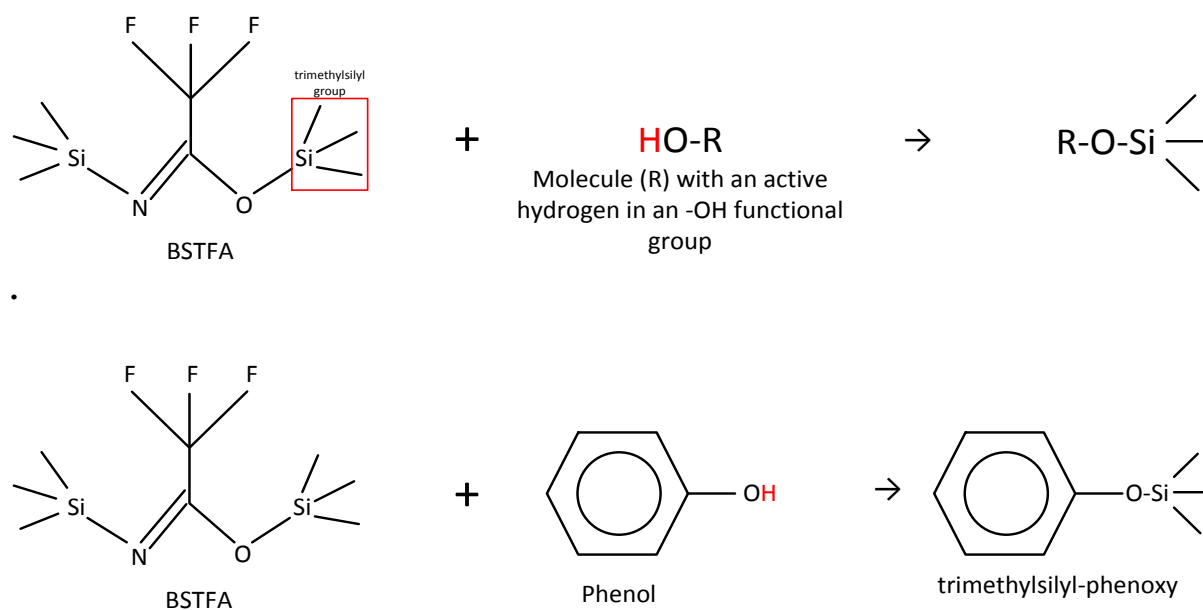
Figure 19. Silylation of the –OH functional group on molecule R (top) and phenol (bottom)

BSTFA reacts with functional groups in the order of Alcohols>Phenols>Carboxyl Acids>Primary Amine> Secondary Amine (Sigma Aldrich, 1997). Since the functional

groups derivatized first are –OH based groups, and these were detected in the biosolids in the FTIR analysis (see 3.3.1), BSTFA was chosen as a derivatizing reagent for the bio-oils.

3.4.2 Bio-oil Preparation

During preliminary investigations into the bio-oil composition, samples were prepared by concentrating 5mL of the filtered bio-oil solution down to at least 5000ppm bio-oil in biosolids to compensate for the anticipated poor peak resolution. The poor peak resolution was anticipated due to the –OH groups detected in the FTIR; these groups are known to separate poorly in GC columns (Schummer et al., 2009). The preliminary investigations confirmed that the bio-oil chromatographs were very poor and the samples required derivation before analysis.

For derivatized samples, 0.01g of BSTFA was used (approx. 100μL) for up to 5mg. For masses of bio-oil greater than 5mg of bio-oil, another 0.01g of BSTFA was added. This ratio was chosen based on methods outlined by Orata (Orata. F, 2011) ensuring the 2:1 molar ratio of BSTFA to active hydrogen is met (Sigma Aldrich, 1997). The bio-oil/BSTFA solution was diluted to approximately 1mL volume with a weighed amount of hexane and was heated at 65°C for 30 minutes to ensure full derivatization. To observe the impact of derivatization procedure, two underivatized samples of the bio-oil produced at 700°C and 800° were prepared using only bio-oil and DCM.

Hexane was used as the solvent for the derivatized bio-oil and standards instead of DCM. When DCM was used as the solvent after erroneous calibration curves (example shown in Figure 20) were produced. The effect where two different concentrations of 2,4-dimethylphenol produce the same peak area is due to the derivatized compound not being sufficiently soluble in DCM. As it is not soluble in DCM, the GC autosampler cannot take a representative sample from the solution, as a portion of the derivatized compound has precipitated. The solubility issues arise as DCM is a midrange polarity solvent, whereas the derivatized samples are non-polar due to the replacement of the polar functional groups with the trimethylsilyl group.

To fully dissolve the derivatized compounds the solvent for the bio-oils and standard was changed to hexane, which has a relative polarity of 0.009, compared to DCM's 0.309. The highest concentration standard was also reduced from 1000 ppm to 400 ppm as 400ppm still encompasses the concentration range in the bio-oil standards and decreases the risk that the high concentration of derivatized compounds will not be soluble.
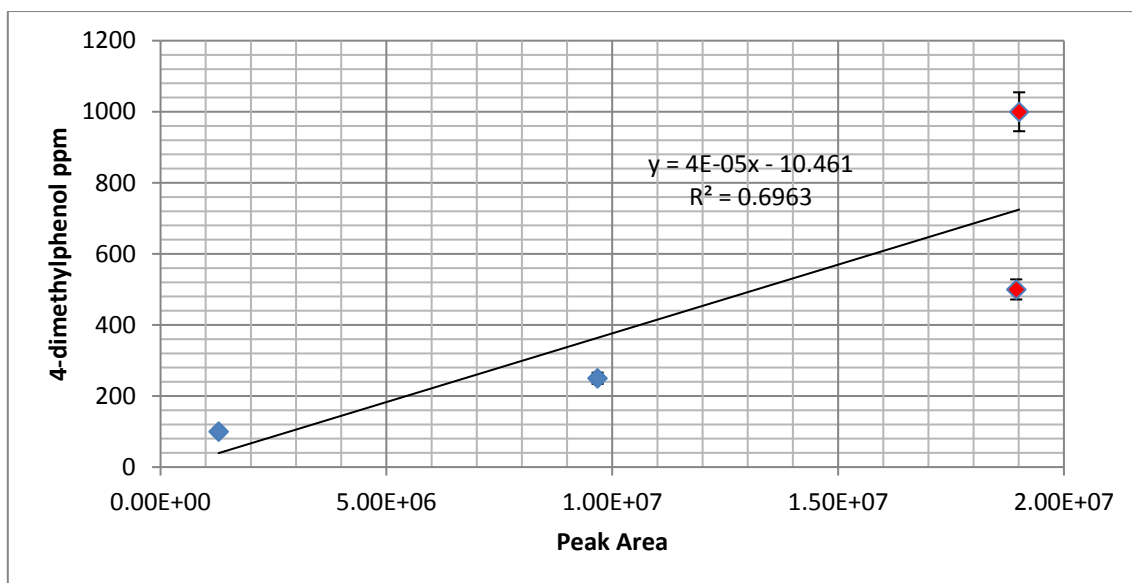
Figure 20. External calibration curve for 2,4-dimethylphenol, showing complications arising to solvent choice and standard concentration

3.4.3 Chromatographic analysis of Bio-oils

Samples were analyzed in a Varian 3800 Gas Chromatogram with a 30 m long x 0.25 mm diameter fused silica column connected to a Varian 1200L quadrupole Mass Spectrometer operated in 40-500 total ion chromatogram scan mode. The injection temperature was $250°C$ with a starting temperature of $60°C$, held for 3 minutes, followed by a $5°C$/min heating rate to $250°C$ which was held for 5 minutes. The total run time was 46 minutes. The carrier gas was 1mL/min of helium with a split ratio of 15.

The peaks of the chromatograms in the GC-MS analysis of the bio-oils were identified using NIST library identification and the GC-MS 'MS DataView' software. Peaks were integrated and the 15 to 17 largest peaks at each temperature were identified. The peaks were then sorted and placed into sets based on structure and functional group. Samples were analyzed with GC-FID to determine the peak area of the components that were identified in the GC-MS analysis as previous studies have done (I. Fonts, Azuara, Lázaro, et al., 2009). The same column, heating program, gas flows and spilt ratio were used for the FID analysis to determine the peak area, and for the quantification. A full collection of chromatograms from stockpiled biosolids bio-oils can be found in the attached Appendix B - Chromatograms.

A calibration curve for phenols was prepared using and ACID-M16C standard (high purity standards), and 3-ethylphenol (Sigma Aldrich). The standards were first derivatized with a 2:1 volume ratio of standard to BSTFA and an equal volume of hexane to BSTFA was added

to aid in dissolution. This mixture was heated and reacted the same way as the bio-oil samples (section 3.3.5). The original aim was to use GC-MS for all analyses but after an extended breakdown of the Mass Spectrometer it was decided that GC-FID would be used for quantification. In comparison to GC-MS, GC-FID is more sensitive, but peaks cannot be identified without a standard to compare the retention times with.

3.4.4   Improvement between Derivatized and Underivatized Samples

Figure 21 compares the GC-MS chromatograms of two bio-oil samples from the same pyrolysis experiment, Figure 21a is derivatized with BSTFA and Figure 21b is underivatized. The 15-17 largest peaks are labelled with the compound that has the best mass spectra match to the peak, based on identification by matching peak spectra to spectra in the NIST library. The derivatized compounds are presented as their underivatized forms. Peaks 4, 11, 15 and 17 are identified as the same compound in the derivatized sample; peaks 3, 9, 13 and 14 have been identified as similar compounds and peaks 1, 2, 6, 7, 8, 10 and 16 are not identified amongst the largest peaks in the derivatized sample. Peaks 5 and 12 are groups of peaks that were not identifiable due to poor separation between the peaks. Notably, the second largest peak, phenol, was not identified in the underivatized sample. The presence of phenol was confirmed in section 3.4.5 and was likely misidentified as allophanic acid, phenyl ester in the underivatized sample, judging by the elution time of the peaks in Figure 21. Peaks 3 and 4 in Figure 21b have also been resolved into three peaks that have been identified as 2, 3 and 4 methylphenol.

From Table 8 there are significant differences between the derivatized and underivatized sample. The reason for the difference in the identification of the peaks is the significant smearing of peaks that can be seen in Figure 21b, especially in the first 14 min of the analysis. The reason for the poor resolution, and differences between the chromatograms, is that the bio-oil contains many compounds that separate poorly. From the derivatized chromatogram, it can be seen that the bio-oils contained a significant amount of phenols and carboxyl acids, by peak area. As mentioned in section 3.4.1, the functional groups of phenols and carboxyl acids, –COOH and –OH, respectively, separate poorly (Wenclawiak, Jensen, & Richert, 1993), so are hard to identify in Figure 21b. In the derivatized samples the functional groups have had the active hydrogen replaced by the trimethylsilyl group by the BSTFA (see 3.4.1), causing the peaks to be better separated for easier identification.
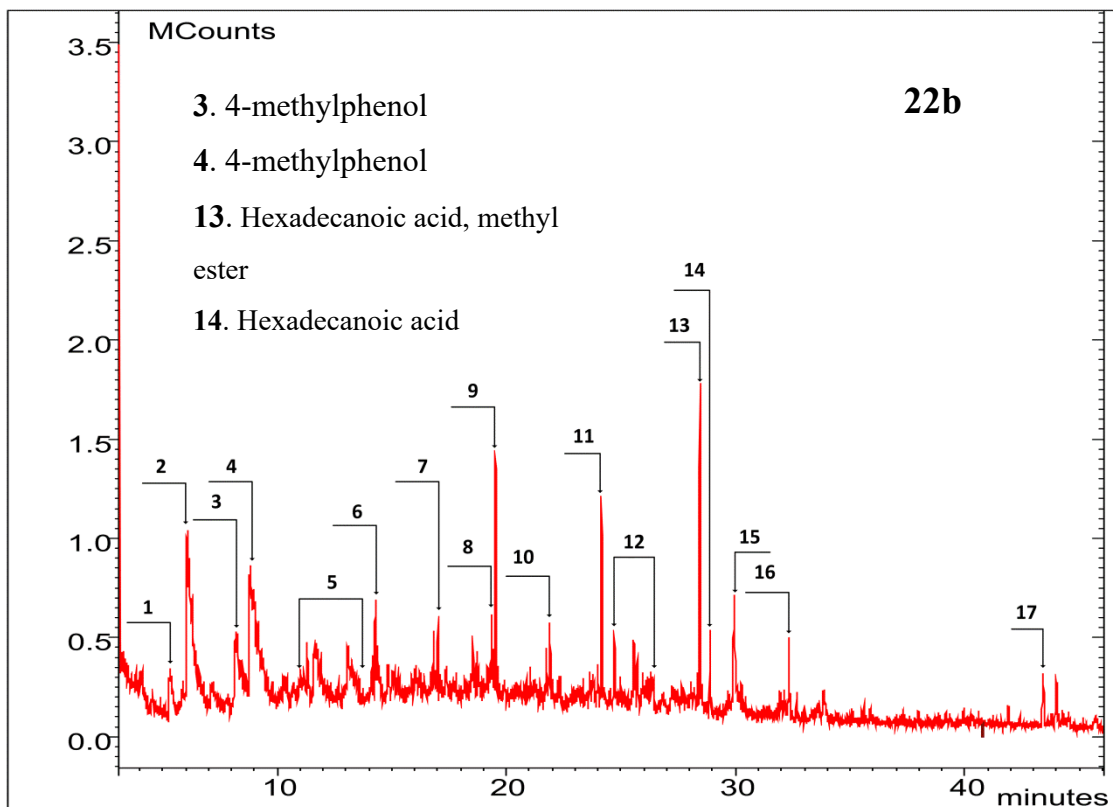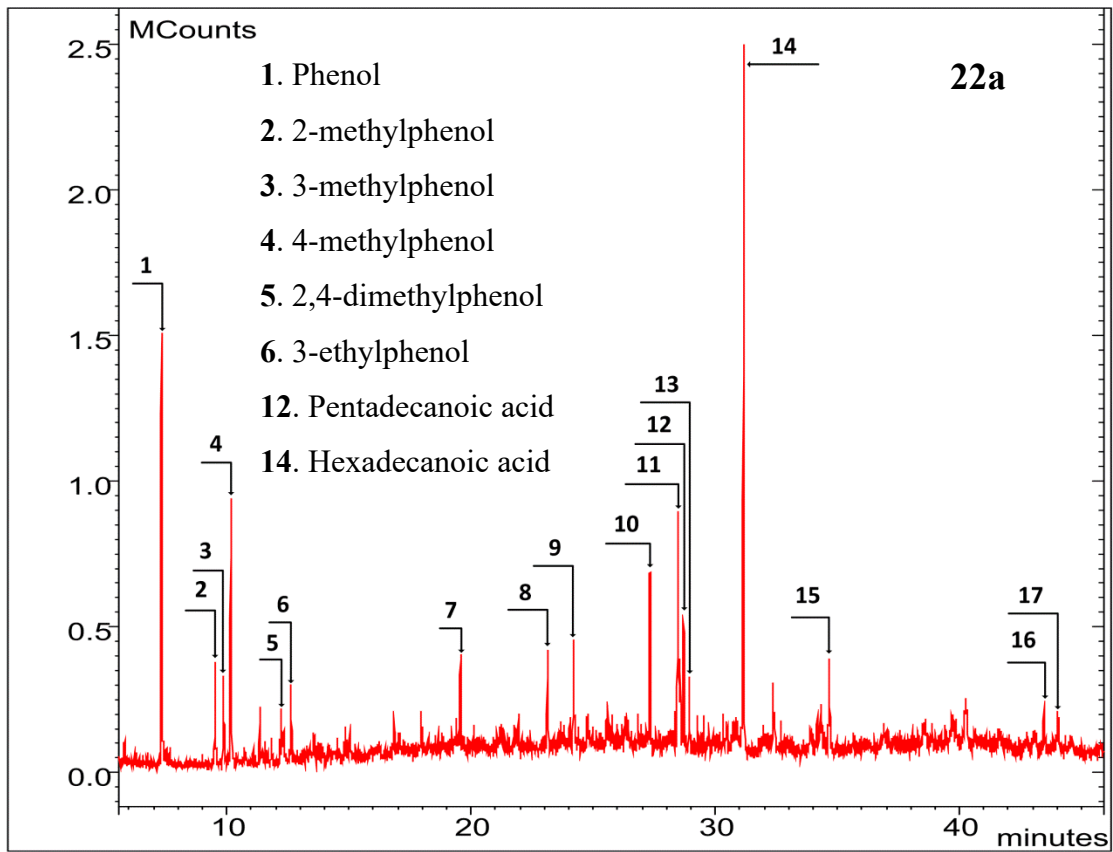
Figure 21. Chromatograms of derivatized (a) and non-derivatized (b), 700°C bio-oil samples. With phenols, pentadecanoic acid and hexadecanoic acid peaks labelled.

Table 8. Compounds identified in derivatized and underivatized sample

Peak	Derivatized			Underivatized		
	Retention Time [min]	Compound[a]	Area [Counts]	Retention Time [min]	Compound	Area [Counts]
1	7.325	Phenol	5.84E+06	5.038	2-Cyclopenten-1-one, 3-methyl-	2.14E+06
2	9.515	2-methylphenol	1.25E+06	6.074	Allophanic acid, phenyl ester	1.47E+06
3	9.863	3-methylphenol	1.33E+06	8.213	4-methylphenol	4.22E+06
4	10.165	4-methylphenol	3.56E+06	8.828	4-methylphenol	8.76E+06
5	12.190	2,3-dimethylphenol	3.84E+05	11.5-12	Unidentifable peaks	
	12.25	2,4-dimethylphenol	9.13E+05			
	12.303	2,6-dimethylphenol	4.19E+05			
6	12.639	3-ethylphenol	1.10E+06	14.281	Cyclohexasiloxane, dodecamethyl-	2.40E+06
7	19.57	Octadecane	1.32E+06	17.008	Decane, 2,3,5-trimethyl-	9.29E+05
8	23.144	Dodecanoic acid	1.02E+06	19.352	Trichloroacetic acid, undecyl ester	3.24E+06
9	24.183	Tritetracontance	1.55E+06	19.522	Hexadecane	3.24E+06
10	27.328	Tetradecanoic acid	1.91E+06	21.891	heptadecane, 2,6,10,15-tetramethyl-	9.89E+05
11	28.474	Nonadecanenitrile	3.21E+06	24.154	Tritetracontane	2.65E+06
12	28.555	Pentadecanoic acid	1.46E+06	24.5-26.5	Unidentifable peaks	
13	28.929	14-methyl-pentadecanoic acid	5.21E+05	28.443	Hexadecanenitril	4.66E+06
14	31.169	Hexadecanoic acid	8.39E+06	28.88	Hexadecanoic acid, methyl ester	1.33E+06
15	34.68	Octadecanoic acid	1.06E+06	29.955	n-hexadecanoic acid	4.75E+06
16	43.419	Cholest-3-ene, (5.alpha)-	1.237e+06	32.337	Ocadecanenitrile	1.25E+06
17	44.08	Cholest-4-ene	998139	43.421	Cholest-3-ene, (5.alpha)-	1.13E+06

[a]Compounds in derivatized sample are given as their underivatized forms

3.4.5 Quantification of Phenols

With improved peak separation, identified compounds can now be quantified with an external standard. To create an external standard a series of samples containing known concentrations of the analyte of interest were injected into the GC-FID and analyzed with the same heating program as the bio-oil samples.

Using an external calibration curve allows for a definitive identification of the compound in the standard, as the peaks in the bio-oil sample can be compared to the peaks in the standard in terms of retention time. Comparing the peaks in the external standard with the peaks in the derivatized sample in Figure 23, most of the phenols identified using library identification are present.

For the phenols calibration curve, a 16 component Acids Extractable standard (ACID-M16C) from high purity standards was used. The standard contained 16 different phenol components, all 2000±20 ppm in DCM. A weighed amount of standard was derivatized with BSTFA, in the same manner as the bio-oil samples, and hexane was used to dilute the standard to create the calibration curve. The concentration of the components in each sample was calculated using the mass of the standard, BSTFA and hexane and the uncertainty in the concentration of each point calculated in EES (section 3.5).

The standards were then analyzed with a hexane blank and the bio-oil samples. The peaks in the sample chromatograms were integrated to determine the response of the detector to the known amount of that compound and the calibration curves were created. There were three methylphenol isomers detected in the bio-oils 2-methylphenol, 3-methylphenol and 4-methylphenol (Table 8). The standard contained 1000 $\mu g/mL$ each of 2-Methylphenol and 4-Methylphenol added, there is some conversion of 2-methylphenol and 4-methylphenol to 3-methylphenol during the heating of the sample, which can be seen in the emergence of a 3-methylphenol peak in the standard, after derivatization. The total amount of methylphenols in the sample is still 2000 $\mu g/mL$, as the conversion ratio is 1:1. The methylphenol isomers were quantified with the curve for total methylphenol as the amount and type of ions produced by each methylphenol isomer molecule is the same. There were 3 dimethylphenol isomers; 2,3-dimethylphenol, 2,4-dimethylphenol and 2,6-dimethylphenol. 2,4-dimethylphenol was also used to quantify the other 2,x-dimethylphenol isomers due to the similarity between the compounds and the very small difference between their retention times. Figure 22 shows an example calibration curve for phenol, using the standards from the first curve in Table 9, plus the blank.
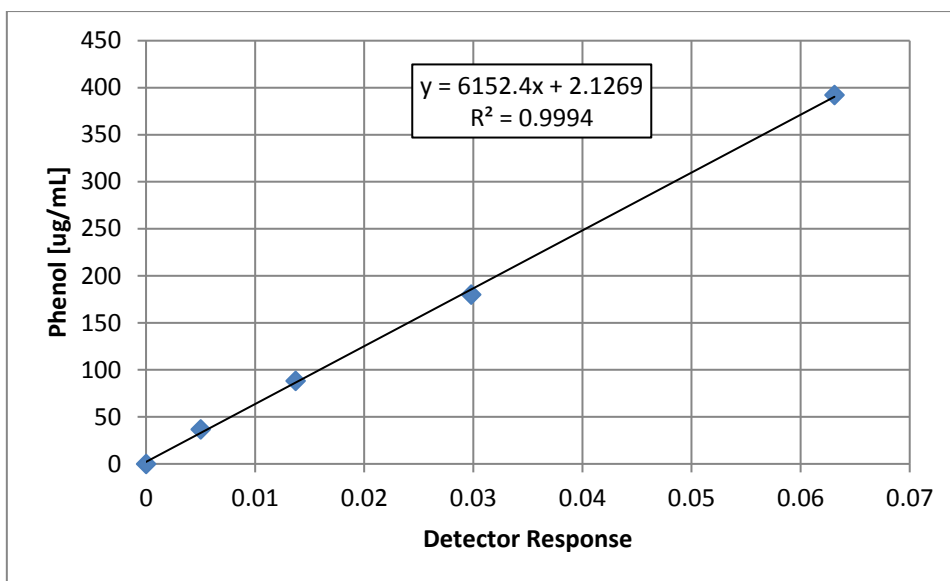
Figure 22. Calibration curve for Phenol, using standards in Table 9.

As the column was not used for a period of a few months between the first and second batches, a second calibration curve was prepared for the second and third set of experiments. The curves were all prepared in the manner described above. The concentrations of the calibration points and the curve coefficients are presented below in Table 9.

Table 9. Point concentrations and coefficients of calibration curves (the blank is included in the curve but is not shown in the table).

Components	Pt. 1 [ppm]	Pt. 2 [ppm]	Pt.3 [ppm]	Pt. 4 [ppm]	Pt. 5 [ppm]	Slope	Intercept	R^2
						Coefficients		
1st Curve								
Phenol	392.24	179.93	88.32	36.75	N/A	6152.4	2.127	0.9994
Methylphenols	N/A	359.86	176.65	73.50	N/A	5116.6	-1.381	0.9933
Dimethylphenols	N/A	179.93	88.32	36.75	N/A	11030	-1.235	0.9997
2nd Curve								
Phenol	387.77	176.56	63.45	41.14	21.33	1093.4	0.6197	0.9966
Methylphenols	775.54	353.12	126.9	82.28	42.66	953.77	3.9107	0.9961
Dimethylphenols	387.77	176.56	63.45	41.14	21.33	1254	1.9888	0.996

Using the calibration curves, the concentration of each of the compounds in the bio-oil samples was determined based on relationship between peak area and compound

concentration. The calculated amount of each compound was then used to determine the yield of that compound in terms of the biosolids volatile solids.

The presence of phenol, methylphenols, and dimethylphenols in the bio-oil was confirmed. However, the peak eluting at 12.6 min (peak 6 in Figure 21a), that had been identified as 3-ethylphenol, did not correspond to the 11.9 min retention time of the 3-ethylphenol peak in the 3-ethylphenol standard. Therefore, 3-ethylphenol peak in the MS was misidentified, despite consistent identification with spectra from the NIST library. In three samples the spectra match probability of the 12.6 min peak corresponding to 3-ethylphenol was greater than 80% and the lowest probability among the other samples was 60%. This highlights the importance of using standards to definitively identify and quantify compounds in bio-oil, as even a peak with a consistent high level of spectra match to a database compound could still be misidentified. The standard peaks are overlayed with the sample peaks in Figure 23. The standards for all the phenols, except 3-ethylphenol, overlap with the sample peaks. Calibration is also important for accurate quantification; which is explained in greater detail section 4.1.2.
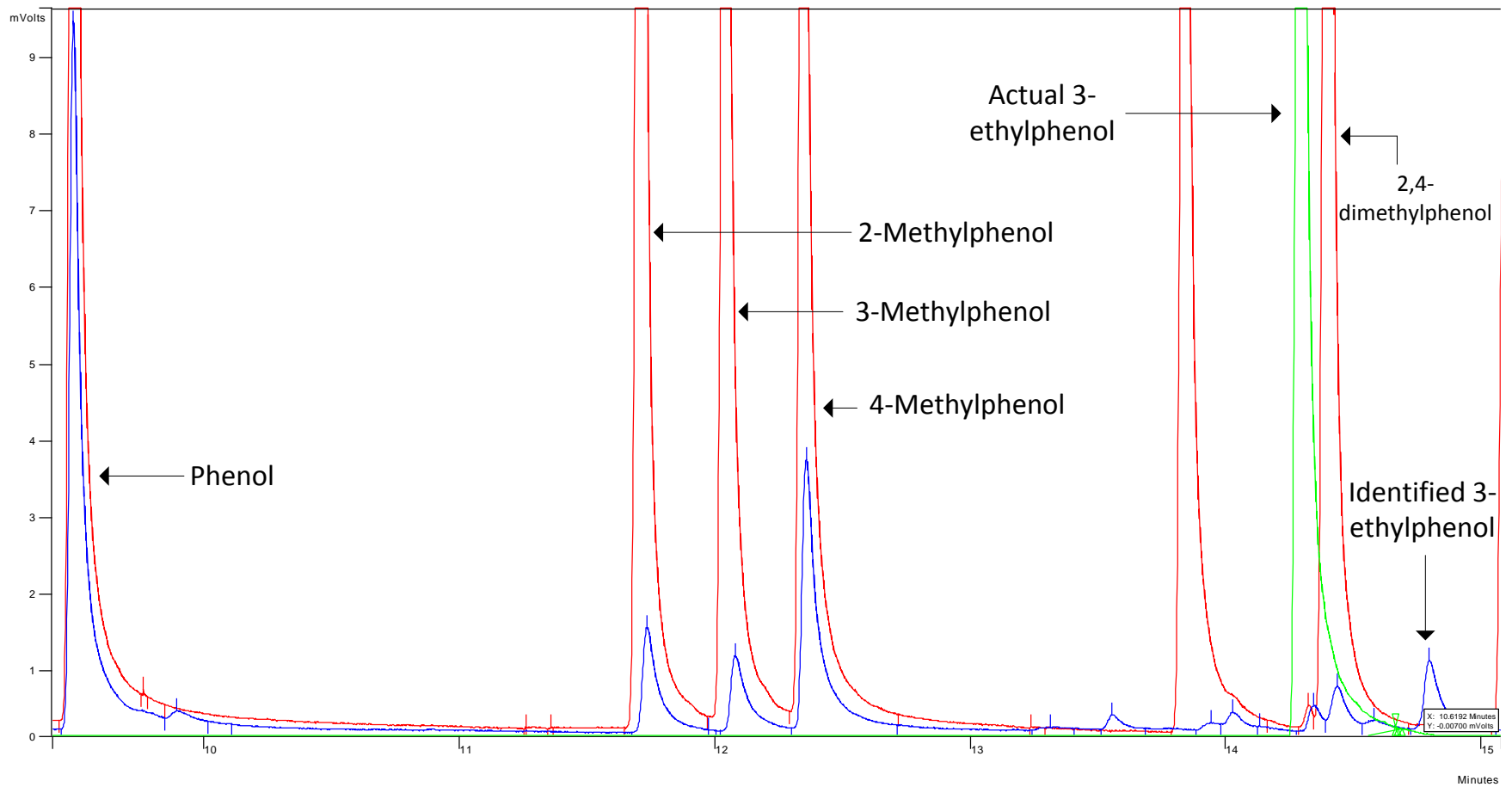
Figure 23. Overlaid chromatograms of single ring phenols standard (red), 3-ethylphenol standard (green), sample (blue)

3.4.6 Carboxylic Acids Quantification

After the temperature effect experiments 3.2.1, it was found that the proportion of phenols in the area was lower than the peak area % suggested. The proportion of phenols in the area, based on the peak area % of peaks, was up to ten times higher than the actual percentage of phenols, based on quantification with a standard. As the amount of phenols in the bio-oil was lower than anticipated, the next largest group of compounds, based on preliminary analyses, was quantified. This group was the fatty acids.

Based on the GC-MS, peak areas, the majority of the fatty acids were pentadecanoic and hexadecanoic fatty acid. Calibration curves were prepared using pure samples of these compounds, sourced from Sigma Aldrich. Weighted portions of hexadecanoic and pentadecanoic acid again were derivatized with BSTFA, with at least a 2:1 molar ratio of BSTFA to acid, in the same manner as in section 3.4.2. The derivatized compounds were then diluted with weighed amounts of DCM as the solvent, as suggested by the method outlined in (Jana Šťávová, Josef Beránek, Eric P. Nelson, Bonnie A. Diep, & Alena Kubátová, 2011) to produce a starting mixture with a concentration of 1596 µg/mL hexadecanoic acid and 870.6 µg/mL pentadecanoic acid. The pentadecanoic acid portion of the starting mixture was prepared to a lower concentration as the pentadecanoic peak had a smaller peak area than that of the hexadecanoic acid. The starting mixture was then diluted further to create three standard calibration points. The concentrations of these points and the coefficients of the curves are provided in Table 10.

Table 10. Calibration point concentrations and coefficients for carboxylic acids

Component	Pt. 1 [ppm]	Pt. 2 [ppm]	Pt. 3 [ppm]	Coefficients m	c	R^2
Hexadecanoic	693.7	354.4	161.6	5966.94	-40.58	0.9977
Pentadecanoic	378.4	193.3	88.17	7641.17	-86.36	0.9908

After the standards were prepared it was found that the peak identified by MS Dataview as 14-methylpentadecanoic acid was the pentadecanoic acid peak, as determined by the standard. The hexadecanoic acid peak, the majority contributor the peak area of the fatty acids, was correctly identified by MS Dataview.
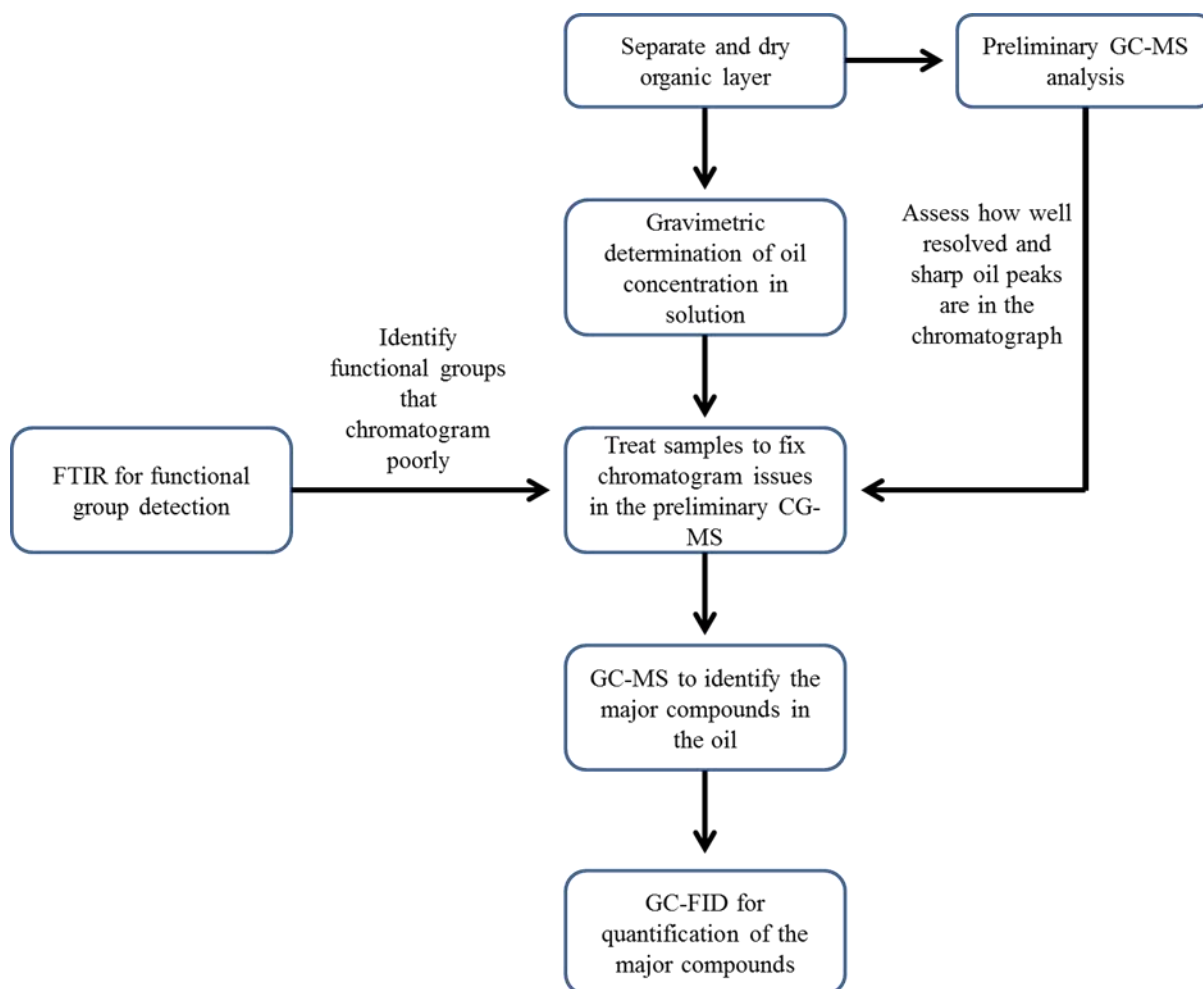
Figure 24. Graphical description of bio-oils analysis

3.5 Data Analysis

Values were divided into two categories; values that were measured directly using instruments and calculated values which were derived from the measured values. The error of the measured values was assumed to be the absolute error of the instrument, as indicated on the instruments specifications. The error of the calculated values was determined using the uncertainty propagation function of Engineering Equation Solver (EES) (F Chart Software, 2015) to determine the probable error of the calculated values based upon the absolute error the measured values they were derived from. EES calculates the uncertainty using the method described in NIST technical note 1297 where;

For a value, Y, calculated via $Y = f(X_1, X_2, \dots X_i)$, its uncertainty U_Y is given by;

$$U_Y = \sqrt{\sum_i \left(\frac{\delta Y}{\delta X_i}\right)^2 U_X^2} \qquad (11)$$

The uncertainty in the measured and calculated values was used to weight the data points to fit more accurate models with the R package for statistical modelling and computing (R Development Core Team, 2008). The points were assigned weights using the equation;

$$Weight = \frac{1}{uncertainity^2}$$

(12)

R was used to analyze the relationships between the variables in the collected data, to fit models and check the models for significance and predictive power. The models fitted to data are discussed in Results and Discussion.

4 Results and Discussion

This chapter provides the results obtained from the experiments and methodologies discussed in the Methodology chapter. The chamber rebuild, and the explanation for the decision to continue using the rebuilt chamber, are also discussed in this chapter.

4.1 Temperature Effects Experiments

The samples were prepared as described in section 3.3.2 and were heated to 400°C, 500°C, 600°C, 700°C or 800°C, then maintained at that temperature for 10 minutes. As discussed in section 3.2.1, 300°C was also tested but no further work was done at this temperature as no bio-oil could be recovered at 300°C. Figure 25 shows example temperature profiles, and the average microwave power consumed at each temperature. The temperature and power profiles for all the experiments can be found in the attached Appendix A - Experimental Results and Calculations. There is no obvious correlation between the temperature and the microwave energy consumed (p=0.74) in Figure 25. However, the average energy consumption for 800°C is significantly higher than the other temperatures.
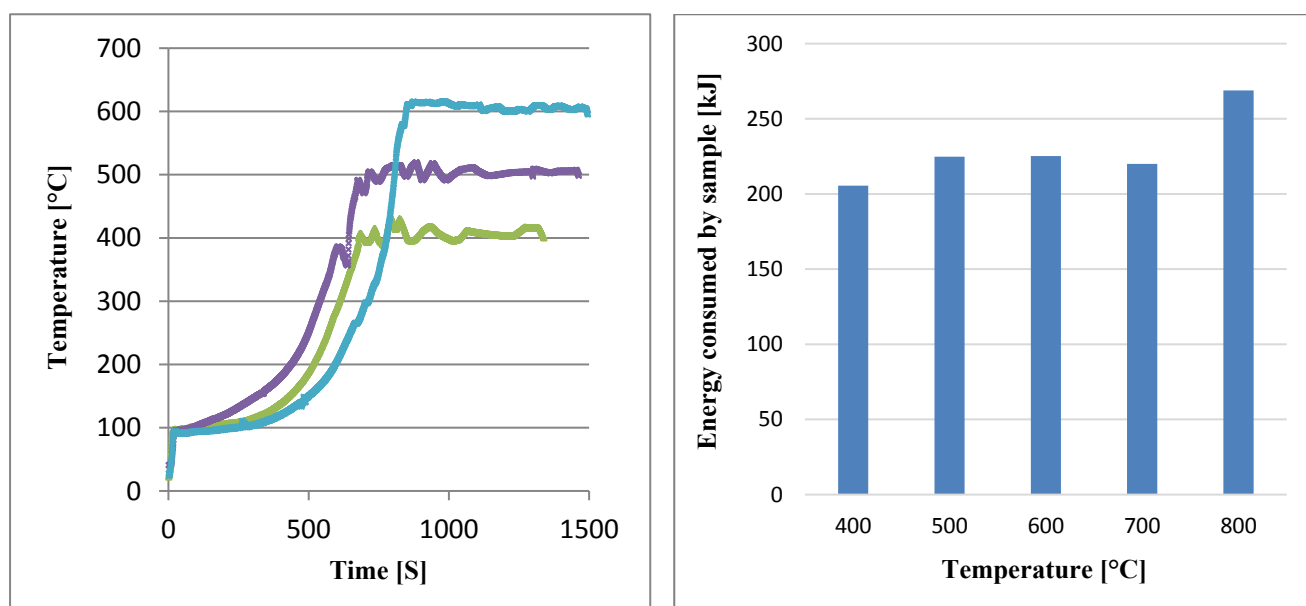
Figure 25. Example temperature profiles and average power consumed at each temperature

4.1.1 Bio-oil Yield

Table 11 shows the bio-oil, biochar and gas yields and the moisture loss from the pyrolysis, the data is an average of triplicate experiments. DAF remaining is the percentage of the dry, ash free (DAF) solids that remained at the end of the pyrolysis. Total biochar refers to the percentage of the total dry biosolids remaining after the experiment, water loss is the

percentage of the moisture removed during the pyrolysis. In all cases the final biochar was nearly dry and there was no significant correlation between pyrolysis temperature and water loss. The moisture detected in the biochar likely intruded after biochar was removed from the chamber.

The bio-oil yield is the percentage of the DAF solids converted into condensable, recoverable bio-oils, the gas yield is the balance mass loss divided by the DAF mass in the sample and is assumed to be non-condensable gases, such as CH_4 and CO produced during the pyrolysis. Previous studies on microwave pyrolysis of sewage waste have reported 38wt % yields of these gases (Domínguez et al., 2008). There is a scarcity of studies that have examined MWAP of stockpiled biosolids, but comparing the bio-oil yields in this study to those obtained through MWAP of other sewage wastes the bio-oil yield is very low. As the intent of this study is to explore the production of bio-oil via MWAP from these stockpiled biosolids, the focus remained on maximizing and assessing the bio-oil yield.

Table 11. Bio-oil produced and mass losses of sample

Temperature	DAF mass Remaining [%]	Total Biochar [%][a]	Water Loss [%]	Bio-oil Yield [%]	Gas Yield [%][b]
400°C	63.62	88.03	97.68	0.28	36.10
500°C	59.37	87.42	98.55	0.74	39.89
600°C	42.48	84.37	97.18	0.79	56.73
700°C	44.45	82.08	98.75	1.27	54.28
800°C	30.76	69.16	98.28	1.42	67.82

[a] Percentage of dry biosolids; [b] Calculated by difference

Other researchers found higher bio-oil yields from higher volatile solids sewage waste. Bio-oil yields (adjusted to DAF basis) ranging between 5.98% (using "wet sewage sludge", 1000°C pyrolysis temperature, 20 min pyrolysis time) (Domínguez et al., 2008) to 66.95% (using "sewage sludge", 500°C, 10 min pyrolysis time) (Tian et al., 2011) are shown in Table 12. The volatile solids content of the sewage waste used in these studies is higher than the stockpiled biosolids, between 55% and 76%, with correspondingly lower ash contents. Higher ash contents are reported to favour gas production, due to the interaction of the metals in the ash with the evolving pyrolysis gases (I. Fonts, Azuara, Gea, & Murillo, 2009). In particular, the ash of the stockpiled biosolids also contains a high proportion of aluminum, as

well as other heavy metals which may be acting as a catalyst for gas phase reactions. Aluminum salts and catalysts have previously been studied for cracking the tar portion of biomass pyrolysis (Bulushev & Ross, 2011; Shen & Yoshikawa, 2013). Most studies also report that bio-oil yields are maximized around ~500°C (Tian et al., 2011; Xie et al., 2014; J. Zhang et al., 2014), whereas the bio-oil yield was maximized at 800°C for this study. This may be explained by the biosolids being stockpiled, allowing for further degradation of the volatile matter into gases through microbial action. Biosolids stored in stockpiles are a source of greenhouse gas emissions for this reason (Majumder et al., 2014). The degradation of the organic matter during storage may also explain the bio-oil yields being maximized at 800°C, with a large increase in yield at 700°C; a large portion of the degradable organic matter has being consumed by bacteria and much of the remaining matter only decomposes under extreme conditions, i.e. very high temperatures. This study later tested stockpile biosolids (section 3.2.2) and fresher biosolids (section 3.2.3) in the same reactor, bio-oil yields from the fresher biosolids were in line with other studies. Stockpiled biosolids bio-oil yields remained low.

Table 12. Bio-oil yields from sewage sludge pyrolysis in other studies

Study	(Domínguez et al., 2008)	(Tian et al., 2011)	(J. Zhang et al., 2014)	(Xie et al., 2014)	These Experiments
VS [%]	65	55.5	75.5	68.57	43.5
Bio-oil Yield [%]	5.98	65.95	40.00	8.6	0.28-1.42

4.1.2 Bio-oil Composition

Table 13 shows the fraction of the phenols in bio-oil as determined from the calibration standards, as well as the proportion of the methylphenol and dimethylphenol isomers. The peak area fraction of the components is also shown. As mentioned in sections 3.4.4, 3.4.5 and 3.4.6, peak area fraction is not necessarily accurate for determining the actual proportion of a component. These are included in Table 13 to highlight the unreliability of using peak area fraction.

The '-1' and '-2' denote bio-oils produced in repeat experiments at that temperature. The DAF yield of the phenols, which is the mass of the product, divided by the DAF mass of the biosolids (17.813g). This calculation was done using the amount of a product determined by

quantification using peak area fraction, and the amount determined by quantification using the calibration curve (see 3.4.5). Both values are presented in Table 13.

To determine the peak area of the compounds in the GC-FID chromatograms, a peak area reject of $50\mu V^*sec$ was used, this value was chosen after tests showed that there was little change in the number of peaks detected with a peak area reject below this value, and many of the peaks were already close to background noise. The yield of the phenols (sum of phenol, the methylphenols and the dimethylphenols) calculated using the calibration curve was lower than the phenols yield calculated using the peak area fraction.

The difference between the total phenols percentage in bio-oil and the peak area fraction in Table 13 is extremely large, even discounting the misidentified ethylphenol peak (see 3.4.5) and the peaks that were below threshold, such as the dimethylphenol peaks in the 400°C bio-oil. In the bio-oil produced at 400°C the peak area fraction of total phenols in the bio-oil is ten times higher than the actual proportion. Possible reasons for this are; 1) the method of assessing proportions of compounds in bio-oil based on peak area fraction overestimates the proportions of compounds in the oil. Some studies report an excess of 100 compounds, as detected by GC-MS (Lin et al., 2012). A likely explanation is there are compounds in the bio-oil that cannot be resolved into peaks effectively without further sample pretreatment. This is supported by the actual percentages being lower in each case, indicating that there is a portion of the bio-oil that is not being detected, inflating the peak area fraction of the compounds that are detected. 2) The detector has a stronger response to the single ring phenols derivatives than the other compounds in the bio-oil, resulting in the peak area of the phenols being exaggerated when compared to the peaks of the other components.

This difference between the peak area fraction and the actual proportion of the compound, as well as the misidentified peaks in Table 13, indicates that qualitative assessments based on NIST Library identification and peak area fraction may be unreliable. Assessing the relationship between temperature and yields with this method was ineffective for these bio-oils as the maximum phenols yield was determined to be at 700°C with this method, as opposed to 800°C. The calculated concentrations of the repeat 700°C samples (700°C-1 and 700°C-1 Rpt) were within 5% of each other when using the calibration curve. Using peak area fraction, there was a 19.6% difference between the samples. This supports the finding that using peak area fraction is unreliable for estimating the concentrations of components.

Table 13. Proportions of phenols and carboxylic acids in the samples

| Sample | Sample Conc. [ug/mL] | Phenols[a] | | | | | | | | | Carboxylic Acids[b] | Other/ Unknown |
		Peak Area %	Actual %	DAF Yld using Peak Area % [DAF mass%]	DAF Yld using Actual % [DAF mass%]	DAF Yld Phenol [DAF mass%]	DAF Yld Methyl-phenols [DAF mass%]	2-Meth /3-Meth /4-Meth %	DAF Yld Dimethyl-phenols [DAF mass%]	2,3-Dimeth /2,4Dimeth /2,6-Dimeth %	Peak area %	Peak area %
400°C – 1	812 ± 61	87.56	4.58	0.00236	0.00012	0.0012	-	-	-	-	6.14	6.30
500°C – 1	610 ± 61	30.90	15.65	0.00069	0.00035	0.000232	0.000119	0.22/0.13/0.64	6.86E-05	0/0.59/0.41	36.85	32.25
500°C – 2	4205 ± 71	89.77	6.62	0.00340	0.00025	0.00014	8.96E-05	0.26/0.14/0.6	2.08E-05	0.36/0.13/0.50	2.38	7.84
600°C – 1	2263 ± 72	17.04	4.89	0.00164	0.00047	0.000219	0.000164	0.17/0.11/0.72	8.86E-05	0/0.44/0.56	36.64	46.33
600°C – 2	2120 ± 71	53.86	5.43	0.00620	0.00063	0.000406	0.00022	0.24/0.12/0.64	8.31E-05	0/0.46/0.54	26.37	19.78
700°C – 1	2143 ± 72	38.74	19.85	0.00502	0.00257	0.00139	0.000864	0.23/0.16/0.61	0.00032	0.26/0.22/0.52	20.96	40.30
700°C – 2	2850 ± 72	72.96	7.09	0.00774	0.00075	0.000413	0.000261	0.27/0.15/0.58	7.75E-05	0.12/0.38/0.50	14.41	12.63
700°C – 1 Rpt	2928 ± 72	48.17	20.4	0.00625	0.00242	0.00132	0.00105	0.23/0.14/0.62	0.00027	0.18/0.61/0.20	18.57	33.26
800°C – 1	3836 ± 71	48.89	21.25	0.00672	0.00292	0.00149	0.00106	0.24/0.18/0.58	0.000383	0.25/0.14/0.60	18.41	32.70
800°C – 2	3200 ± 73	42.10	25.15	0.00482	0.00288	0.00148	0.000984	0.26/0.16/0.57	0.00041	0.25/0.21/0.54	19.53	38.36

[a] Phenol, 2-methylphenol, 3-methylphenol, 4-methylphenol, 2,3-dimethylphenol, 2,4-dimethylphenol, 2,6-dimethylphenol.

[b] dodecanoic acid, tetradecanoic acid, 14-methyl-pentadecanoic acid, hexadecanoic acid, octadecanoic acid.

4.1.3 Phenols Quantification and Yield

Figure 26 shows the average yield of the phenol, total methylphenols, total dimethylphenols and total phenols on a DAF basis. The compounds were identified and quantified using GC-FID and the external calibration standard. The yield of each compound increases with temperature and weighted (according to relative uncertainty in each measurement) linear models were fitted to the data using R (R Development Core Team, 2008). The fitted relationships between the compound yields and temperatures (400°C-800°C) are as follows;

$$\ln(Total\ Phenols\ Yld.) = 0.00768 * T[°C] - 12.110; \qquad R^2 = 0.9233 \qquad (13)$$

$$\ln(Phenol\ Yld.) = 0.00777 * T[°C] - 13.125; \qquad R^2 = 0.8585 \qquad (14)$$

$$\ln(Methylphenol\ Yld.) = 0.00588 * T[°C] - 12.220; \qquad R^2 = 0.8347 \qquad (15)$$

$$\ln(Dimethylphenol\ Yld). = 0.01189 * T[°C] - 16.531; \quad R^2 = 0.8197 \qquad (16)$$

The R models also found significance at the 5% level for each of the relationships between compound yield and temperature. At 400°C, only phenol was present in detectable amounts. There was no significant relationship between the proportions of the dimethylphenol and methylphenol isomers and temperature.

The proportion of phenols in the bio-oil was between 4.57% at 400°C to 25.15% at 800°C, a higher proportion of phenols than from pyrolysis of non-stockpiled sewage wastes. The phenols are likely formed from the decomposition of lignin, which is a component of sewage sludge (Su et al., 2015), in the biosolids. This is reinforced by the increase in the phenolic yield with temperature as lignin decomposes at higher temperatures, with the highest lignin degradation rates occurring at over 750°C. The -OH functional groups detected in the FTIR analysis also suggest the presence of lignin. Lignin is also less decomposable than other components of biomass (Mihai Brebu & Cornelia Vasile, 2010) so the relative proportion of them in the biosolids would increase as more volatile components degrade during storage – explaining the higher proportion of phenols. While the phenols proportion was roughly 25%, at maximum, the overall yield of the bio-oil was low. The maximum mass of phenols produced was only 0.052g from 17.813g of dry ash-free biosolids.
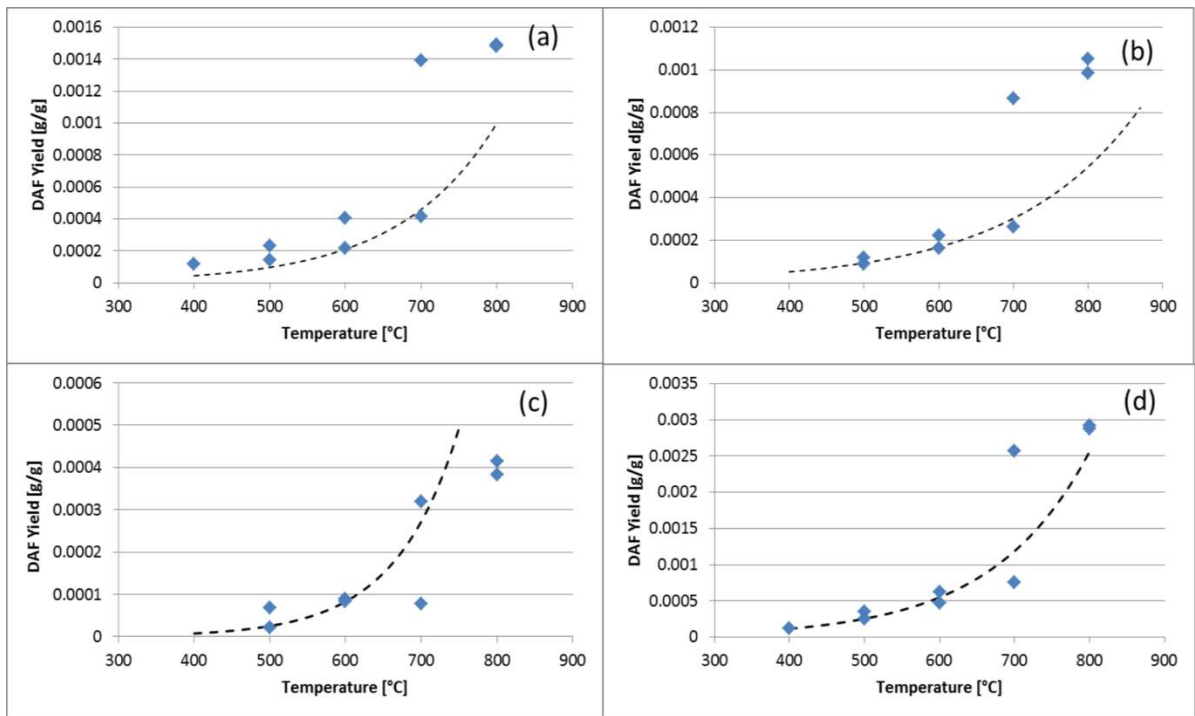
Figure 26. Phenols Yields, in grams of compound per gram of dry, ash-free biosolids (DAF), against pyrolysis temperature. (a) Phenol, (b) Total Methylphenols, (c) Total Dimethylphenols, (d) Total Phenols

4.2   Rebuilt Chamber

The chamber was rebuilt (see 3.1.1) due to the corrosion of the chamber interior, and concerns over whether the nitrogen gas flow was properly entraining the pyrolysis gases. Figure 27 compares the averaged bio-oil yields of the old chamber versus the new when the same biosolids were held at 700°C for 5-45 min. The bio-oil yields in the new chamber are consistently higher with the largest increases occurring at 5 min, with a 300% increase, and 45 min with a 200% increase.
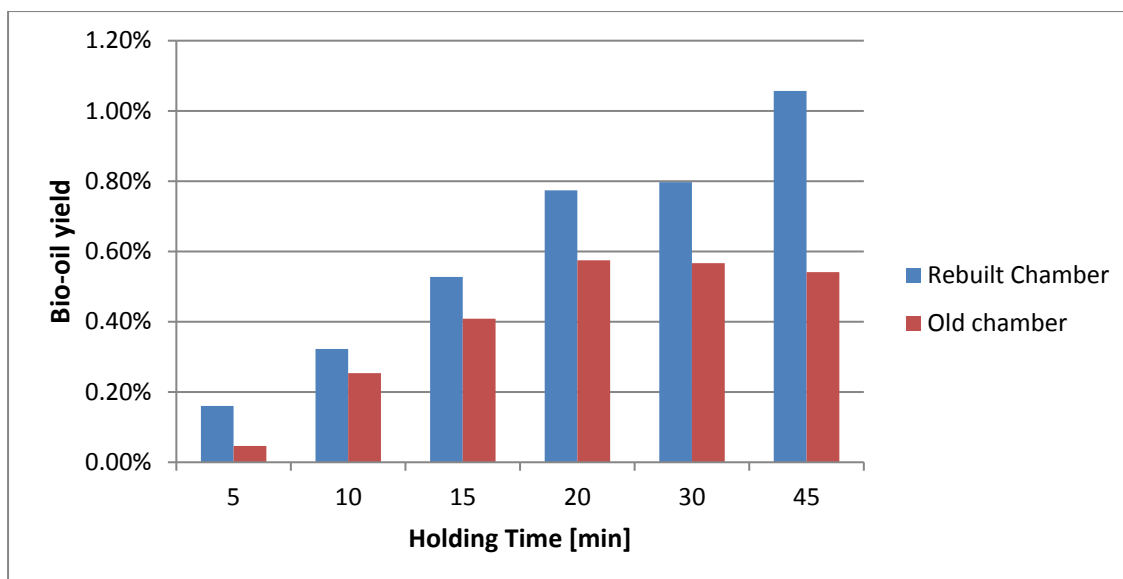
Figure 27. Bio-oil yields of old chamber vs rebuilt

The reason for the increase in the bio-oil yield is likely the reduced residence times of the pyrolysis gases, longer residence times decrease bio-oil yields as more bio-oil cracking reactions take place (Neves et al., 2011). In the rebuilt chamber, hot pyrolysis gases would entrain into the nitrogen gas flow, being cooled and rapidly removed. In the old chamber the nitrogen gas may be removing the pyrolysis gases via random mixing and not directed flow. In the rebuilt chamber, the N_2 flows from the chamber base, around the sample beaker in the centre of the chamber, to the outlet on the opposite side, this more complete flow of gases through the chamber may also eliminate pockets of un-eluted gas that occurred in the old chamber, preventing water and volatiles from condensing in these areas. Qualitatively, this is supported by the rebuilt chamber being nearly completely dry after an experiment, while the old chamber had remaining moisture. Moisture was also observed to flow into the condenser column at an earlier time than in the old chamber.

Less energy was absorbed by the sample in the rebuilt chamber than the old chamber. The difference in energy absorption decreased with pyrolysis time, from a 33% energy absorption reduction to 19%, from 5 min to 45 min. A proposed explanation is moisture was removed from the rebuilt chamber at a higher rate than in the old chamber, reducing the amount of MW energy that was wasted on heating steam and refluxing water. At longer pyrolysis times, the difference between the energy consumption of the old and rebuilt chambers decreased. This is because water was slowly removed from the old chamber, decreasing the wasted energy used to heat the unremoved water.

It was decided to continue work using the new chamber, as the main objective of this project was to assess the feasibility of MWAP for generating bio-oil from biosolids and the new chamber improved both yields and lowered energy requirements, making the process more feasible.

4.3 Pyrolysis times

The experiments discussed in this section are the 500°C and 700°C pyrolysis time experiments that were conducted in the rebuilt chamber. For the pyrolysis time experiments 80 g of the Lot 2 biosolids (see 3.3.1) was mixed with activated carbon in a dry ratio of 1:10. The mixture was then pyrolysed using the heating method in section 3.2.1. The produced bio-oils and biochar were collected and analyzed using the methods described in the Methodology. Figure 16 shows how the pyrolysis time was defined for these experiments.

4.3.1 Bio-oil yields

Figure 28 shows the bio-oil yield at each pyrolysis time for both pyrolysis temperatures. The fitted curve is a generalized logistic curve of the form;

$$Y(t) = A + \frac{K - A}{(1 + e^{-Bt})^{\frac{1}{v}}} \tag{17}$$

A is the lower asymptote, as the lowest possible bio-oil that could be produced is zero the equation becomes;

$$DAF\ Oil\ Yiled = \frac{K}{(1 + e^{-Bt})^{\frac{1}{v}}} \tag{18}$$

The unknown parameters were regressed using non-linear least-squares regression in R. A logistic curve was chosen as the data shows a logarithmic relationship between DAF bio-oil yield and pyrolysis time with $p<0.05$ and an adjusted R^2 of 0.8024 and 0.5712 for 500°C and 700°C respectively. However, as there is a limited amount of volatile solids in the biosolids sample, there is a maximum amount of bio-oil that can be produced, so incorporating an asymptote plateau into the model is appropriate.

Unlike in section 4.1, the DAF yields in Figure 28 followed the bio-oil yield trend found elsewhere in literature with the bio-oil yield being higher at 500°C than at 700°C (Xie et al., 2014). At 500°C there was a slight decrease in the yield at 45 minutes one possible

explanation is that the maximum bio-oil yield under the experimental conditions occurs around 30 minutes, whereupon all the volatile solids that can decompose to bio-oil have been pyrolysed. The biosolids samples used for the 500°C for 45 minutes experiments produced less bio-oil and may also have contained less volatile solids that could be converted into bio-oil. The overall amount of volatile solids pyrolysed increased from 30 - 45minutes for 500°C, as shown in Table 14 but produced gas instead of bio-oils.
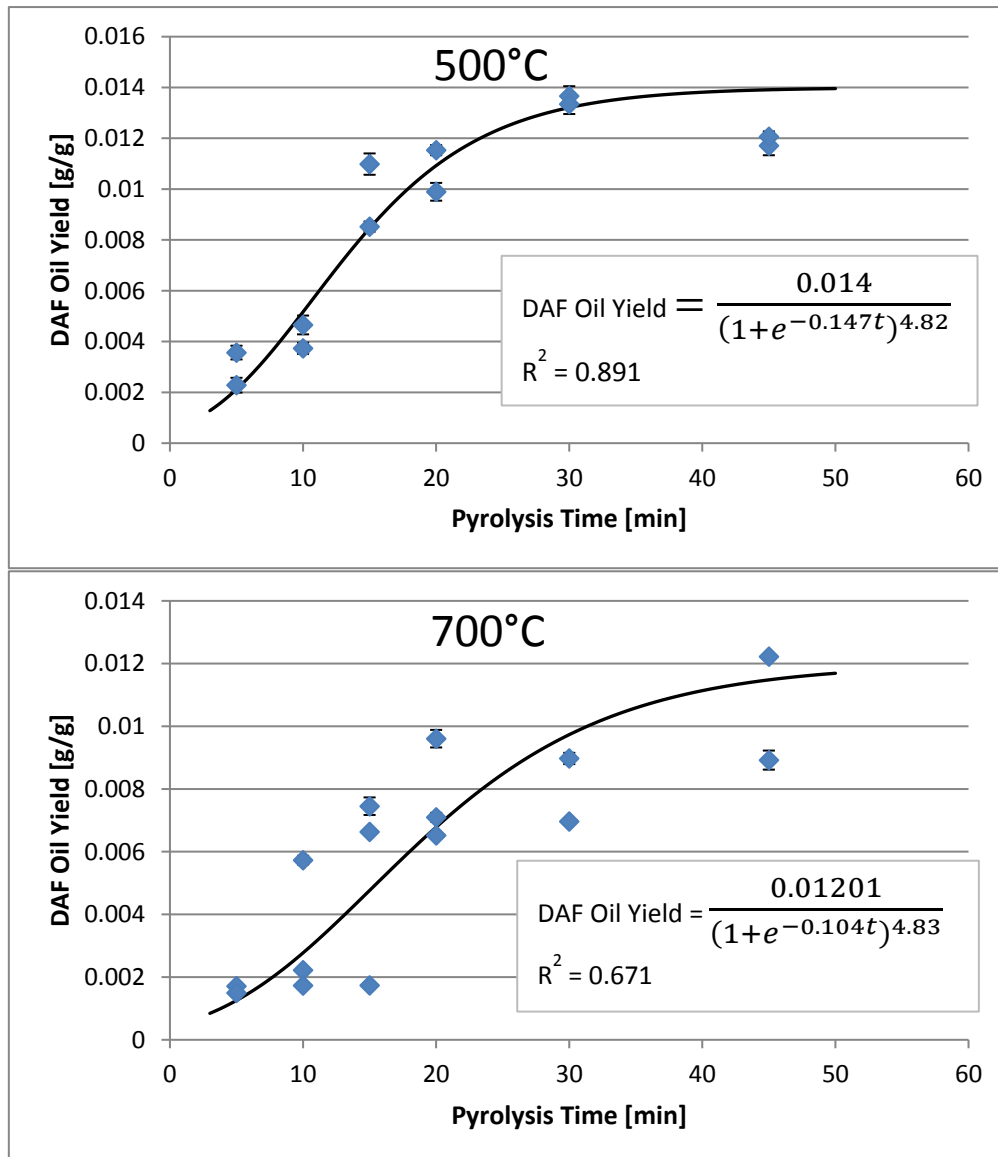
Figure 28. DAF Bio-oil yield with pyrolysis time at 500°C (top) and 700°C (bottom).

Table 14 contains the data for the bio-oil, biochar and gas yields, as well as volatile and total mass for the pyrolysis time experiments. For both temperatures, the highest rate of total mass loss occurs from 0-5 min, which is where we see the smallest rate of bio-oil production, indicating that reactions that produce lighter, non-condensable gases dominate at shorter

pyrolysis times. As the pyrolysis proceeds, the dry mass loss rate decreases, with less mass loss occurring between 5-30 min than 0-5 min. The rate of bio-oil production increases during this time. This suggests that the reaction rate of the gas producing reactions is higher than that of the bio-oils. From studies of the gas fraction produced from sewage sludge pyrolysis, the non-condensable gases produced are mainly H_2, CO, CO_2 and smaller alkanes, such as butane (Menéndez et al., 2004). Of the available volatile matter, only 59.54% and 64.77% was decomposed, at a maximum, for 500°C and 700°C respectively. This suggests that not all of the volatile matter is thermally decomposable in the oxygen free environment of pyrolysis.

Table 14. Mass losses and product yields of the pyrolysis time experiments

500°C					
Pyrolysis Time [min]	Total Mass Loss[c] [%]	Volatile Mass Loss %	Bio-oil[b][%]	Gas[ab] [%]	Biochar[b] [%]
5	47.97	37.57	0.29	37.28	62.43
10	47.57	36.52	0.42	36.10	63.48
15	50.04	44.88	0.98	43.91	55.12
20	50.46	46.22	1.07	45.15	53.78
30	51.51	49.58	1.35	48.23	50.42
45	51.66	59.54	1.19	58.36	40.46
700°C					
Pyrolysis Time [min]	Total Mass Loss[c] [%]	Volatile Mass Loss %	Bio-oil[b] [%]	Gas[ab] [%]	Biochar[b] [%]
5	50.13	41.07	0.16	40.91	59.09
10	52.28	44.36	0.32	44.04	55.96
15	50.20	47.72	0.53	47.1	52.81
20	51.77	55.56	0.77	54.79	45.21
30	54.50	56.04	0.80	55.24	44.76
45	57.03	64.77	1.06	63.71	36.29

[a]Calculated by difference. [b]Dry basis. [c]Includes moisture.

4.3.2 Bio-oil Composition

As shown in Figure 29, the most notable difference between 500°C and 700°C is that the pentadecanoic acid was not present in 500°C. The unquantified portion of the bio-oil contains alkanes, other fatty acids, nitriles and cholesterols (see **Table 8**) as well as compounds that couldn't be identified due to lack of corresponding standard (see 3.4.3). The pentadecaonic acid peak appeared to be present in the 500°C but was too small to be accurately quantified. The averaged DAF bio-oil yields and mass of the quantified components in the bio-oil are presented in **Error! Reference source not found.**.

Table 15. Yield and masses of quantified bio-oil components at each pyrolysis time (average values)

500°C								
Pyrolysis Time [min]	**Bio-oil mass [g]**	**Phenol** Yield [g/gDAF]	**Methylphenol** 2-Meth /3-Meth /4-Meth %*	Yield [g/gDAF]	**Dimethylphenol** 2,3-Dimeth /2,4Dimeth /2,6-Dimeth %*	Yield [g/gDAF]	**Hexadecanoic Acid** Yield [g/gDAF]	**Pentadecanoic Acid** Yield [g/gDAF]
5	7.24E-02	2.00E-04	0.29/0.24/0.47	3.86E-05	0.36/0.33/0.32	1.83E-05	3.36E-04	-
10	1.04E-01	2.45E-05	0.26/0.20/0.54	3.19E-05	0.35/0.34/0.31	2.16E-05	2.96E-04	-
15	2.42E-01	1.05E-04	0.40/0.24/0.36	7.40E-05	0.25/0.45/0.32	3.74E-05	4.33E-04	-
20	2.65E-01	1.89E-04	0.50/0.30/0.20	8.05E-05	0.30/0.39/0.30	6.68E-05	6.84E-04	-
30	3.34E-01	2.12E-4	0.25/0.15/0.60	1.82E-04	0.26/0.44/0.30	6.38E-05	5.56E-04	-
45	2.94E-01	1.62E-04	0.26/0.15/0.59	1.45E-04	0.27/0.44/0.28	4.40E-05	4.18E-04	-
700°C								
Pyrolysis Time [min]	**Bio-oil mass [g]**	**Phenol** Yield [g/gDAF]	**Methylphenol** 2-Meth /3-Meth /4-Meth %*	Yield [g/gDAF]	**Dimethylphenol** 2,3-Dimeth /2,4Dimeth /2,6-Dimeth %*	Yield [g/gDAF]	**Hexadecanoic Acid** Yield [g/gDAF]	**Pentadecanoic Acid** Yield [g/gDAF]
5	2.81E-02	5.09E-06	0.27/0.24/0.48	6.32E-06	0.34/0.36/0.3	5.39E-06	5.39E-04	5.61E-05
10	7.99E-02	9.67E-05	0.24/0.19/0.56	5.10E-05	0.24/0.44/0.31	2.66E-05	1.50E-03	8.43E-05
15	1.50E-01	1.28E-04	0.26/0.17/0.57	7.39E-05	0.21/0.50/0.28	4.09E-05	2.54E-04	1.12E-04
20	1.65E-01	1.55E-04	0.24/0.16/0.60	8.33E-05	0.18/0.50/0.32	4.13E-05	2.71E-04	1.07E-04
30	1.97E-01	1.53E-04	0.30/0.18/0.53	7.18E-05	0.23/0.46/0.31	4.21E-05	3.86E-04	1.54E-04
45	2.49E-01	2.14E-04	0.15/0.11/0.74	1.13E-04	0.28/0.44/0.28	3.37E-05	3.60E-04	1.84E-04
Volatile Mass = 24.763g								

4.3.2.1   500°C Pyrolysis Time Composition

At 500°C, the yield of the phenols, methylphenols, dimethylphenols, and total phenols, increased to a maximum yield at 30 minutes with a log-linear relationship to pyrolysis time with significance at the 5% level. The relationship between DAF bio-oil yields and pyrolysis time had a better F-statistic when a log-linear model was used than with a linear model. The R values were low for the modelled relationships, indicating that variables other than pyrolysis time had a significant impact on the yields of phenols;

$$Total\ Phenols\ DAF = 9.43x10^{-5}\ln(t) - 7.61x10^{-5}; \qquad\qquad R^2 = 0.4783 \qquad (19)$$

$$Phenol\ DAF = 7.62x10^{-5}\ln(t) - 1.504x10^{-4}; \qquad\qquad R^2 = 0.664 \qquad (20)$$

$$Total\ Methylphenols\ DAF = 4.71x10^{-5}\ln(t) - 6.00x10^{-5}; \qquad R^2 = 0.644 \qquad (21)$$

$$Total\ Dimethylphenols\ DAF = 1.37x10^{-5}\ln(t) - 8.62x10^{-6}; \quad R^2 = 0.509 \qquad (22)$$

The plateau of the yields of these components occurred at the same pyrolysis time as the overall bio-oil yield in Figure 28. There was no significant relationship between the methylphenol isomers in the bio-oil, with the average proportion of 2, 3 and 4 methylphenol being 0.33/0.21/0.46. The 2,6-dimethylphenol proportion was relatively constant at 30% of the total dimethylphenols at all pyrolysis times. The 2,3-dimethylphenol decreased with pyrolysis time from 36% to 27% of dimethylphenols while the 2,4-dimethylphenol increased from 33% to 44%. The hexadecanoic acid yield followed a similar trend to the phenols; linearly increasing with pyrolysis time, except the plateau of the hexadecanoic acid yield occurred at 20 minutes.

4.3.2.2   700°C Pyrolysis Time Composition

At 700°C, the yield of all the phenols for the pyrolysis time tests was best described with log-linear models. The there was a significant, positive relationship between the DAF yield and all phenols components across the pyrolysis times. The log-linear fits for the phenols components are shown below. At 700°C, the phenols components were far better correlated to pyrolysis time than at 500°C. As mentioned in section 4.1.3, the rates of lignin degradation to phenols are highest at around 750°C. The rates of phenols production from lignin degradation may be close to maximized. In this situation, length of the pyrolysis is a more important variable (up till the lignin in the biosolids is exhausted);

$$Total\ Phenols\ DAF = 1.561x10^{-4}\ln(t) - 2.415x10^{-4}; R^2 = 0.9019 \qquad\qquad (23)$$

$$Phenol\ DAF = \ 8.556x10^{-5}\ln(t) - 1.344x10^{-4}; R^2 = 0.8363 \qquad (24)$$

$$Total\ Methylphenols\ DAF = 4.034x10^{-5}\ln(t) - 6.084x10^{-5}; R^2 = 0.8027 \qquad (25)$$

$$Total\ Dimethylphenols\ DAF = 4.283x10^{-6}\ln(t) - 3.837x10^{-6}; R^2 = 0.5175 \qquad (26)$$

The distribution of the dimethylphenol isomers did not change with pyrolysis time and the average proportion was 0.24/0.45/0.30 of 2,3/2,4/2,6-dimethylphenol. The proportion of 2-methylphenol in the total methylphenol did not vary significantly and was an average of 24.2%. The 3-methylphenol proportion decreased with pyrolysis time while the 4-methylphenol increased. The hexadecanoic and pentadecanoic acid yields are also proportional to pyrolysis time, the hexadecanoic acid increased with a log-linear relationship while the pentadecanoic relationship to pyrolysis was best fitted with a linear curve (F-statistic of 22.41 to 10.49);

$$Hexadecanoic\ Acid\ DAF = \ 1.36610^{-4}\ln(t) - 1.546x10^{-4}; R^2 = 0.7854 \qquad (27)$$

$$Pentadecanoic\ Acid\ DAF = \ 3.214x10^{-6}t + 5.130x10^{-5}; R^2 = 0.6615 \qquad (28)$$

The mass yield of the quantified components increased with pyrolysis time at both 500°C and 700°C (see **Error! Reference source not found.**), but the quantified proportion of the oil mass decreased (Figure 29). This suggests that additional compounds were being formed at longer pyrolysis times, possibly due to secondary reactions, or that some of the components in the bio-oil have formation rate that initially lags behind the quantified components. In the bio-oils produced at 500°C, the quantified proportion approximately halved after 5 minutes. For bio-oils produced at 700°C the reduction in the quantified proportion was less, from about 14% at 5 and 10 min, to about 10% for the other pyrolysis times. The quantified proportion of the bio-oil was also very stable after 10 minutes, suggesting that the composition of the bio-oil produced at 700°C had less variation with time, than the bio-oil produced at 500°C.
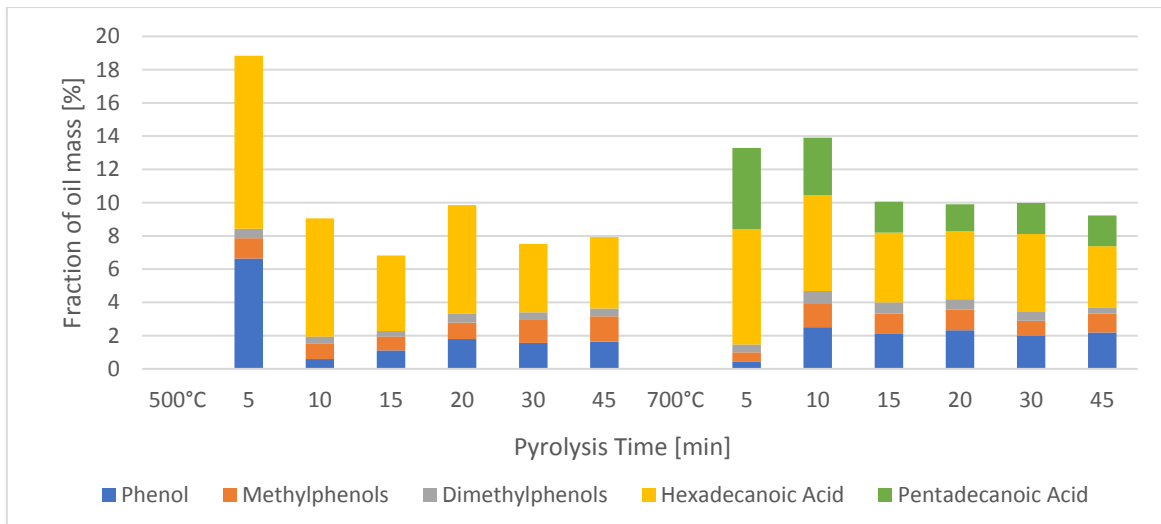
Figure 29. Percentage of the quantified compounds at 500°C (left) and 700°C (right) pyrolysis time bio-oils.

4.3.3 Bio-oil Energy Efficiency Analysis

The bio-oil energy efficiency refers to how much of the microwave energy absorbed by the biosolids can be recovered by combusting the bio-oil, not accounting for energy losses during combustion. The lower heating value (LHV) of the bio-oils, as received, was calculated using the method described in section 3.3.6. The bio-oil for all tests ranged between 30-33 kJ/kg LHV, which is within the 30-40 kJ/kg HHV reported by other studies (Isabel Fonts et al., 2012; L. Zhang et al., 2014).

For the 500°C bio-oils, there was no significant difference between the LHV of the bio-oils at the analyzed pyrolysis times of 5 minutes, 30 minutes and 45 minutes, so the average value was used in Table 16. As the LHV did not vary significantly with pyrolysis time, the efficiency was determined by only the mass of oil that could be produced, compared to the energy consumed. At 20 minutes the amount of energy used per gram of oil produced was the lowest, providing an efficiency of 3.10%.

At 700°C, the LHV has a slight positive relationship with pyrolysis time. The maximum energy efficiency of 2.28% occurred at 45 minutes but the energy efficiency at the time was similar to that of 15 – 30 minutes, with the lowest energy efficiency in that range being only 16.5% lower than the 45 minutes efficiency. Overall, the bio-oil energy efficiency is very poor due to the low bio-oil yield of the pyrolysis. Despite the chamber rebuild, the oil yields were still more than three times lower than those found in other works (see Table 12).

Table 16. Energy analysis of the 500°C and 700°C pyrolysis time bio-oils

500°C				
Pyrolysis Time [min]	LHV [kJ/g]	kJ absorbed/g biosolids	kJ/ g Bio-oil produced	Energy Efficiency
5	31.17	1.97	2274.91	0.91%
10	30.94	1.86	1432.43	1.32%
15	30.71	2.09	694.17	2.71%
20	30.48	2.02	608.31	3.08%
30	30.01	3.35	801.18	2.30%
45	30.71	3.41	926.29	2.03%

700°C				
Pyrolysis Time [min]	LHV [kJ/g]	kJ absorbed/g biosolids	kJ/ g Oil produced	Energy Efficiency
5	31.91	1.41	2862.59	0.71%
10	32.14	1.66	2065.50	1.19%
15	32.36	2.10	969.35	2.19%
20	32.33	2.51	1041.83	2.03%
30	32.24	2.61	1082.35	1.95%
45	33.22	3.00	944.62	2.28%

4.4 Storage Effects

The bio-oil yields from the Temperature Effects Experiments and Pyrolysis times experiments were lower than the bio-oil yields from other research, even after the chamber rebuild. For this reason, it became necessary to explore the possibility that the storage time had adversely impacted the bio-oil yields from the stockpiled biosolids.

To examine the effect of storage time; biosolids were collected at a local wastewater treatment plant and the entire amount was refrigerated in a sealed container within an hour of collection to prevent degradation and used in all experiments. The storage was done in two batches, in both cases the biosolids were placed into aluminum trays, in a 1.25-inch-thick layer, turned every week, and stored outside in an undercover area for 4 to 30 days. The biosolids were stored during the periods of 01/05-28/05 and 4/06-04/07. The average temperature, humidity and total rainfall (though the biosolids were kept out of the rain) during these times are noted in Table 17. The weather was similar over both storage periods, except for rainfall. The moisture content of the biosolids was adjusted to 60% for all experiments as some studies suggest that the moisture content impacts the bio-oil production (Beneroso et al., 2014a). 60% was chosen as at 1 week and 11 days storage time, the moisture content of the biosolids was almost 60% naturally. The biosolids were then pyrolysed at 500°C and 700°C for 20 minutes.

Table 17. Meteorological data for the storage periods.

01/05-28/05	Min Temperature [°C]	Max Temperature [°C]	Rainfall [mm]
Mean	21.2	29.8	
Lowest	15.4	27.2	0
Highest	24.7	31.7	0.4
Total			0.4
04/06-04/07	**Min Temperature [°C]**	**Max Temperature [°C]**	**Rainfall [mm]**
Mean	17.5	27.1	
Lowest	10.4	19.9	0
Highest	21.6	29.8	40.8
Total			57.8

4.4.1 Volatile solids and Bio-oil Yield

The volatile solids (VS) of the biosolids was tracked during the storage time using the method in section 3.3.1 and is presented in Figure 30. From Figure 30, the VS content of the biosolids decreases with storage time, with the most rapid VS loss occurring between 0-4 days and 4-7 days when the amount of labile carbon was highest. The biosolids used for the 500°C experiments had a steadier decrease in VS content with time, while the 700°C had a much sharper loss of VS with 90% of VS loss occurring in the first week of storage. This may be explained by the slightly higher temperature during May, promoting the growth of bacteria which consumed the VS. The DAF oil yield at 700°C generally decreases with temperature, with an increase in bio-oil yield notably occurring at 4 days.

A log-linear curve describes the relationship between bio-oil yield and storage time slightly better than a linear equation, with an F-test statistic of 15.34 to 17.42. Equations (29) and (30) give the relationship between DAF bio-oil and storage time (in days). Note the equations have been rearranged to have bio-oil yield on the left-hand side instead of $\ln(Bio\text{-}oil\ yield)$.

$$700°C\ Bio\text{-}oil\ yield\ \left[\frac{g_{oil}}{gDAF}\right] = 0.0907e^{-0.0223t} \qquad\qquad R^2 = 0.56 \qquad (29)$$

$$500°C \text{ Bio-oil yield } \left[\frac{g_{oil}}{gDAF}\right] = 0.0294e^{-0.0234t} \qquad\qquad R^2 = 0.295 \qquad (30)$$

While the scatter in the data points means that an exact curve is difficult to fit, the relationship between storage time and DAF oil yield is very significant with p=0.00129. The DAF oil yield was higher at 700°C than at 500°C, contrary to literature where the maximum bio-oil yield is generally identified as being around 500 - 550°C (see 4.1.1).

During experiments, it was observed that volatiles began to rapidly flow into in the first condenser between 280°C to 300°C, while the sample was heating to pyrolysis temperature, and continued to flow for the duration of the experiment. TG and DTG analysis of fresh sewage waste in other studies has observed sharp mass loss peaks in this temperature range (Gao et al., 2014). This formation of volatiles at 300°C was not observed with the older, stockpiled Victorian biosolids.

The decay of both the DAF oil yield and the VS with storage time indicates the effect of aging is two-fold, the VS content decreases while the proportion of the VS that pyrolyzes to bio-oil also decreases under these conditions. This supports the suggestion in section 4.1.1 that the low bio-oil yields are due to the extended storage time of those biosolids. The increase in the bio-oil yield at 4 days could be due to inhomogeneity in the biosolids, or a VS degradation effect, where the slightly degraded VS have been broken into smaller molecules and is easier to pyrolyze into bio-oil. The 500°C experiments have a less clear pattern than the 700°C. The 21 days experiments for the 500°C storage time set could be discounted as the total bio-oil produced differed significantly in each repeat, with values of 0.111g, 0.78g and 0.25g. The stored sludge batch used in these experiments may not have been homogenized as well as in the other experiments. If the 21 days experiment data points are kept, the relationship is not significant with p = 0.4. If the data points are discarded there is a relationship between storage time and DAF oil yield at the 5% significance level (p=0.0394), for the log-linear model. Based on these findings it seems that storage does not impact the bio-oil yields when the biosolids are pyrolysed at 500°C.
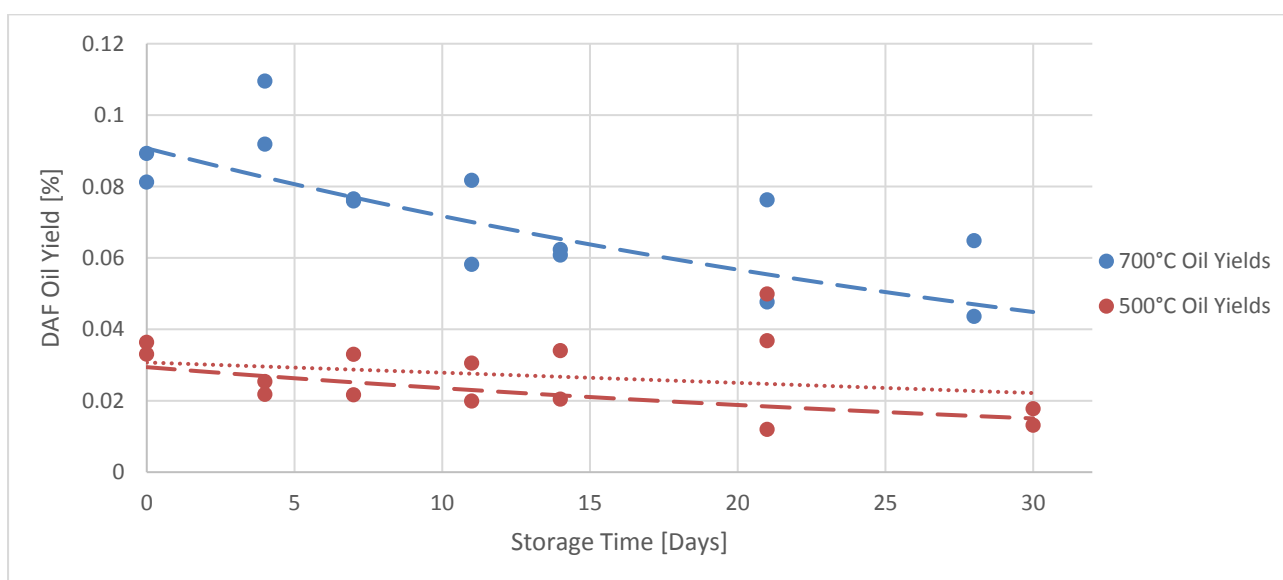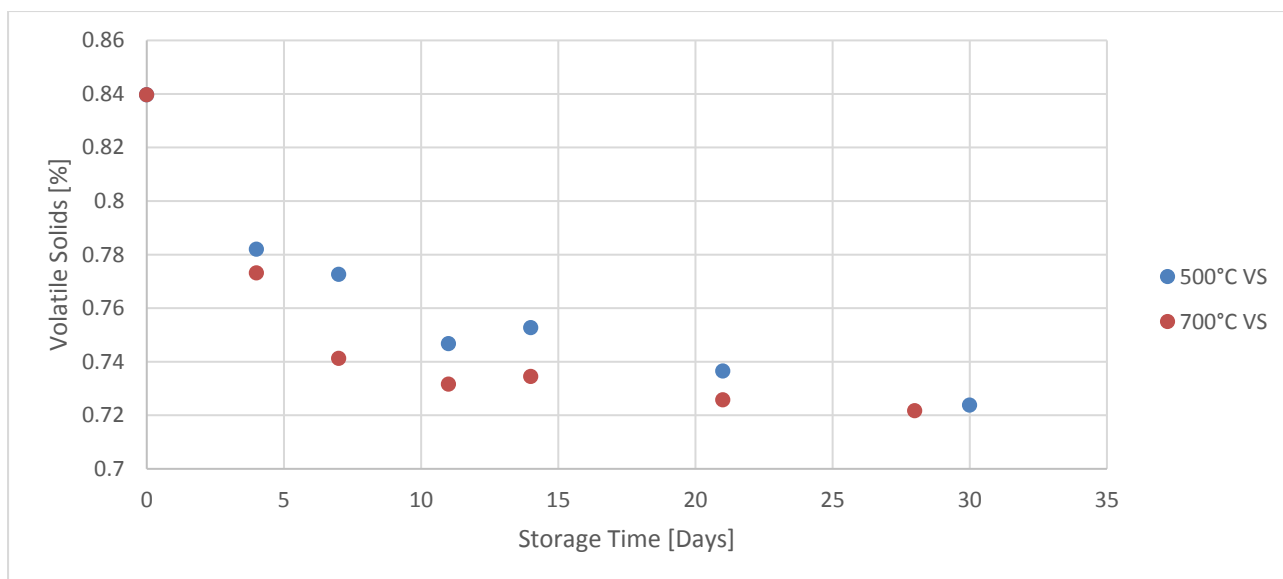
Figure 30. Volatile solids (top) and DAF oil yield (bottom) versus storage time for 500°C and 700°C.

4.4.2 Bio-oil Composition

The DAF yields of the quantified components in the bio-oil and the volatile mass of the biosolids pyrolysed are presented in Table 18. The quantified components had a lower proportion in the bio-oil than with the stockpiled biosolids, with a wider range of compounds being produced, based on the number of peaks in the GC-FID chromatograms. The quantified components were a maximum of 12.4% of the bio-oil, at 700°C, 28 days storage time. The net mass of the single ring phenols in the bio-oil did not change significantly with storage time at neither 500°C or 700°C. These findings are in agreement with those in section 4.1.3, where it was postulated that the phenols from the biosolids are predominately from lignin,

which degrades quite slowly, and storage time has less of an impact on their yield than other on components in the bio-oil.

At 500°C there was no significant change in the proportion of methylphenol and dimethylphenol isomers. The proportion of 2/3/4-methylphenol isomers was an average of 0.14/0.11/0.75. The average proportion of 2,3/2,4/2,6-dimethylphenol isomers was 0.23/0.40/0.37. At 700°C there was a significant relationship between storage time and the proportions of both the methylphenol and dimethylphenol isomers. For the methylphenol isomers, the 3-methylphenol proportion decreased with storage time while the 4-methylphenol proportion increased. The 2,3-dimethylphenol and 2,4-dimethylphenol proportions decreased with pyrolysis time, while the 2,6-dimethylphenol increased.

The combined hexadecanoic and pentadecanoic acid yields at 700°C decreased with the storage time with a relationship (p=0.0463) that was best described with a log-linear model, similar to the total bio-oil yield. The decrease in yield of the total bio-oil and total yield of carboxylic acids was similar, with the slope of model being -0.0234 and -0.0253 respectively. Considering each carboxylic acid separately, hexadecanoic acid itself had a negative relationship to pyrolysis time with a significance of p=0.00809, meaning that longer storage times reduce it yields. The pentadecanoic acid yield also had a slight negative relationship to storage time at 700°C.

For the experiments at 500°C, the combined hexadecanoic and pentadecanoic acid yields did not have a relationship at the 5% significance level with p=0.0653. Individually, a log-linear model of the pentadecanoic acid showed a significant, negative relationship between the pentadecanoic acid yield, and storage time, with a significance of p=0.0305. The hexadecanoic acid did not have a significant dependency on storage time at 500°C. It should be noted that the stockpiled biosolids produced no quantifiable amount of pentadecanoic acid at 500°C (see 4.3.2).

Table 18. DAF yields and masses of quantified components in storage time tests

500°C								
Storage time [days]	**Phenol**	**Methylphenol**		**Dimethylphenol**		**Hexadecanoic**	**Pentadecanoic**	**Volatile Mass**
	DAF Yld [g/gDAF]	**2-Meth /3-Meth /4-Meth %***	**DAF Yld [g/gDAF]**	**2,3-Dimeth /2,4Dimeth /2,6-Dimeth %***	**DAF Yld [g/gDAF]**	**DAF Yld [g/gDAF]**	**DAF Yld [g/gDAF]**	**[g]**
0	1.52E-04	0.13/0.11/076	2.35E-04	0.21/0.37/0.41	5.70E-05	1.49E-03	8.74E-04	24.22
7	1.17E-04	0.15/0.12/0.74	1.83E-04	0.23/0.40/0.37	4.90E-05	1.01E-03	6.28E-04	22.29
14	1.95E-04	0.14/0.20/0.74	2.84E-04	0.23/0.42/0.35	7.30E-05	1.49E-03	9.89E-04	21.72
21	4.31E-04	0.13/0.09/0.78	5.82E-04	0.20/0.43/0.37	1.42E-04	2.62E-03	2.54E-03	21.25
30	9.33E-05	0.15/0.13/0.72	1.49E-04	0.29/0.38/0.34	3.97E-05	1.01E-03	3.38E-04	20.88
700°C								
Storage time [days]	**Phenol**	**Methylphenol**		**Dimethylphenol**		**Hexadecanoic**	**Pentadecanoic**	**Volatile Mass**
	DAF Yld [g/gDAF]	**2-Meth /3-Meth /4-Meth %***	**DAF Yld [g/gDAF]**	**2,3-Dimeth /2,4Dimeth /2,6-Dimeth %***	**DAF Yld [g/gDAF]**	**DAF Yld [g/gDAF]**	**DAF Yld [g/gDAF]**	**[g]**
0	4.35E-04	0.16/0.13/0.72	3.65E-04	0.29/0.47/0.23	1.70E-04	4.18E-03	2.01E-03	24.23
7	4.70E-04	0.13/0.10/0.76	1.64E-05	0.24/0.52/0.24	1.90E-04	2.83E-03	1.30E-03	21.39
14	3.90E-04	0.15/0.13/0.72	1.53E-04	0.21/0.36/0.43	2.05E-04	3.67E-03	1.74E-03	21.19
21	4.30E-04	0.14/0.11/0.74	3.45E-04	0.23/0.38/0.39	2.60E-04	2.39E-03	1.58E-03	20.95
28	1.15E-03	0.12/0.09/0.79	8.75E-04	0.13/0.44/0.43	1.16E-04	2.72E-03	1.79E-03	20.82

*These proportions are averaged values so may not add to 1.

From the elemental analysis, the most significant change in the CHNS content of the bio-oil was the decrease in the carbon content of the bio-oil at 700°C with longer storage times. Three samples of bio-oil were analysed for each temperature, bio-oil from the fresh biosolids, bio-oil produced from biosolids in the middle of the storage period, and at the end of the storage. The reduction in carbon content is expected as a greater proportion of the organic carbon in the biosolids would be oxidized to CO_2 during storage (Majumder, Livesley, Gregory, & Arndt, 2015). The reduced carbon content is the primary contributor to the lower energy content of the pyrolysis bio-oil (as determined by the method in 3.3.6).

Table 19. Elemental composition and calorific value of the bio-oils and biosolids

	Storage days	C [%]	H [%]	N [%]	S [%]	O [%]	Energy Content [kJ/g]
500°C	0	69.11	9.25	8.64	0.00	13.01	31.59
	11	54.25	8.68	5.71	0.32	31.03	26.50
	30	64.27	7.95	7.36	0.31	20.11	28.41
700°C	0	68.92	8.93	7.66	0.00	14.49	32.18
	14	60.06	7.78	8.55	0.35	23.26	24.27
	28	53.57	8.23	6.66	0.34	31.19	23.46
Biosolids	0	34.12	5.61	6.04	0.68	37.50	12.77

4.4.3 Bio-oil Energy Efficiency Analysis

Comparing the energy efficiency of the stockpiled Victorian biosolids (see Table 16) to that of the stored local biosolids (see Table 20). The energy efficiency is higher with lower storage times as both the bio-oil yield and the calorific value of the bio-oil is higher. For 500°C bio-oil at 21 days storage time, the value for the calorific value was averaged from the relationship between the analysed bio-oils as there was no relationship between storage time and calorific value at 500°C (though there was at 700°C). 21 days was examined since the 21 days storage bio-oil yields were of interest as outliers (as noted in 4.4.1) and the average bio-oil yield at 3 weeks was similar to that achieved with fresh biosolids. The efficiency at 3 weeks was still lower than that of the bio-oils from the fresh biosolids though. The highest energy efficiency in this study was achieved with 700°C pyrolysis of the fresh biosolids at 13.35%.

Table 20. Energy analysis of 500°C and 700°C bio-oil

500°C Pyrolysis of Stored Biosolids			
Biosolids Storage Days	kJ absorbed/ g biosolids	kJ/ g Oil Produced	Energy Efficiency
0	2.19	188.88	9.89%
11	2.46	323.81	3.99%
21	3.05	248.18	5.92%
30	1.90	436.2	2.98%
700°C Pyrolysis of Stored Biosolids			
Biosolids Storage Days	kJ absorbed/ g biosolids	kJ/ g Oil Produced	Energy Efficiency
0	3.87	136.01	13.35%
14	4.15	229.22	5.67%
28	4.49	302.05	3.56%

4.5 Key Findings

- Phenols and carboxylic acid were 25% and 17% of the bio-oil by mass, respectively, and were the largest components of the bio-oil.
- Energy efficiency was highest for stockpiled biosolids at 15 mins and 20 mins for 500°C and 700°C.
- Bio-oil yields were maximized at 30 min at 500°C where they plateaued. At 700°C, bio-oil yields were maximized, where they were beginning to plateau.
- The bio-oil yields from the stored local biosolids were higher than that of the stockpiled Victorian biosolids.
- Shorter storage times increased bio-oil yields. 700°C bio-oil yields were higher.
- The mass of produced phenols stayed the same over storage time while the mass of fatty acids decreased. This supports the theory that the sludge degrades over time until only very stable compounds (like phenol-producing lignin) remain.

5 Economic Analysis

The aim of this section is to develop a framework to assess the economic feasibility of using microwave assisted pyrolysis to treat biosolids. This is not a comprehensive analysis and larger scale testing is required before definitive conclusions can be drawn. The purpose of this analysis is to conduct a preliminary assessment and develop a framework that could be used for larger scale studies.

5.1 Value Generation from Biosolids by Microwave Assisted Pyrolysis

A goal of this project (see 1.3) was to determine how MWAP compared as a biosolids management technique that could be used on its own, or in combination with traditional biosolids management methods. The comparison was done based upon the cost of beneficial biosolids use, which is an average of $300/ dry tonne in Australia (Australian and New Zealand Biosolids Partnership, 2015). It was assumed that a cost of less than $300/ dry tonne corresponded to net savings for biosolids beneficial use, and constituted a positive net present value. The beneficial use aspect of MWAP was also considered as some of the biosolids stored at Melbourne Water WWTPs are unsuitable for land application, which is the majority beneficial use of biosolids in Australia.

5.1.1 Production of Bio-oil

The produced bio-oil is a potential source of energy and chemicals. For the purposes of this analysis, it is assumed that each of these uses of the bio-oil is mutually exclusive (i.e. if the bio-oil is used for chemicals it can't be used for energy). For the quantified components of the bio-oil, the reference wholesale prices, based upon averaged market prices from the Molbase Chemical Marketplace (MOLBASE, 2015) along with the maximum mass of the compound produced in the stockpiled biosolids MWAP, are shown in Table 21.

Table 21. Values of components and masses produced

Component	Price[a]	Highest component mass from stockpiled biosolids [g/g biosolids]
Phenol	$1.39/kg	0.0265
2-Methylphenol	$24kg	0.00449
3-Methylphenol	$3.40/kg	0.00262
4-Methylphenol	$6.54/kg	0.0107
2,3- Dimethylphenol	$2.08/kg	0.0017
2,4- Dimethylphenol	$10.60/kg	0.001
2,6-Dimethylphenol	$4.03/kg	0.0041
Hexadecanoic Acid	$1.22/kg	0.0169
Pentadecanoic Acid	$750/kg	0.00455

[a] Sale prices taken from Molbase reference price (MOLBASE, 2015).

While some of the components are have high monetary value, their mass fraction is low. There may be more valuable components within the oil but the overall mass of oil produced from the stockpiled biosolids is low, as discussed in section 4. The pentadecanoic acid price is larger than the other quantified components, which is due to less pentadecanoic acid being produced industrially. The primary use for pentadecanoic acid is for tracking milk fat consumption (Smedman A, Gustafsson I, Berglund L, & Vessby B, 1999) as well as perfume manufacture. The high price may simply reflect the amounts that are produced, as there is only a small demand. As the prices in Table 21 are sale prices, profit margins were used to determine the value of the chemical components. Values of 5.44%, and 9.63% were used for the margins and were based upon the average net profit margin on product sales for the chemical manufacturing industry being 5.44% for each quarter (as of Nov 2016) and the twelve trailing month average being 9.63% (CSImarket.com Inc, 2016). It should be noted that these margins may not necessarily apply to chemicals produced via MWAP, but due to lack of data on such chemicals, the profit margins of chemicals produced through conventional processes were applied to this scenario.

The use of the bio-oil for energy would allow some of the energy used in the MWAP to be offset. The energy of the bio-oil, versus the energy consumption is shown in Table 16 and Table 19. Use of the bio-oil in this way would be simpler than extracting individual components, as the bio-oil may be able to be burned onsite, and the combustion would

dispose of the bio-oil, which contains environmental pollutants, such as phenols. The oil may need upgrading though, which would increase costs, due to high oxygen content.

5.1.2 Mass Reduction

The stockpiled biosolids studied were approximately 40% water by mass. This is low compared to the average water content of biosolids in Australia, which is typically 79% by mass (Australian and New Zealand Biosolids Partnership, 2016). For land application, the most commonly used method in Australia (see 2.2), the largest single cost is transportation, which could be decreased via mass reduction through the application of MWAP. As shown in section 4.1.1, the MWAP almost completely dries the biosolids. In addition, a smaller amount of the total mass is lost through thermochemical decomposition. This mass loss lowers the cost of the transportation. For stockpiled biosolids the total mass loss averaged around 50%, leading to potentially significant savings in disposal of the final product of the MWAP, when compared to untreated stockpiled biosolids. In Australia, the average distance biosolids are transported from metropolitan areas is 200-300 km (Darvodelsky, 2012), and this distance is expected to grow as increasing production of biosolids requires transportation longer distances to dispose of the biosolids. If the resulting biochar from the MWAP is to be disposed to landfill, the decreased mass will also lower the costs of landfill levy fees, which are about $75/tonne in Victoria (John Marsden Associates, 2014). The median cost for transporting solid waste in the typical 20 tonne tipper is $2/tonne.hr (John Marsden Associates, 2014). To calculate the transportation costs, it was assumed that it takes three hours for the biosolids or biochar to be transported to its destination, based upon the typical 300 km transport distance, costing $6/tonne. This provides a total cost of $81/tonne for landfill disposal of generic biosolids (including the moisture). It should be noted that these expenses could be avoided if the biochar could be left onsite but this option would undermine the goal of reducing the amount of biosolids in stockpiles. The biosolids stockpiles would simply be replaced with biochar.

5.1.3 Beneficial Use of Biochar

The conversion of the biosolids to biochar from the MWAP is a useful benefit of the process. Previous studies have found that the heavy metals in sewage waste are well incorporated into pyrolysis biochar and are not available to leach into the environment (Evita Agrafioti, George Bouras, Dimitrios Kalderis, & Evan Diamadopoulos, 2013; Taoze Liu, Bangyu Liu, & Wei Zhang, 2013). The high temperature and application of microwave radiation also results in the death of the pathogens that existed in the biosolids (Hong et al., 2004). The sterility and

low risk of contamination of biochar compared to biosolids, as well as the reduction in mass, means that there are more avenues of disposal or end-use for the biochar than biosolids.

The calorific value of the biochar was not considered as a beneficial use. The ash content of the biochar is 60% at minimum. This high ash content poses significant technical challenges; in particular the high proportion of aluminum will contribute to slagging. (Niu, Tan, & Hui, 2016). The production of fly ash from the combustion of biochar would also negate any advantages biochar offers by better incorporating heavy metals into the char matrix (see 2.3.1.1).

The most probable use of the biochar is application as a fertilizer, since biochar contains the phosphorus from the sewage waste, and this phosphorus is in a bio-available form (Taoze Liu et al., 2013). A study on the effects of applying biosolids to Australian farm land found that for Victoria, the average value of a dry tonne of biosolids, when applied to farmland is $7.08/dry tonne in fertilizer substitution value (McLaughlin et al., 2008). Based on the 31% increase fertilizer prices since the study, the current value would be $9.27/dry tonne.

The final solutions to manage the biochar are:

1: Apply the biochar to farm land. The reduced transport costs also improve the feasibility of this method.

2: Dispose to landfill. The low heavy metal leaching and sterile nature of the biochar mean that the contamination risk is lower than that of biosolids. This would increase the acceptability of disposing of the sewage waste to landfill. As before, the reduction in mass lowers the transportation cost, as well as landfill levies. This option is not ideal as the only beneficial use of the biosolids is bio-oil production, leaving the biochar as waste.

The above scenarios for MWAP value generation are encapsulated in equations (31) and (32). If the biochar is applied to agricultural land a flat $9.70 is added per dry tonne:

$$Value\ Generation\ with\ chemical\ recovery \left[\frac{\$}{Dry\ Tonne\ Biosolids} \right]$$
$$= Chemical\ Price \left[\frac{\$}{Dry\ Tonne\ Biosolids} \right] * Profit\ Margin \tag{31}$$

$$Value\ Generation\ with\ energy\ recovery\ \left[\frac{\$}{Dry\ Tonne\ Biosolids}\right] \quad (32)$$

$$= Energy\ produced\ \left[\frac{MWh}{Dry\ Tonne\ Biosolids}\right] * \frac{\$60}{MWH}$$

5.2 Cost of Microwave Assisted Pyrolysis Process

The obvious cost to consider for MWAP is the energy needed to run the apparatus. The energy consumption of the magnetron and the system peripherals depends upon the amount of power outputted from the magnetron, but it has been suggested (Industrial Microwave Systems, 2012) that total system efficiencies for a 2.45 GHz system ranges between 50-75%. For this analysis, the energy cost was set at $60/MWh, which is the wholesale price of energy in Victoria (Origin Energy, 2016). The energy efficiencies (η) used were 50% and 60%, the lower energy efficiencies were assumed to account for the peripherals required by the process. The MWAP apparatus would be located onsite at a WWTP, so all connection and service prices are already factored in. An alternative susceptor is required for the pyrolysis process, given the wholesale price of activated carbon ($1000/tonne). Biosolids were mixed with activated carbon in a 10:1 dry ratio. The other major variable running cost is the nitrogen needed to elute the gases and maintain the inert conditions in the chamber.

The wholesale price for nitrogen is $0.014/L, based on bulk price of nitrogen from BOC (BOC Pricing, 2016). Determining the nitrogen cost is difficult as the amount of nitrogen required for a residence time of 6.3 seconds depends upon the void volume in the pyrolysis chamber. It is also possible to use a nitrogen purge to inert the chamber, then remove the volatiles using only pump suction without nitrogen eluting the gases. Or the non-condensable gases could be recycled to elute the volatiles. Due to the different equipment and process setups possible, it was assumed that the chamber was 2 m³ to allow for 1 tonne of biosolids to be placed inside and that 20m³/min of nitrogen was supplied to maintain the residence time to the same duration as the pyrolysis experiments in section 3.2.

The cost of the MWAP treatment is calculated with equation (34), while the *Biochar disposal* is calculated using equation (35) or (36). Equation (35) calculates the cost if biochar is disposed of via landfill. Equation (36) calculates the cost if the biochar is applied to agricultural land:

$$Cost \left[\frac{\$}{Dry\ Tonne\ Biosolids}\right]$$

$$= \frac{Energy\ Absorbed\ by\ biosolids \left[\frac{MWh}{dry\ tonne\ biosolids}\right] * \frac{\$60}{MWh}}{\eta}$$

$$+ \$100(AC\ costs) + 20000[L_{N_2}/dry\ tonne] * pyrolyis\ time\ [min]$$

$$* 0.014[\frac{\$}{L_{N_2}}]\ + Biochar\ disposal\ [\$/dry\ tonne] \tag{33}$$

$$Energy\ absorbed\ by\ biosolids \left[\frac{MWH}{Dry\ Tonne\ Biosolids}\right]$$

$$= Total\ Power\ Absorbed\ during\ experiment\ [MWH]$$

$$* \frac{1}{dry\ sample\ mass\ [dry\ tonne]} \tag{34}$$

$$Biochar\ landfill\ disposal \left[\frac{\$}{Dry\ Tonne\ Biosolids}\right] \tag{35}$$

$$= \frac{\$81}{Dry\ \%\ of\ Biochar} * (1 - Mass\ Loss\ \%)$$

$$Biochar\ agricultural\ disposal \left[\frac{\$}{Dry\ Tonne\ Biosolids}\right] \tag{36}$$

$$= \frac{\$6}{Dry\ \%\ of\ \ Biochar} * (1 - Mass\ Loss\ \%)$$

5.3   Final Cost of Biosolids Microwave Assisted Pyrolysis

The final cost of microwave assisted pyrolysis for several different cases is presented in Table 22 to Table 29. The final cost per dry tonne of the microwave pyrolysis treatment is calculated as follows;

$$Final\ Cost = Cost - Value\ Generation \tag{37}$$

The final cost was calculated for four different cases across two energy efficiencies and two profit margins on chemical sales. The values for energy efficiencies and profit margins were chosen for the reasons in sections 5.1.1 and 5.2.

- Case (a): 50% efficiency and 5.44% margin
- Case (b): 60% efficiency and 5.44% margin
- Case (c): 50% efficiency and 9.63% margin
- Case (d): 60% efficiency and 9.63% margin.

These cases were then applied to the two different scenarios for biochar handling, landfill disposal and agricultural application. The values in the table are averaged results of duplicate or triplicate experiments and are in units of Australian dollars ($AUD) per dry tonne of biosolids processed. Note that cases (a) and (b), and (c) and (d), have the same final cost with energy recovery as these cases have the same energy efficiency. For this reason, the final cost with energy recovery is only presented in tables once for each energy efficiency. Final costs that are lower than the average cost of beneficial biosolids use in Australia ($300) are highlighted green for clarity. The values that were up to 10% over the average cost ($330) are indicated in yellow. These conditions are conditions possibly worth further investigation as they are just over the average cost. The chemical or energy value generated from the MWAP is also shown.

In no case does the MWAP generate value (i.e. displays a negative final cost). Table 22 and Table 23 show the final costs of microwave pyrolysis at 500°C. With landfill disposal, the cost of the microwave pyrolysis treatment was lower than the average cost for beneficial biosolids at 5 minutes pyrolysis time for cases (b) and (d) for chemical recovery, and case (c) for energy recovery. The cases in Table 22 with 10 minutes or less pyrolysis times that were not below average cost were within 10% of it. With agricultural application, pyrolysis times 15 minutes or less had a final cost less than the average cost of beneficial use of biosolids. At 20 minutes pyrolysis time, energy recovery, and chemical recovery for case (b) and (d) were within 10% of the average cost. For 500°C, energy recovery produced a lower final cost than chemical recovery.

Table 24 and Table 25 show the final costs of microwave pyrolysis treatment at 700°C. The final cost was lower than the average beneficial use cost for pyrolysis times 10 minutes or less, for all landfill disposal scenarios. Additionally, the final cost was within 10% of the average beneficial cost for chemical recovery with cases (c) and (d). With agricultural application of the biochar, the final costs are lower overall, with the final cost being higher than $300 for pyrolysis times longer than 15 minutes for cases (a) and (b). At 20 minutes pyrolysis time, the final value was lower than the average beneficial use cost, or within 10%,

for all cases. Compared to 500°C, at 700°C the final costs were lower with chemical recovery than with energy recovery, due to the bio-oils containing the high value pentadecanoic acid at this temperature.

Table 26 and Table 27 show the final costs and value of the chemicals and energy from microwave pyrolysis, at 500°C, of the aged biosolids from lot 3 (Table 7). The mass reduction and the oil production is significantly higher than with the stockpiled biosolids (see Figure 30). The final cost was still higher than $300/ dry tonne, due to the additional moisture that needed to be removed and volatile matter absorbing energy as it thermally decomposes. The final cost of the microwave pyrolysis with agricultural application was lower than the Australian average cost with case (d) with chemical recovery at 0, 21 and 30 days aging for case (d) and 30 days aging for cases (b) and (c). A few more cases were within 10% of the Australian average cost. With landfill, no storage times produced a final cost lower than the Australian average cost of $300 for beneficial use.

The final costs of microwave pyrolysis of stockpiled biosolids at 700°C are shown in Table 28 and Table 29. For landfill, the final cost was below the Australian beneficial use average with chemical recovery for cases (b), (c) and (d) at 21 days aging only. Chemical recovery with case (a) at 21 days and case (d) at 0 days were within 10% of the average cost. With agricultural application of the biochar, 21 days storage time is lower cost than the average Australian cost with chemical recovery for all cases. With case (d), all aging times had a lower cost except 7 days. With the higher chemical recovery profit margin, 0 and 28 days were within 10% of the average beneficial cost with case (c). The only energy recovery case that was close to the Australian average cost was case (c) at 21 days.

Table 22. Stockpiled biosolids pyrolysis at 500°C with landfill disposal of biochar. Values in AUD.

Pyrolysis Time [min]	Case [a]		Case [b]	Case [c]		Case [d]	Value with Chemical Recovery [5.44%]	Value with Chemical Recovery [9.63%]	Value with Energy Recovery
	Chem Recovery	Energy Recovery	Chem Recovery	Chem Recovery	Energy Recovery	Chem Recovery			
5	$311.76	$311.01	$292.05	$311.73	$291.31	$292.03	$0.03	$0.06	$0.78
10	$321.20	$320.11	$303.90	$321.18	$302.82	$303.88	$0.02	$0.04	$1.11
15	$360.08	$357.54	$339.63	$360.04	$337.09	$339.60	$0.05	$0.09	$2.59
20	$403.28	$400.51	$379.43	$403.23	$376.65	$379.38	$0.07	$0.12	$2.84
30	$510.17	$506.68	$476.04	$510.09	$472.55	$475.96	$0.10	$0.17	$3.58
45	$572.16	$569.08	$539.33	$572.10	$536.25	$539.27	$0.08	$0.14	$3.16
Australian Average = $300									

Table 23. Stockpiled biosolids pyrolysis at 500°C with agricultural application of biochar. Values in AUD.

Pyrolysis Time [min]	Case [a]		Case [b]	Case [c]		Case [d]	Value with Chemical Recovery [5.44%]	Value with Chemical Recovery [9.63%]	Value with Energy Recovery
	Chem Recovery	Energy Recovery	Chem Recovery	Chem Recovery	Energy Recovery	Chem Recovery			
5	$237.02	$236.28	$217.32	$236.99	$216.57	$217.29	$9.73	$9.76	$10.48
10	$245.96	$244.88	$228.67	$245.95	$227.58	$228.65	$9.72	$9.74	$10.81
15	$287.94	$285.40	$267.49	$287.90	$264.95	$267.45	$9.75	$9.79	$12.29
20	$331.65	$328.88	$307.80	$331.60	$305.02	$307.75	$9.77	$9.82	$12.54
30	$439.86	$436.38	$405.73	$439.79	$402.24	$405.65	$9.80	$9.87	$13.28
45	$502.03	$498.95	$469.20	$501.97	$466.12	$469.14	$9.78	$9.84	$12.86
Australian Average = $300									

Table 24. Stockpiled biosolids pyrolysis at 700°C with landfill disposal of biochar. Values in AUD.

Pyrolysis Time [min]	Case [a]		Case [b]	Case [c]		Case [d]	Value with Chemical Recovery [5.44%]	Value with Chemical Recovery [9.63%]	Value with Energy Recovery
	Chem Recovery	Energy Recovery	Chem Recovery	Chem Recovery	Energy Recovery	Chem Recovery			
5	$267.36	$268.72	$266.07	$254.30	$255.66	$253.01	$1.67	$2.96	$0.31
10	$305.00	$305.75	$303.72	$289.07	$289.82	$287.80	$2.48	$4.39	$0.55
15	$346.64	$351.03	$341.91	$327.33	$331.71	$322.60	$3.09	$5.46	$1.62
20	$378.24	$381.50	$374.09	$367.81	$360.63	$353.22	$5.39	$9.55	$1.88
30	$438.58	$444.53	$432.28	$414.36	$420.30	$408.06	$5.75	$10.18	$2.26
45	$535.79	$540.56	$529.90	$506.56	$511.32	$500.66	$8.17	$14.47	$2.23
Australian Average = $300									

Table 25. Stockpiled biosolids pyrolysis at 700°C agricultural application of biochar. Values in AUD.

Pyrolysis Time [min]	Case [a]		Case [b]	Case [c]		Case[d]	Value with Chemical Recovery [5.44%]	Value with Chemical Recovery [9.63%]	Value with Energy Recovery
	Chem Recovery	Energy Recovery	Chem Recovery	Chem Recovery	Energy Recovery	Chem Recovery			
5	$195.32	$196.68	$182.26	$194.03	$183.62	$180.97	$11.37	$12.66	$10.01
10	$235.64	$236.40	$235.64	$234.37	$220.47	$218.44	$12.18	$14.09	$10.25
15	$274.98	$279.37	$274.98	$270.25	$260.06	$250.94	$12.79	$15.16	$11.32
20	$308.26	$311.51	$308.26	$304.10	$290.65	$283.24	$15.09	$19.25	$11.58
30	$372.01	$377.96	$347.79	$365.71	$353.73	$341.49	$15.45	$19.88	$11.96
45	$472.38	$477.14	$443.14	$466.48	$447.90	$437.24	$17.87	$24.17	$11.93
Australian Average = $300									

Table 26. Aged biosolids pyrolysis at 500°C with landfill disposal of biochar. Values in AUD.

Storage Time [days]	Case [a]		Case [b]	Case [c]		Case [d]	Value with Chemical Recovery [5.44%]	Value with Chemical Recovery [9.63%]	Value with Energy Recovery
	Chem Recovery	Energy Recovery	Chem Recovery	Chem Recovery	Energy Recovery	Chem Recovery			
0	$430.83	$466.53	$393.36	$391.32	$429.06	$353.85	$51.30	$90.81	$15.60
7	$488.18	$510.52	$444.47	$463.63	$466.81	$419.92	$31.87	$56.42	$8.98
14	$453.38	$489.89	$414.17	$418.08	$450.68	$378.87	$31.87	$56.42	$9.53
21	$441.17	$512.23	$397.16	$380.14	$468.21	$336.12	$79.25	$140.29	$7.60
30	$398.69	$423.44	$372.25	$375.56	$397.00	$349.12	$30.03	$53.15	$9.31
Australian Average = $300									

Table 27. Aged biosolids pyrolysis at 500°C with agricultural application of biochar. Values in AUD.

Storage Time [days]	Case [a]		Case [b]	Case [c]		Case [d]	Value with Chemical Recovery [5.44%]	Value with Chemical Recovery [9.63%]	Value with Energy Recovery
	Chem Recovery	Energy Recovery	Chem Recovery	Chem Recovery	Energy Recovery	Chem Recovery			
0	$361.90	$397.60	$324.43	$322.39	$360.13	$284.92	$61.00	$100.51	$25.30
7	$418.79	$441.13	$375.08	$394.24	$397.42	$350.53	$41.57	$66.12	$19.23
14	$378.29	$414.81	$339.08	$342.99	$375.60	$342.49	$55.53	$90.83	$17.30
21	$373.14	$444.19	$329.13	$312.10	$400.18	$268.09	$88.95	$149.99	$17.90
30	$317.94	$342.69	$291.50	$294.81	$316.25	$268.37	$39.73	$62.85	$14.97
Australian Average = $300									

Table 28. Aged biosolids pyrolysis at 700°C with landfill disposal of biochar. Values in AUD.

Storage Time [days]	Case [a] Chem Recovery	Energy Recovery	Case [b] Chem Recovery	Case [c] Chem Recovery	Energy Recovery	Case [d] Chem Recovery	Value with Chemical Recovery [5.44%]	Value with Chemical Recovery [9.63%]	Value with Energy Recovery
0	$468.66	$528.07	$414.86	$382.82	$488.68	$329.01	$111.46	$197.30	$37.63
7	$536.60	$534.65	$482.67	$502.12	$499.94	$448.19	$44.77	$79.25	$39.00
14	$496.77	$552.32	$439.13	$409.72	$532.20	$352.08	$113.02	$200.07	$27.50
21	$319.10	$384.60	$291.98	$242.11	$373.03	$214.99	$99.96	$176.94	$23.94
28	$506.86	$596.64	$444.51	$401.11	$566.41	$338.76	$137.30	$243.05	$19.95
Australian Average = $300									

Table 29. Aged biosolids pyrolysis at 700°C with agricultural application of biochar. Values in AUD.

Storage Time [days]	Case [a] Chem Recovery	Energy Recovery	Case [b] Chem Recovery	Case [c] Chem Recovery	Energy Recovery	Case [d] Chem Recovery	Value with Chemical Recovery [5.44%]	Value with Chemical Recovery [9.63%]	Value with Energy Recovery
0	$399.73	$472.49	$345.93	$313.88	$419.75	$260.08	$121.16	$207.00	$47.33
7	$467.20	$483.05	$413.28	$432.72	$430.55	$378.80	$99.23	$168.19	$37.20
14	$421.69	$511.97	$364.04	$334.63	$457.11	$276.99	$122.72	$209.77	$29.65
21	$251.06	$330.96	$223.94	$174.08	$304.99	$146.96	$109.66	$186.64	$28.61
28	$426.11	$545.63	$363.76	$320.36	$485.66	$258.01	$147.00	$252.75	$25.10
Australian Average = $300									

5.4   Final Costs Analysis

The final cost per dry tonne of stockpiled biosolids increases with pyrolysis time at 500°C and 700°C. The reason for this is the energy and nitrogen costs increase, while the value generated does not increase as rapidly. The mass reduction lowers the cost of transportation, as described in 5.1.2, and the reduced costs from the mass reduction is large compared to the value generated from the oil, particularly for landfill disposal. At 500°C, for 5 min pyrolysis time, the value of the oil generated is $0.78 and the cost saved due to mass reduction for landfill is a much larger $65. Most of the mass loss occurs within 5 minutes the material reaching the pyrolysis temperature, as moisture is removed around 100°C and the volatile matter in the biosolids has begun to pyrolyse (see Table 14). At 500°C, from 5-45 min pyrolysis time, mass loss increases from 48 - 52%, and from 51 - 60% for 700°C. The savings from the mass reduction increase only slightly and the phosphorus value (for agricultural application only) is fixed. The increase in oil with pyrolysis time does not compensate for the running costs.

Compared to the stockpiled biosolids with a pyrolysis time of 20 minutes, the aged biosolids produced significantly more bio-oil (compare oil yields in Table 11, Table 14 and Figure 29). However, the higher oil yield from the increased volatile mass of the fresher biosolids was not enough to offset the increased energy consumption from the higher water content. Generally, case (d) was required for the MWAP to be cheaper than beneficial use. It should be noted that the water content of the aged biosolids (60%) is far lower than the average Australian moisture content for fresh biosolids, so the energy cost to remove the water would be higher for most biosolids.

Overall, the MWAP was the most cost effective for the stockpiled biosolids at shorter pyrolysis times due to the savings from mass reduction not increasing with pyrolysis time and increased bio-oil production not offsetting the nitrogen and energy costs. While the aged biosolids generated more chemical and energy value (see Table 22 to Table 29) through bio-oil production than stockpiled biosolids, the higher MWAP cost offset any value generation.

5.5   Final Costs Analysis Limitation

The analysis presented in this section does not consider the capital expenditure that would be needed to install a MWAP process, nor the technical challenges of such an installation. Larger scale tests that consider specific scenarios of MWAP, such as how much biosolids will be processed, whether the oil will be separated into its chemical components or used for

energy, are needed to evaluate these aspects of MWAP. Even if the final cost per dry tonne of biosolids is lower than the average cost in Australia, the savings may not be sufficient to justify the capital expense of constructing the MWAP process, or the increased technical complexity of the plant. Due to the simplicity of burning the bio-oil for energy – it may be the best use of the bio-oil, even if chemical recovery can have lower costs based on this analysis.

The chemical value of the oil is based upon only the quantified compounds. There may be unquantified compounds in the oil that are high value and significantly improve the economics of MWAP. The chemical value of the oil is likely an underestimate but is based upon what could be quantified during this project. Assessing the composition of the oil with methods such as peak area fraction and matching spectra of peaks to a database is not sufficiently accurate in identifying what compounds are present and in what amounts (see 3.4.3 and 4.1.2).

As the MWAP incorporates the heavy metals into the biochar it does not remove them and only prevents them leaching. The biochar still contains the heavy metals, and in a higher concentration than the biosolids, due to the MWAP reducing the biosolids mass. For this reason, the biochar still may be deemed unsuitable for agricultural application or landfill. The landfill and transportation savings could also be eliminated by not transporting the biochar and instead stockpiling it onsite. This approach would be cheaper and helpful if the biochar couldn't be applied to agriculture, but undermines one goal of this project, as mentioned in section 5.1.2.

6   Conclusions, Recommendations and Outlook

The conclusions from the research and activities in each chapter are presented in this chapter. At the end of this section possible areas for future work are identified and a brief statement overall success of the process at producing bio-oil from the stockpiled biosolids is given.

6.1   Methodology

Most studies identified groups of compounds using peak area fraction to determine compound proportions in bio-oil (section 2.6). In section 4.1.2, using peak area fraction to determine proportions of bio-oil was compared to using an external calibration standard. This work found that using peak area fraction over-estimated the amount of the compound in the oil by up to ten-fold. As shown in sections 3.4.5 and 3.4.6, identifying compounds using databases of peak spectra can misidentify compounds in the bio-oil. External standards allow for definitive identification of the compounds in the oil. Quantifying the compounds allows the value of chemicals in the oil to be more confidently assessed.

6.2   Results and Discussion

The greatest constituents in the bio-oil were phenols and carboxylic acids. Bio-oil from stockpiled biosolids had a maximum phenolic content of 25% and a maximum biosolids DAF mass yield of 0.29% (section 4.1.3). The carboxylic acids were at most 17% of the oil and had a maximum yield of 0.054% by weight. Only hexadecanoic acid was detected in the stockpiled bio-oils pyrolysed at 500°C, but pentadecanoic acid was also quantified in the bio-oils produced at 700°C (section 4.3.2). Pentadecanoic acid was detected in the bio-oils produced at both 500°C and 700°C from the stored biosolids (Table 18). Longer pyrolysis times increased the bio-oil yield up to the point where all the volatile matter that could be thermally decomposed into bio-oil had been pyrolysed.

The bio-oil yield of the biosolids that were stored for a month was higher than the stockpiled biosolids (see Figure 30). The bio-oil yield decreased with storage time and likewise the volatile content. This suggests that as biosolids age, microbial action not only decreases the volatile matter, but increases the proportion of the matter that goes to non-condensable gases (see 4.4.1). All quantified compounds in the stockpiled biosolids bio-oil were detected and quantified in the aged biosolids bio-oil. There were peaks present in the stored for up to a month biosolids bio-oil that were not present in the stockpiled biosolids and these were not quantified, since this fell outside the scope of this work. While the proportion of phenols and fatty acids in the aged biosolids bio-oil was lower than that of the stockpiled biosolids, the

higher bio-oil yield meant that the produced mass of these components was higher. The mass of phenols produced was constant with storage time, while the mass of fatty acids generally decreased (see **Error! Reference source not found.** and Table 18). This supports the idea that the volatile matter in stockpiled biosolids has a higher proportion of lignin, and other components that do not degrade under atmospheric conditions, as the easily degraded organic components have volatilized during storage (see section 4.1.3).

The design of the pyrolysis chamber is critically important to energy consumption and bio-oil production. Due to the mechanisms of microwave heating (see 2.5.3.1), the walls of the pyrolysis chamber are cooler than the pyrolysis off-gases. Rapidly removing the pyrolysis gases prevents them from condensing in the pyrolysis chamber, and absorbing additional energy as they are reheated. This can be seen with the improvements in energy consumption and bio-oil yield between the first and second redesigned chambers (section 4.2).

6.3   Economic Analysis

This study suggests that MWAP of biosolids is economically feasible in some circumstances for the stockpiled biosolids; the final cost of MWAP of stockpiled biosolids from the Victorian WWTPs was lower than the Australian average cost of beneficial biosolids agricultural application for shorter pyrolysis times (see section 5.4). Shorter pyrolysis times had a lower final cost for all temperatures and economic cases considered with the stockpiled biosolids. With more favourable conditions in the economic analysis (i.e. higher efficiency and chemical profit margins) the final for agricultural application cost was lower than the Australian average for times up to twenty minutes. Longer pyrolysis times produced more bio-oil, but this was offset by the increased energy consumption and nitrogen costs. MWAP at 700°C had a lower final cost than 500°C for both stockpiled and aged biosolids (see Table 22 to Table 29) due to higher amounts of bio-oil produced (in particular, the production of high value pentadecanoic acid) and higher mass reduction.

The mass reduction of the biosolids reducing transport costs and the associated reduction in landfill levies are significant factors in the final cost. The case where biosolids are applied to agricultural land as biochar is cheaper than landfill, though this presumes that agricultural application of the biosolids will be permitted (see 5.4).

In both the aged bio-oil and stockpiled bio-oil the pentadecanoic acid was the largest contributor to the chemical value of the bio-oil, due to its high price (Table 21), despite being only a small proportion of the bio-oil. The chemical value in the bio-oil is a conservative

estimate for this reason, as a large proportion of the bio-oil was still unquantified, so there may be similarly valuable components that are only a small proportion of the bio-oil.

While the aged biosolids produced more bio-oil, the overall processing costs were still greater than the Australian beneficial use average of $300 dry/tonne in most cases (see Table 26 to Table 29). This is due to the energy required to remove the moisture and pyrolyze the volatile matter. This suggests that fresher biosolids are much better in terms of bio-oil production, and may better overall if they could be cheaply and quickly dried first. If the biosolids could be sufficiently solar dried and processed before the organic matter had been degraded to the extent of the stockpiled biosolids, the costs would decrease and the final cost would be lower.

6.4   Recommendations

- Due to the complex composition of the bio-oil, there are likely to be additional valuable compounds not identified in this study. Future studies should utilize the methods in this study to quantify a larger proportion of the bio-oil to better assess the bio-oil value.

- Future studies should design processes in such a way as to eliminate, or reduce the use of nitrogen. The nitrogen is a significant proportion of the costs and the proportion would need to be drastically lowered for a full-scale process.

- The ideal biosolids for bio-oil production are fresh (high volatile matter content) but dry. Further work should focus on biosolids that are fresh but have undergone a drying process, such as a short period of solar drying or centrifuging.

- Larger scale tests should be carried out on suitable biosolids to determine the scalability of MWAP, how scaling up effects energy efficiency, and identify problems that arise with larger volumes of biosolids treated.

- Larger scale studies should employ a more comprehensive methodology for the assessment of the final cost of the process. In particular, determining how feasible it is to extract individual components from the bio-oil, considering what peripheries would be needed by the process, and comparing the final cost against the costs of the specific WWTP the biosolids came from.

6.5   Overview

The stockpiled biosolids produced low amounts of bio-oil due to the degradation of the volatile matter during storage. The produced bio-oil is very complex so it is challenging to quantify each component in the bio-oil. The process consumed a large amount of energy as well as nitrogen and susceptor. The process is also technically complex with its use of microwave energy and requires careful design to prevent inefficiencies, as shown by the impact of the chamber redesign. Specialized equipment is also needed, such like the microwave compatible thermocouples, and power measuring equipment.

However, biosolids that were stored for less time than the stockpiled biosolids had a higher oil yield and the increased energy cost from the higher moisture content can be lowered with pre-drying. For this reason, MWAP should be investigated further as a treatment fresher biosolids instead of stockpiled biosolids. While the mass of biosolids in stockpiles would not be decreased, treating fresher biosolids with MWAP instead of long-term stockpiling would prevent the growth of the stockpiles.

7 References

Alter power Systems. (2003). TM0-TMA 2.45GHz remotable Microwave Heads, Air Cooled (TMA) or Water Cooled (TM0). In A. P. Systems (Ed.).

Alter power Systems. (2006). CM340-CM440 E&F series, Technical Note. In A. P. Systems (Ed.), (1st, 5th Revision ed.).

Australian and New Zealand Biosolids Partnership. (2015). Benefits of Land Application. Retrieved from https://www.biosolids.com.au/info/benefits-of-land-application/

Australian and New Zealand Biosolids Partnership. (2016). Australian Biosolids Statistics. Retrieved from https://www.biosolids.com.au/guidelines/australian-biosolids-statistics/

AWA. (2012). *The Management of Biosolids in Australia*. Retrieved from https://www.awa.asn.au/Documents/Position_Paper_Biosolids.pdf

Beneroso, D., Bermúdez, J. M., Arenillas, A., & Menéndez, J. A. (2014a). Influence of the microwave absorbent and moisture content on the microwave pyrolysis of an organic municipal solid waste. *Journal of Analytical and Applied Pyrolysis, 105*(0), 234-240. doi:http://dx.doi.org/10.1016/j.jaap.2013.11.009

Beneroso, D., Bermúdez, J. M., Arenillas, A., & Menéndez, J. A. (2014b). Integrated microwave drying, pyrolysis and gasification for valorisation of organic wastes to syngas. *Fuel, 132*(0), 20-26. doi:http://dx.doi.org/10.1016/j.fuel.2014.04.064

Beverly Microwave Division. Magnetron Theory of Operation. Retrieved from http://67.225.133.110/~gbpprorg/mil/herf/Magnetron_Theory.pdf

BOC Pricing. (2016). Nitrogen, Industrial Grade, Extra High Pressure, Compressed, Cylinder Pack. In BOC (Ed.). https://www.boc.com.au/shop/en/au/nitrogen--industrial-grade--compressed-032-pk.

Bridgwater, A. V. (2012). Review of fast pyrolysis of biomass and product upgrading. *Biomass and Bioenergy, 38*(0), 68-94. doi:http://dx.doi.org/10.1016/j.biombioe.2011.01.048

Britannica, E. (2014). http://www.britannica.com/EBchecked/topic/357510/magnetron.

Bulushev, D. A., & Ross, J. R. H. (2011). Catalysis for conversion of biomass to fuels via pyrolysis and gasification: A review. *Catalysis Today, 171*(1), 1-13. doi:http://dx.doi.org/10.1016/j.cattod.2011.02.005

Centre for Industrial Education. (2014, 2/1/2014). Benzene and methylbenzene. Retrieved from http://www.essentialchemicalindustry.org/chemicals/benzene.html

Clarke Energy. (2014). Landfill Gas. Retrieved from http://www.clarke-energy.com/landfill-gas/

Clarke, R. M., & Cummins, E. (2014). Evaluation of "Classic" and Emerging Contaminants Resulting from the Application of Biosolids to Agricultural Lands: A Review. *Human and Ecological Risk Assessment: An International Journal, 21*(2), 492-513. doi:10.1080/10807039.2014.930295

CSImarket.com Inc. (2016). Chemical Manufacturing Industry Profitability. Retrieved from http://csimarket.com/Industry/industry_Profitability_Ratios.php?ind=101

Cyr, M., Coutand, M., & Clastres, P. (2007). Technological and environmental behavior of sewage sludge ash (SSA) in cement-based materials. *Cement and Concrete Research, 37*(8), 1278-1289. doi:http://dx.doi.org/10.1016/j.cemconres.2007.04.003

Dai, Q., Jiang, X., Wang, F., Chi, Y., & Yan, J. (2013). PCDD/Fs in wet sewage sludge pyrolysis using conventional and microwave heating. *Journal of Analytical and Applied Pyrolysis, 104*(0), 280-286. doi:http://dx.doi.org/10.1016/j.jaap.2013.07.005

Darvodelsky, P. (2012). *Biosolids Snapshot* (J206). Retrieved from http://www.environment.gov.au/protection/national-waste-policy/publications/biosolids-snapshot

Datta, A. K. (2001). *Handbook of Microwave Technology for Food Application*: CRC Press.

Department of the Environment AUS. (2013). *Factsheet- Biosolids Profile*. Retrieved from http://www.environment.gov.au/system/files/resources/0a517ed7-74cb-418b-9319-7624491e4921/files/factsheet-biosolids.pdf.

Domínguez, A., Fernández, Y., Fidalgo, B., Pis, J. J., & Menéndez, J. A. (2008). Bio-syngas production with low concentrations of CO2 and CH4 from microwave-induced pyrolysis of

wet and dried sewage sludge. *Chemosphere, 70*(3), 397-403. doi:http://dx.doi.org/10.1016/j.chemosphere.2007.06.075

Domínguez, A., Menéndez, J. A., Fernández, Y., Pis, J. J., Nabais, J. M. V., Carrott, P. J. M., & Carrott, M. M. L. R. (2007). Conventional and microwave induced pyrolysis of coffee hulls for the production of a hydrogen rich fuel gas. *Journal of Analytical and Applied Pyrolysis, 79*(1–2), 128-135. doi:http://dx.doi.org/10.1016/j.jaap.2006.08.003

Dominguez, A., Menendez, J. A., Inguanzo, M., Bernad, P. L., & Pis, J. J. (2003). Gas chromatographic–mass spectrometric study of the oil fractions produced by microwave-assisted pyrolysis of different sewage sludges. *Journal of Chromatography A, 1012*(2), 193-206. doi:http://dx.doi.org/10.1016/S0021-9673(03)01176-2

Domínguez, A., Menéndez, J. A., Inguanzo, M., & Pis, J. J. (2005). Investigations into the characteristics of oils produced from microwave pyrolysis of sewage sludge. *Fuel Processing Technology, 86*(9), 1007-1020. doi:http://dx.doi.org/10.1016/j.fuproc.2004.11.009

Domínguez, A., Menéndez, J. A., Inguanzo, M., & Pís, J. J. (2006). Production of bio-fuels by high temperature pyrolysis of sewage sludge using conventional and microwave heating. *Bioresource Technology, 97*(10), 1185-1193. doi:http://dx.doi.org/10.1016/j.biortech.2005.05.011

Domínguez, A., Menéndez, J. A., & Pis, J. J. (2006). Hydrogen rich fuel gas production from the pyrolysis of wet sewage sludge at high temperature. *Journal of Analytical and Applied Pyrolysis, 77*(2), 127-132. doi:http://dx.doi.org/10.1016/j.jaap.2006.02.003

Dominquez, A., Fernandez, G., Fidalgo, J., Pis, J., & Menendez, J. (2009). Bio-syngas production with low concentrations of CO2 and CH4 from microwave-induced pyrolysis of wet and dried sewage sludge. *Chemosphere.*

Donatello, S., & Cheeseman, C. R. (2013). Recycling and recovery routes for incinerated sewage sludge ash (ISSA): A review. *Waste Management, 33*(11), 2328-2340. doi:http://dx.doi.org/10.1016/j.wasman.2013.05.024

Egan, M. (2013). Biosolids management strategies: an evaluation of energy production as an alternative to land application. *Environmental Science and Pollution Research, 20*(7), 4299-4310. doi:10.1007/s11356-013-1621-1

EPA Victoria. (2004). *Biosolids Land Application*. http://www.epa.vic.gov.au/~/media/Publications/943.pdf.

ESCWA. (2003). *Waste-water Treatment Technologies: A General Review*. Retrieved from http://www.igemportal.org/Resim/Wastewater%20Treatment%20Technologies_%20A%20general%20rewiev.pdf

Evan Pert, Yuval Carmel, Amikam Birnboim, Tayo Olorunyolemi, David Gershon, Jeff Calame, . . . Jr, O. C. W. (2001). Temperature Measurements during Microwave Processing: The Significance of Thermocouple Effects.

Evita Agrafioti, George Bouras, Dimitrios Kalderis, & Evan Diamadopoulos. (2013). Biochar production by sewage sludge pyrolysis. *Journal of Analytical and Applied Pyrolysis*(101), 6.

F Chart Software. (2015). Engineering Equaiton Solver (Version 2015) [Equation Solver]: F-Chart Software.

Fernandez, Y., Arenillas, A., & Angel Menendez, J. (2011). Microwave Heating Applied to Pyrolysis *Advances in Induction and Microwave Heating of Mineral and Organic Materials* (pp. 723-748): InTech.

Fernández, Y., Arenillas, A., & Menéndez, J. Á. (2011). Microwave Heating Applied to Pyrolysis. In Stanislaw (Ed.), *Advances in Induction and Microwave Heating of Mineral and Organic Materials*.

Fonts, I., Azuara, M., Gea, G., & Murillo, M. B. (2009). Study of the pyrolysis liquids obtained from different sewage sludge. *Journal of Analytical and Applied Pyrolysis, 85*(1–2), 184-191. doi:http://dx.doi.org/10.1016/j.jaap.2008.11.003

Fonts, I., Azuara, M., Lázaro, L., Gea, G., & Murillo, M. B. (2009). Gas Chromatography Study of Sewage Sludge Pyrolysis Liquids Obtained at Different Operational Conditions in a Fluidized Bed. *Industrial & Engineering Chemistry Research, 48*(12), 5907-5915. doi:10.1021/ie900421a

Fonts, I., Gea, G., Azuara, M., Ábrego, J., & Arauzo, J. (2012). Sewage sludge pyrolysis for liquid production: A review. *Renewable and Sustainable Energy Reviews, 16*(5), 2781-2805. doi:http://dx.doi.org/10.1016/j.rser.2012.02.070

Gao, N., Li, J., Qi, B., Li, A., Duan, Y., & Wang, Z. (2014). Thermal analysis and products distribution of dried sewage sludge pyrolysis. *Journal of Analytical and Applied Pyrolysis, 105*(0), 43-48. doi:http://dx.doi.org/10.1016/j.jaap.2013.10.002

García-Orenes, F., Guerrero, C., Mataix-Solera, J., Navarro-Pedreño, J., Gómez, I., & Mataix-Beneyto, J. (2005). Factors controlling the aggregate stability and bulk density in two different degraded soils amended with biosolids. *Soil and Tillage Research, 82*(1), 65-76. doi:http://dx.doi.org/10.1016/j.still.2004.06.004

Gerling Applied Engineering. (2005). Dual Directional Waveguide Coupler.

Hayes. B. (2002). *Microwave Synthesis* Retrieved from http://faculty.swosu.edu/tim.hubin/share/Microwave%20Synthesis.pdf

Hong, S. M., Park, J. K., & Lee, Y. O. (2004). Mechanisms of microwave irradiation involved in the destruction of fecal coliforms from biosolids. *Water Research, 38*(6), 1615-1625. doi:http://dx.doi.org/10.1016/j.watres.2003.12.011

Houillon, G., & Jolliet, O. (2005). Life cycle assessment of processes for the treatment of wastewater urban sludge: energy and global warming analysis. *Journal of Cleaner Production, 13*(3), 287-299. doi:http://dx.doi.org/10.1016/j.jclepro.2004.02.022

Industrial Microwave Systems. (2012). Frequently Asked Questions: 2450MHz vs. 915MHz.

J.A. Menéndez , A. Arenillas, B. Fidalgo, Y. Fernández, L. Zubizarreta, E.G. Calvo, & Bermúdez, J. M. (2009). Microwave heating processes involving carbon materials. *Fuel Processing Technology*, 1-8.

Jahirul, M. I., Rasul, M. G., Chowdhury, A. A., & Ashwath, N. (2012). Biofuels Production through Biomass Pyrolysis —A Technological Review. *Energies, 5*(12), 1-50.

Jana Št'ávová, Josef Beránek, Eric P. Nelson, Bonnie A. Diep, & Alena Kubátová. (2011). Limits of detections for the determination of mono- and dicarboxylic acids using gas and liquid chromatographic methods coupled with mass spectrometry. *Journal of Chromatography B, 879*(17-18). doi:doi:10.1016/j.jchromb.2010.11.027

Jindarom, C., Meeyoo, V., Rirksomboon, T., & Rangsunvigit, P. (2007). Thermochemical decomposition of sewage sludge in CO2 and N2 atmosphere. *Chemosphere, 67*(8), 1477-1484. doi:http://dx.doi.org/10.1016/j.chemosphere.2006.12.066

John Marsden Associates. (2014). *Estimate of the cost of hazardous waste in Australia*. https://www.environment.gov.au/system/files/resources/d1889716-2b06-44e1-a62c-3e67ff3d595f/files/cost-hazardous-waste.pdf.

Key, D. (2005). *Composting Biosolids*. Paper presented at the 68th Annual Water Industry Engineers and Operators Conference, Bendigo.

Kim, K.-R., & Owens, G. (2010). Potential for enhanced phytoremediation of landfills using biosolids – a review. *Journal of Environmental Management, 91*(4), 791-797. doi:http://dx.doi.org/10.1016/j.jenvman.2009.10.017

Lappin, G. R., & Sauer, J. D. (Eds.). (1989). *Alpha Oelfins Applicatins Handbook* (10th ed.).

Le Barc'H, N., Grossel, J. M., Looten, P., & Mathlouthi, M. (2001). Kinetic study of the mutarotation of D-glucose in concentrated aqueous solution by gas-liquid chromatography. *Food Chemistry, 74*(1), 119-124. doi:http://dx.doi.org/10.1016/S0308-8146(01)00139-X

Lin, H., & Ma, X. (2012). Simulation of co-incineration of sewage sludge with municipal solid waste in a grate furnace incinerator. *Waste Management, 32*(3), 561-567. doi:http://dx.doi.org/10.1016/j.wasman.2011.10.032

Lohninger. H. (2011). *Occurrence and Use of Alkanes*

Lundin, M., Olofsson, M., Pettersson, G. J., & Zetterlund, H. (2004). Environmental and economic assessment of sewage sludge handling options. *Resources, Conservation and Recycling, 41*(4), 255-278. doi:http://dx.doi.org/10.1016/j.resconrec.2003.10.006

Majumder, R., Livesley, S. J., Gregory, D., & Arndt, S. K. (2014). Biosolid stockpiles are a significant point source for greenhouse gas emissions. *Journal of Environmental Management, 143*(0), 34-43. doi:http://dx.doi.org/10.1016/j.jenvman.2014.04.016

Majumder, R., Livesley, S. J., Gregory, D., & Arndt, S. K. (2015). Storage management influences greenhouse gas emissions from biosolids. *Journal of Environmental Management, 151*, 361-368. doi:http://dx.doi.org/10.1016/j.jenvman.2015.01.007

McLaughlin, M., Bell, M., Nash, D., Pritchard, D., Whatmuff, M., Warne, M., . . . Penney, N. (2008). Benefits of using biosolid nutrients in Australian agriculture - a national perspective.

Meca Electronics, I. (2010). *Isolater and Circulator Basics*

Melbourne Water. (2014). Waste to Resources.   Retrieved from https://www.melbournewater.com.au/whatwedo/Liveability-and-environment/waste/Pages/Waste-to-resources.aspx

Menedez, J., Arenillas, A., Fidalgo, B., Fernandez, Y., Zuizarreta, E. G. C., & Bermudez, J. M. (2010). Microwave heating processes involving carbon materials. *Fuel Processing Technology*(91), 1-8.

Menéndez, J. A., Domínguez, A., Inguanzo, M., & Pis, J. J. (2004). Microwave pyrolysis of sewage sludge: analysis of the gas fraction. *Journal of Analytical and Applied Pyrolysis, 71*(2), 657-667. doi:http://dx.doi.org/10.1016/j.jaap.2003.09.003

Menéndez, J. A., Inguanzo, M., & Pis, J. J. (2002). Microwave-induced pyrolysis of sewage sludge. *Water Research, 36*(13), 3261-3264. doi:http://dx.doi.org/10.1016/S0043-1354(02)00017-9

Mihai Brebu, & Cornelia Vasile. (2010). THERMAL DEGRADATION OF LIGNIN - A REVIEW. *Cellulose Chemistry and Technology, 9*(44), 353-363.

Mills, N., Pearce, P., Farrow, J., Thorpe, R. B., & Kirkby, N. F. (2014). Environmental & economic life cycle assessment of current & future sewage sludge to energy technologies. *Waste Management, 34*(1), 185-195. doi:http://dx.doi.org/10.1016/j.wasman.2013.08.024

MOLBASE. (2015). MOLBASE Chemical B2B E-Commerce Platform.   http://www.molbase.com/

Murakami, T., Suzuki, Y., Nagasawa, H., Yamamoto, T., Koseki, T., Hirose, H., & Okamoto, S. (2009). Combustion characteristics of sewage sludge in an incineration plant for energy recovery. *Fuel Processing Technology, 90*(6), 778-783.

National Electronics. (2007). Industrial Isolator 2722 162 11171. In R. Electronics (Ed.).

Navas, A., Machín, J., & Navas, B. (1999). Use of biosolids to restore the natural vegetation cover on degraded soils in the badlands of Zaragoza (NE Spain). *Bioresource Technology, 69*(3), 199-205. doi:http://dx.doi.org/10.1016/S0960-8524(99)00003-6

Nave. R. (2014). The Magnetron. Retrieved from http://hyperphysics.phy-astr.gsu.edu/hbase/Waves/magnetron.html

Neves, D., Thunman, H., Matos, A., Tarelho, L., & Gómez-Barea, A. (2011). Characterization and prediction of biomass pyrolysis products. *Progress in Energy and Combustion Science, 37*(5), 611-630. doi:http://dx.doi.org/10.1016/j.pecs.2011.01.001

Niu, Y., Tan, H., & Hui, S. e. (2016). Ash-related issues during biomass combustion: Alkali-induced slagging, silicate melt-induced slagging (ash fusion), agglomeration, corrosion, ash utilization, and related countermeasures. *Progress in Energy and Combustion Science, 52*, 1-61. doi:http://dx.doi.org/10.1016/j.pecs.2015.09.003

NRMMC. (2004). *Guidelines for Sewage Systems Biosolid Management*.

Okuda, T., Nishijima, W., Sugimoto, M., Saka, N., Nakai, S., Tanabe, K., . . . Okada, M. (2014). Removal of coagulant aluminum from water treatment residuals by acid. *Water Research, 60*(0), 75-81. doi:http://dx.doi.org/10.1016/j.watres.2014.04.041

Omar, R., & Robinson, J. P. (2014). Conventional and microwave-assisted pyrolysis of rapeseed oil for bio-fuel production. *Journal of Analytical and Applied Pyrolysis, 105*(0), 131-142. doi:http://dx.doi.org/10.1016/j.jaap.2013.10.012

Orata. F. (2011). Derivatization Reactions and Reagents for Gas Chromatography Analysis *Advanced Gas Chromatography – Progress in Agricultural, Biomedical and Industrial Applications* http://cdn.intechopen.com/pdfs/32817.pdf.

Origin Energy. (2016). Powering Business.   Retrieved from https://www.originenergy.com.au/business/commercial-and-industrial/newsletter.html

Pan, S.-C., Lin, C.-C., & Tseng, D.-H. (2003). Reusing sewage sludge ash as adsorbent for copper removal from wastewater. *Resources, Conservation and Recycling, 39*(1), 79-90. doi:http://dx.doi.org/10.1016/S0921-3449(02)00122-2

Petroleum UK. (2013). Alkene types and structures. Retrieved from http://www.petroleum.co.uk/alkene-chemistry

Pritchard, D., Penney, N., McLaughlin, M., Rigby, H., & Schwarz, K. (2010). Land application of sewage sludge (biosolids) in Australia: risks to the environment and food crops. *Water Science and Technology, 62*(1), 48.

R Development Core Team. (2008). R: A language and environment for statistical computing. (Version 3.2.4). www.R-project.org: R Foundation for Statistical Computing.

Roberts, J. D. (1977). Alkanes *Basic Organic Chemistry*.

Schummer, C., Delhomme, O., Appenzeller, B. M. R., Wennig, R., & Millet, M. (2009). Comparison of MTBSTFA and BSTFA in derivatization reactions of polar compounds prior to GC/MS analysis. *Talanta, 77*(4), 1473-1482. doi:http://dx.doi.org/10.1016/j.talanta.2008.09.043

Shen, Y., & Yoshikawa, K. (2013). Recent progresses in catalytic tar elimination during biomass gasification or pyrolysis—A review. *Renewable and Sustainable Energy Reviews, 21*, 371-392. doi:http://dx.doi.org/10.1016/j.rser.2012.12.062

Sidhu, J. P. S., & Toze, S. G. (2009). Human pathogens and their indicators in biosolids: A literature review. *Environment International, 35*(1), 187-201. doi:http://dx.doi.org/10.1016/j.envint.2008.07.006

Sigma Aldrich. (1997). BSTFA- Product Specification. Retrieved from http://www.sigmaaldrich.com/Graphics/Supelco/objects/4800/4747.pdf

SITA Australia. (2010). Green Energy Production.

Smedman A, Gustafsson I, Berglund L, & Vessby B. (1999). Pentadecanoic acid in serum as a marker for intake of milk fat:

relations between intake of milk fat and metabolic risk factors1. *American Journal of Clinical Nutrition, 69*(1), 22-29.

Sturm, G., Verweij, M., Stankiewicz, A., & Stefanidis, G. (2014). Microwaves and microreactors: Design challenges and remedies. *Chemical Engineering Journal*(243), 147-158.

Su, Y., Zhu, W., Gong, M., Zhou, H., Fan, Y., & Amuzu-Sefordzi, B. (2015). Interaction between sewage sludge components lignin (phenol) and proteins (alanine) in supercritical water gasification. *International Journal of Hydrogen Energy, 40*(30), 9125-9136. doi:http://dx.doi.org/10.1016/j.ijhydene.2015.05.072

T.J. Buckley, & E.S. Domanski. (1988). *EVALUATION OF DATA ON HIGHER HEATING VALUES AND ELEMENTAL ANALYSIS FOR REFUSE-DERIVED FUELS* US National Bureau of Standards.

Taoze Liu, Bangyu Liu, & Wei Zhang. (2013). Nutrients and Heavy Metals in Biochar Produced by Sewage Sludge Pyrolysis: Its Application in Soil Amendment *Pol. J. Environmental Studies, 23*(1), 4.

Technical Glass Products. (2010). Properties of Fused Quartz. Retrieved from https://www.technicalglass.com/enlarged_technical/lg_property_value.html

Tian, Y., Zuo, W., Ren, Z., & Chen, D. (2011). Estimation of a novel method to produce bio-oil from sewage sludge by microwave pyrolysis with the consideration of efficiency and safety. *Bioresource Technology, 102*(2), 2053-2061. doi:http://dx.doi.org/10.1016/j.biortech.2010.09.082

Turovskiy, I. (2000). Biosolids or Sludge? The Semantics of Terminology. Retrieved from http://www.wwdmag.com/biosolids-or-sludge-semantics-terminology

Tyagi, V. K., & Lo, S.-L. (2013). Microwave irradiation: A sustainable way for sludge treatment and resource recovery. *Renewable and Sustainable Energy Reviews, 18*(0), 288-305. doi:http://dx.doi.org/10.1016/j.rser.2012.10.032

UN-Habitat, U. N. H. S. P. (2008). *GLOBAL ATLAS OF EXCRETA, WASTEWATER SLUDGE, AND BIOSOLIDS MANAGEMENT: MOVING FORWARD THE SUSTAINABLE AND WELCOME USES OF A GLOBAL RESOURCE*.

US EPA. (2007). *Methodology for Thermal Efficiency and Energy Input Calculations and Analysis of Biomass Cogeneration Unit Characteristics* https://www3.epa.gov/airtoxics/utility/fnl_biomass_cogen_TSD_04_19_07.pdf.

van de Voort, F. R., Laureano, M., Smith, J. P., & Raghavan, G. S. V. (1987). A Practical Thermocouple for Temperature Measurement in Microwave Ovens1. *Canadian Institute of Food Science and Technology Journal, 20*(4), 279-284. doi:http://dx.doi.org/10.1016/S0315-5463(87)71200-0

Wang, N., Yu, J., Tahmasebi, A., Han, Y., Lucas, J., Wall, T., & Jiang, Y. (2014). Experimental Study on Microwave Pyrolysis of an Indonesian Low-Rank Coal. *Energy & Fuels, 28*(1), 254-263. doi:10.1021/ef401424p

Wang, X., Morrison, W., Du, Z., Wan, Y., Lin, X., Chen, P., & Ruan, R. (2012). Biomass temperature profile development and its implications under the microwave-assisted pyrolysis condition. *Applied Energy, 99*(0), 386-392. doi:http://dx.doi.org/10.1016/j.apenergy.2012.05.031

Wenclawiak, B., Jensen, T., & Richert, J. O. (1993). GC/MS-FID analysis of BSTFA derivatized polar components of diesel particulate matter (NBS SRM-1650) extract. *Fresenius' Journal of Analytical Chemistry, 346*(6-9), 808-812. doi:10.1007/BF00321295

Wu, C., Budarin, V. L., Gronnow, M. J., De Bruyn, M., Onwudili, J. A., Clark, J. H., & Williams, P. T. (2014). Conventional and microwave-assisted pyrolysis of biomass under different heating rates. *Journal of Analytical and Applied Pyrolysis, 107*(0), 276-283. doi:http://dx.doi.org/10.1016/j.jaap.2014.03.012

Xie, Q., Peng, P., Liu, S., Min, M., Cheng, Y., Wan, Y., . . . Ruan, R. (2014). Fast microwave-assisted catalytic pyrolysis of sewage sludge for bio-oil production. *Bioresource Technology, 172*(0), 162-168. doi:http://dx.doi.org/10.1016/j.biortech.2014.09.006

Yin, C. (2012). Microwave-assisted pyrolysis of biomass for liquid biofuels production. *Bioresource Technology, 120*(0), 273-284. doi:http://dx.doi.org/10.1016/j.biortech.2012.06.016

Yu, Y., Yu, J., Sun, B., & Yan, Z. (2014). Influence of catalyst types on the microwave-induced pyrolysis of sewage sludge. *Journal of Analytical and Applied Pyrolysis, 106*(0), 86-91. doi:http://dx.doi.org/10.1016/j.jaap.2014.01.003

Yu, Y., Yu, J., Sun, B., & Yan, Z. (2014). Influence of catalyst ypes on the microwave-induced pyrolysis of sewage sludge. *Journal of Analytical and Applied Pyrolysis*, 6.

Zhang, J., Tian, Y., Zhu, J., Zuo, W., & Yin, L. (2014). Characterization of nitrogen transformation during microwave-induced pyrolysis of sewage sludge. *Journal of Analytical and Applied Pyrolysis, 105*(0), 335-341. doi:http://dx.doi.org/10.1016/j.jaap.2013.11.021

Zhang, L., Xu, C., Champagne, P., & Mabee, W. (2014). Overview of current biological and thermo-chemical treatment technologies for sustainable sludge management. *Waste Management and Research, 32*(7), 586-600.

Zuo, W., Tian, Y., & Ren, N. (2011). The important role of microwave receptors in bio-fuel production by microwave-induced pyrolysis of sewage sludge. *Waste Management, 31*(6), 1321-1326. doi:http://dx.doi.org/10.1016/j.wasman.2011.02.001